Exploring the Astrobiological Potential of Titan's Cryovolcanic Features, Impact Craters, and Liquid Hydrocarbon Lakes & Seas

Presented in Partial Fulfillment of the Requirements for the Degree of

Master of Science

with a Major in

Geology

in the

College of Graduate Studies

University of Idaho

by

Anna Sage Ross-Browning

Major Professor

Jason W. Barnes, Ph.D.

Co-Major Professor

Erika L. Rader, Ph.D.

Committee

Matthew M. Hedman, Ph.D.

Michael S. Strickland, Ph.D.

Departmental Administrator

Alistair M.S. Smith, Ph.D.

December 2023

ABSTRACT

Saturn's moon Titan has garnered significant astrobiological attention due to its Earth-like characteristics, which include its thick atmosphere, meteorological cycle, and long-lasting liquid bodies on its surface. The upcoming Dragonfly mission – scheduled to launch in the 2020s – aims to explore the surface of Titan and to search for past and present signs of habitability. However, Titan's extremely cold average surface temperature of 94 K poses challenges for the existence of liquid water on its surface but for two geologic and astronomical processes – cryovolcanism and impact events. This thesis investigates the features created by these processes – as well as the liquid methane and ethane lakes and seas – and their potential roles in supporting prebiotic or biotic chemistry. Chapter 1 introduces the significance of this work and outlines its structure. In Chapter 2, I analyze the astrobiological potential of cryovolcanic features and impact craters by performing a literature review. In Chapter 3, I use the Beer-Lambert-Bouguer law to examine how light incident on Titan's surface attenuates in impact melt crater pools and the liquid hydrocarbon lakes and seas to determine if photosynthetically available radiation (PAR) could be suitable as a primary or secondary energy source for putative life. Chapter 4 discusses the caveats to this work as well as directions for future research. This work serves as an important discussion about how astrobiological theory may be applied to Titanian environments to assess what habitability- and bio-signatures could be created by prebiotic or biotic chemistry in Titan's unique environments. This thesis will contribute to understanding potential habitability and potential biosignatures in Titan's environments, informing future missions to Titan and other icy moons.

ACKNOWLEDGEMENTS

I am extremely thankful to my advisors Dr. Jason Barnes and Dr. Erika Rader for the support and opportunity to learn and conduct research here at the University of Idaho. Thank you to Dr. Barnes for allowing me to take (a small) part in the Dragonfly mission. Thank you to Dr. Rader for allowing me to tag along and help with fieldwork for other students in the group and inviting me to travel to Iceland with all of you to help you collect data. I would also like to thank my committee members Dr. Michael Strickland and Dr. Matthew Hedman for their wonderful teaching, insightful conversations, and for agreeing to be on my committee. Dr. Hedman, I would especially like to thank you for your infinite patience with me, both as a student in your classes and as a student for which you are a committee member. I am infinitely thankful for your patience and the help you have provided me with over the years.

Thank you also to my undergraduate research advisors, Dr. Tyler Robinson, Mary Anne Limbach, and Dr. Jut Wynne for all the wonderful advisement and for teaching me how to conduct research before even reaching graduate school.

DEDICATION

I would like to dedicate this thesis first and foremost to my parents, my mom, Lisa Flowers Ross, and my dad, Frank Ross, to my husband, Brian Browning, and to my grandparents Margaret and William Ross. The generous and loving support of my parents and grandparents is what made going to college and graduate school to follow my dreams possible in the first place. Thank you for thinking of me and planning for my future even when I was small, and for supporting me in all ways emotional as well. Thank you to my parents for always being supportive and encouraging me to follow my dreams, no matter what they were or are, and for telling me I can do whatever I put my mind to, even when I don't believe it myself. Thank you to my husband for coming to Moscow with me and for being my rock, and for giving me cuddles and ice cream when I am having a bad day. You keep me grounded when my brain is trying to spiral away. Thank you to my uncle Bob Taylor for always inspiring me with your natural curiosity about the world around you. Thank you to all my other family members as well, I love you all so much.

I would also like to thank all my pets, past and present, who have begrudgingly put up with all the cuddles and times I have had to cry into their fur for comfort. Taro, you deserve all the tuna for all the emotional support cuddles and purrs you have given me. Forest, you deserve all the walkies and treats for giving me kisses and trying to play tug-of-war with me to help me de-stress. To all my hamsters and to Cleo the lizard, you deserve all the mealworms and yogurt treats for keeping me in the present.

I would also like to dedicate this thesis to my friends from my hometown, from undergrad, and the friends I have made here in the Moscow-Pullman area. You all are awesome. Thank you especially to Ethan Goff, Hannah Mattsson, and Alexis Lundgren. Even though we are far apart, my love and appreciation for all of you never dwindles. As well, I dedicate this thesis to Mr. Scott Arnold and Mrs. Erin Galinato, my favorite teachers. You both inspired and encouraged my love for learning, and that encouragement is part of the reason I have made it to graduate school. And finally, a thank you to all my plants for inspiring a new love for different scientific disciplines and hobbies and for making my living space green and happy

TABLE OF CONTENTS

LIST OF TABLES

LIST OF FIGURES

CHAPTER 1

INTRODUCTION

> "On [that] day therefore, according to the Gregorian Calendar, the 25th of March, in the year 1655, at about 8 o'clock in the evening, I saw Saturn with his arms stretched out on both sides according to a straight line; and at three o'clock [I observed] a certain little star a distance from him, so situated that if [it] were led straight by the arm, it would run into [Saturn], or at least pass a little lower. And the other, likewise towards the east, was the star b, a little farther removed from Saturn, and the line of the arms much lower. And on this first occasion I suspected that the star was accompanied by Saturn, since I had also noticed it on other occasions close to it, and in a similar position."

- Christiaan Huygens (1659*), Systema Saturnum*, roughly translated from Latin by the author

Over the past 364 years, Saturn's moon Titan has transformed in humanity's eyes from a small, pale, orange dot gracing the flanks of Saturn to an intriguing world with an environment not so unlike that of our own planet Earth. Discoveries made by the Voyagers I (Stone and Miner 1981) and II (Stone and Miner 1982) and Cassini-Huygens (Elachi *et al.* 2005; Lange 2008) missions uncovered vibrant and alien landscapes beneath Titan's hazy atmosphere, where rocks are made of ice and complex organics (Coates *et al.* 2007; Thompson and Sagan 1992) and lakes and seas are composed of liquid methane and ethane (Stofan *et al.* 2007). As a result, Titan has emerged as an intriguing target for in-depth study and exploration by planetary scientists and astrobiologists.

Astrobiology is the field of science in which, i.) Earth-like life is studied in space, microgravity, and lab-created extraterrestrially analogous environments and ii.) the potential for the development of life on other planets and moons is evaluated. It is one of the most interdisciplinary fields in the natural sciences, drawing from diverse subjects including physics, astronomy, geology, chemistry, meteorology, botany, medical sciences, and geospatial sciences, just to name a select few. The absence of confirmed extraterrestrial life presents astrobiologists with the mammoth task of synthesizing information from numerous disciplines and applying this knowledge to extreme and unfamiliar terrains. Astrobiologists must make the determination of whether an extraterrestrial environment is amenable or deleterious to water-based life by studying environments on planets and moons and searching for the

ingredients believed to be necessary for life – namely, liquid water and essential elements – without ever physically stepping foot in those environments.

Currently, several objects in the solar system are of high astrobiological interest. Among these is Titan. Titan appears Earth-like in several respects - it is one of few objects in the solar system to possess an appreciable atmosphere, it is the only object aside from Earth known to host stable surficial liquids, and it experiences familiar geological and meteorological processes. However, Titan is a frigid 94 K (-179.15 ^{O}C) which is much colder than Earth's 294 K average temperature, and much too cold for stable surface water (the universal solvent of life as we know it).

Nevertheless, two environments on Titan's surface have the potential to host transient liquid water for extended periods, possibly up to or greater than 10^2-10^6 years (Artemieva and Lunine 2003; 2005; O'Brien *et al.* 2005; Thompson and Sagan 1992). Such timescales may render these environments amenable to prebiotic chemistry or abiogenesis. These two environments are putative cryovolcanic features and impact melt ponds or pools. The latter will be studied and discussed extensively in the following thesis while the former will be discussed in Chapter 2.

Thus, while Titan at first seems uninhabitable by life as we know it, transient liquid water environments on Titan in the form of cryovolcanic features and impact crater pools are astrobiologically significant for the following reasons:

i. Enough liquid water is generated by large impact events to remain liquid under a slow-growing icy lid for up to or more than 10^2-10^6 (Artemieva and Lunine 2003; 2005; O'Brien *et al.* 2005; Thompson and Sagan 1992). Artemieva and Lunine (2003)'s modeling provides the most comprehensive study regarding impact melt generation by impacts to the surface of Titan. However, their study focuses on craters produced by a 2 km diameter impactor. This size of impactor is predicted to produce a crater with diameter of ~ 20 km (Artemieva and Lunine 2003). Notably, several craters exist on Titan with diameters that far exceed 20 km in diameter, including Selk Crater (80 km in diameter) (Hedgepeth *et al.* 2020), a target location for the Dragonfly mission poised to launch in the late 2020s (Barnes *et al.* 2021). Larger volumes of water can be produced by larger impact events and may experience longer freezing timescales. It is posited that even the freezing timescales experienced by the ~20 km diameter craters could be sufficient for abiogenesis (Artemieva and Lunine 2003): longer freezing timescales only increase the chance for abiogenesis to occur and for life to develop on an in-situ detectable level.

ii. Liquid water produced by an impact event will mix with complex organic sediments produced in Titan's photolytically active atmosphere and rained out onto the icy crust (Artemieva and Lunine 2003). Complex organics mixed into the liquid water column could provide essential elements needed for prebiotic chemistry to develop in the impact crater pool (Artemieva and Lunine 2003; Thompson and Sagan 1992).

iii. Cryovolcanism can generate liquid water or ammonia-water or ammonia-water-methanol slurries in the subsurface that are eruptible (Lopes *et al.* 2007). Near-surface cryomagmas residing in magma chambers, calderas, dikes, or sills may remain in a liquid state for a considerable period before erupting or cooling. These intrusive liquids or slurries offer promising habitats for the development of prebiotic chemistry or abiogenesis. Putative life forms originating in cryomagmas could subsequently be erupted and could survive on the surface for the duration of time in which the cryolavas remain semi-liquid. The existence of cryovolcanism may also imply communication between the surface and the subsurface liquid ammonia-water ocean. If life did not form in the cryomagmas, life that may have formed in the salty, warm ocean below could be forced upwards into the subsurface and eventually extruded or erupted onto the surface (Lopes *et al.* 2007). Any evidence of life, should it exist, might be preserved in these frozen flow features.

Thus, studies of impact melts and cryovolcanic features on Titan are crucial, since the timescales on which water could remain in its liquid phase might be astrobiologically significant. Potential signatures of prebiotic or biotic chemistry (should they exist) could remain detectable in the frozen-over melts to surface-going missions such as Dragonfly. Studies such as this thesis, as well as future studies of Titanian environments by missions such as Dragonfly, can further constrain the likelihood for life to develop in Titanian environments. Additionally, such investigations could help to identify potential biosignatures that may have been left behind by extant life.

Additionally, recent studies have explored the possibility of methane-based life developing in Titan's liquid hydrocarbon lakes and seas (McKay and Smith 2005; Sandström and Rahm 2020; Stevenson *et al.* 2015). However, findings regarding the stability of a hydrocarbon-based cellular membrane in the extreme temperatures experienced by these lakes and seas are varied. Despite this uncertainty, this avenue of astrobiological investigation warrants further exploration, particularly as the potential for sea-going missions on Titan remains a subject of ongoing research (i.e., Lorenz 2017; Stofan *et al.* 2013; Tagliabue *et al.* 2020).

Systematic investigations exploring the types of energies available to putative prebiotic and biotic chemistry in Titanian environments have been limited. By investigating different energies available in these environments – such as solar radiation, forms of heating, or chemical energy gradients – we can gain further insights into the potential for prebiotic or biotic chemistry to develop in these locations.

This thesis will begin with the current introduction section, and then will proceed to Chapter 2, which will contain a literature review. In this literature review, I will outline the current state of knowledge of cryovolcanism, impact cratering, and the lakes and seas of Titan and analyze each location's astrobiological potential, and broadly outline what kinds of life could potentially exist here under the right circumstances. Chapter 3 will contain the main research that comprises the thesis, where I will use a model based upon the Bouguer-Beer-Lambert Law to assess the attenuation with depth of visible wavelengths through impact crater pools and the lakes and seas of Titan, and the astrobiological consequences of my findings. Chapter 4 will outline caveats of this research and future directions for research in this area.

CHAPTER 2

ASTROBIOLOGICAL SIGNIFICANCE OF CRYOVOLCANIC AND IMPACT FEATURES ON SATURN'S MOON TITAN

2.1 ABSTRACT

Saturn's moon Titan is an alien mirror of Earth with its thick atmosphere, active methane meteorological cycle, and liquid hydrocarbon lakes and seas. Although the surface of Titan is well below the freezing point of water, transient surficial liquid water can exist in putative cryovolcanic flows and liquid impact crater melt pools. This transient liquid water might have interacted with complex organics containing essential elements for life, rendering these environments astrobiologically auspicious. Here, I perform a literature review to evaluate various cryovolcanic and crater environments on Titan where sufficient amounts of liquid water may have once existed and assess the astrobiological potential of these environments. Cryovolcanic regions such as Hotei and Tui Regiones, Doom and Erebor Montes have stood up to scrutiny regarding their cryovolcanic origins and appear to be the most promising for astrobiological studies. Other convincing putative cryovolcanic features exist but may require future study before becoming targets for extended or future Titan-going missions. Numerous craters with diameters greater than 20 km exist on Titan. Craters of this size or larger can potentially hold crater melt pools that could have remained partially liquid on astrobiologically relevant timescales. Large craters such as Afekin, Forseti, Guabonito, Hano, Menrva, Paxsi, Selk, Sinlap, and Soi likely boast the largest volumes of melt and thus the longest freezing timescales, with Menrva being the largest crater by far. Life at these locations, should it develop, could survive by utilizing survival strategies such as the development of "antifreeze proteins" and exopolymers, or, in the case of repeated cryovolcanic flow eruptions, cryobiosis/dormancy. Overall, while Titan is a frigid world, it retains high astrobiological potential.

2.2 INTRODUCTION

The Cassini-Huygens mission, flown in the early 2000s, unveiled an Earth-like landscape beneath Titan's opaque, hazy orange atmosphere (Elachi *et al.* 2005; Lunine and Atreya 2008). Dunes of

sediments grace its equatorial region (Radebaugh *et al.* 2008), while its poles are adorned by lakes and seas (Lunine and Atreya 2008; Stofan *et al.* 2007). All these features are animated by an active meteorological cycle (Mitchell and Lora 2016). However, the liquids present on Titan's surface and rained down from the clouds are liquid hydrocarbons – predominantly methane and ethane (Lunine and Atreya 2008; Mitchell and Lora 2016) – instead of water.

Biologically relevant molecules as we know them require a solvent of liquid water to assemble and ultimately develop into life, a process known as abiogenesis. Consequently, the approach to the search for life as we know it (LAWKI) typically follows the mantra, "follow the liquid water" (although a "follow the liquid hydrocarbon" approach could also be considered for Titan (McKay and Smith 2005; Sandström and Rahm 2020; Stevenson *et al.* 2015), as discussed in Chapter 3).

Given Titan's average surface temperature of 94 K, stable, long-lived liquid water cannot exist on its surface. However, two geological and astronomical processes, impact cratering events and cryovolcanism, have the potential to generate transient surficial or near-surficial liquid water (Artemieva and Lunine 2003; 2005; Lopes *et al.* 2007; 2013; Lorenz 1996; Neish *et al.* 2018; O'Brien *et al.* 2005; Wall *et al.* 2009). Cryovolcanism may force liquid ammonia-water mixtures or slurries from Titan's subsurface ocean onto the surface, where the freezing point depression of ammonia may allow for slower freezing of cryoliquids. Repeated eruptions and re-melting could provide temporary habitats for life that uses dormancy and regeneration as a life history strategy. Intrusive cryomagmatic features such as sills, dikes, and chambers could host liquid water or water slurries on longer timescales. Impact cratering events, on the other hand, can generate large volumes of liquid water from the icy crust that may remain liquid for up to 10^4 years or more (Artemieva and Lunine 2003; 2005; O'Brien *et al.* 2005), which may be long enough for prebiotic chemistry or abiogenesis to occur.

In addition to liquid water, life on Earth requires C, H, N, O, P, S – carbon, hydrogen, nitrogen, oxygen, phosphorus, and sulfur. Titan's photolytically active atmosphere produces complex organic 'tholins' (Sagan and Khare 1979) that rain out onto the surface (it is these sediments that comprise the equatorial dunes), and that may contain several if not all these essential elements. When mixed with liquid water, these complex organics can generate biologically relevant molecules such as amino acids (Neish *et al.* 2018; O'Brien *et al.* 2005), giving rise to a veritable "primordial soup".

Necessary ingredients for LAWKI likely exist on Titan. The question remains if these ingredients have mixed with water, are abundant in the correct quantities, and to what extent the products of this mixing have approached a prebiotic or biotic state. Therefore, studying and characterizing the various locations on Titan where cryolavas, cryomagmas, or impact melts are found

are of paramount importance for future surface-going missions such as Dragonfly (Barnes *et al.* 2021; Neish *et al.* 2018).

In this chapter, I discuss Titan's cryovolcanic and impact crater environments where transient liquid water may exist or has existed in the past. I explore the extent to which this water has had contact with essential elements and molecules to spur prebiotic chemical processes, and thus which of these environments may have once hosted (or could still host) prebiotic or biotic chemistry. I then discuss the kinds of life and ecologies that could hypothetically exist in these environments. I emphasize the importance of thinking both critically and creatively about the potential organisms that could exist in Titanian environments – should prebiotic chemistry occur and progress to abiogenesis – in preparation for future missions to Titan and other icy bodies.

2.3 CRYOVOLCANISM

Cryovolcanism – a form of volcanism in which the constituent 'magmas' are water-ice mixtures or slurries as opposed to melted silicate rock (Kargel 1995) – is a poorly understood process that has direct implications for the development of prebiotic chemistry on icy moons such as Titan. Cryovolcanism has been proposed to occur on icy bodies in the outer solar system such as Europa (Roth *et al.* 2014; Sparks *et al.* 2016; 2017) Enceladus (Lorenz 1996; Spencer *et al.* 2009), several Uranian satellites (Schenk and Moore 2020), and has been proposed to occur on Titan as well (Lopes *et al.* 2007; 2013; Schurmeier *et al.* 2023; Wall *et al.* 2009).

In the early 2000's, Cassini imagery revealed the existence of flow-like, lobate features with unexplained origins on Titan (Elachi *et al.* 2005). Initial analysis of radiometric data returned from Cassini VIMS, RADAR, and SAR instrumentation implied the presence of cryovolcanism, as many geologic features appeared analogous to intrusive and extrusive volcanic formations found on Earth's surface (Elachi *et al.* 2005; Lopes *et al.* 2013; Schurmeier *et al.* 2023; Wall *et al.* 2009).

However, the origin of these features on Titan remains uncertain, rendering the existence of cryovolcanism on Titan a controversial topic (Lopes *et al.* 2013). Lack of fine-resolution imagery and conflicting morphological interpretations of Cassini images confound the quantification of the extent of cryovolcanism – whether past or currently active – on Titan. Sources such as Lopes *et al*. (2007), Lopes *et al.* (2013), Wall *et al.* (2009), among others, have interpreted several lobate flow-like features

on Titan to be cryovolcanic. The presence of cryovolcanic features would indicate that endogenic processes have occurred or are occurring on Titan.

Several promising lines of evidence indicate the possibility of cryovolcanic processes occurring in the past. Titan's atmosphere – for example – is enigmatic with its relatively substantial amount of volatile methane gas. Significant amounts of atmospheric methane are difficult to maintain on terrestrial moons and planets without a source of replenishment. Photolysis is a prime factor for depletion of atmospheric methane (Guzmán Marmolejo and Segura 2015; Toublanc 1995). Without replenishment, atmospheric methane at Titan should hypothetically be depleted on timescales of 10^7 to 10^8 years (Lunine and Atreya 2008; Schurmeier *et al.* 2023; Toublanc 1995; Yung *et al.* 1984) in direct contradiction with amounts observed today (Lunine and Atreya 2008; Moore and Pappalardo 2011). Thus, some process or processes must be replenishing atmospheric methane in order to maintain the atmosphere observed at Titan today (Lunine and Atreya 2008). Cryovolcanism is one proposed replenishment mechanism (Lopes *et al.* 2013; Lunine and Atreya 2008). This hypothesis was further bolstered by the discovery of the lobate features on Titan in 2005 (Elachi *et al.* 2005; Lopes *et al.* 2007; Wall *et al.* 2009). These features appear to mimic volcanic flow features, volcanic craters and pits, domes, and shields (Lopes *et al.* 2007; 2013; Wall *et al*. 2009).

However, Moore and Pappalardo (2011) analyzed Cassini imagery and arrived at the conclusion that the "cryovolcanic" features could be more reliably explained by weathering processes resulting from Titan's methanological cycle, and that Titan may not be endogenically active. Citing past inaccurate characterizations of lunar and Martian features as volcanic in origin that were later shown to be features generated by weathering, Moore and Pappalardo (2011) argue for increased caution before characterization of exciting geological features as cryovolcanic, lest they be characterized incorrectly.

As well, cryovolcanism may be a difficult process on Titan. Cryovolcanic activity would require the extrusion of subsurface liquids through fractures and sills in the icy crust, indicated to be some 50-100 km thick (Lunine 2017). Pure water is denser than the ice-I shell, and a solution of water and ammonia is even denser still (Lunine 2017; Soderblom *et al.* 2009). Thus, eruptions onto the surface may prove more difficult on Titan and may thus occur more infrequently than previously suggested by the volume of seemingly volcanically analogous features in Cassini image datasets. Additionally, other hypotheses exist to explain the large amounts of atmospheric methane that have not been depleted as expected.

Reevaluation of these analyses with newer, more finely resolved imagery has since overwritten some prior exogenic interpretations in favor of endogenic ones. Lopes *et al.* (2013)'s re-analysis of newer VIMS, SAR, and RADAR data from subsequent Cassini fly-bys in conjunction with topographic profiles (SARTopo, RADAR stereogrammetry) provides evidence in support of the presence of cryovolcanism in some regions previously "debunked" to be cryovolcanic, such as flows in Hotei and Tui Regiones, the pit of Sotra Patera, Doom and Erebor Montes, and several other lesser- studied features (Lopes *et al.* 2013).

While unconfirmed, it is still believed that cryovolcanism could have occurred or could be occurring to some extent on Titan (Lopes *et al.* 2013; Schurmeier *et al.* 2023). Until more detailed investigations of these features by surface-going spacecraft with in-situ data acquisition capabilities – such as Dragonfly – are achieved, it is likely the cryovolcanism debate will persist. Until cryovolcanism is all but ruled out completely for Titan, I consider potentially cryovolcanically generated features to be of astrobiological significance. Therefore, I include here a discussion of the astrobiological potential of cryovolcanic features should they exist, as hopefully these locations will one day be analyzed by Titan-going missions.

2.3.1 *Putative Cryovolcanic Features on Titan*

On Titan, cryomagmas could be generated in the subsurface ice or forced up and extruded from the global subsurface ocean through various mechanisms such as tidal forcing, radiogenic heating, or by another unknown process (Lorenz 1996). Cryomagmas and cryolavas on Titan are likely to consist of water-ammonia or water-ammonia-methanol mixes or slurries (Lopes *et al.* 2007; Lorenz 1996). If cryovolcanism is indeed an active or past process on Titan, it could create transient environments on the moon's surface or subsurface where liquid water, potentially in contact with complex organics, could exist. These environments offer a promising opportunity for the development of prebiotic chemistry.

In terms of the nature of cryovolcanic features on Titan, it is anticipated that eruptions would be minimally explosive due to the thick atmosphere and the difficulty of forcing cryomagmas through Titan's crust (Lorenz 1996). Instead, effusive eruptions with low topographic profiles and lobate or flow-like shapes are most likely (Lorenz 1996). (Lorenz 1996) posits that it may be difficult to form larger features typical of explosive volcanism, such as cones and stratovolcanoes, on Titan. However, it is plausible that such features could have formed during an earlier epoch in Titan's history.

Effusive cryovolcanism could be promising for putative organisms, as cryovolcanic flows could constitute large bodies of liquid water or slurries that would come into contact and potentially mix with tholins on the surface. Effusive flows would also take time to freeze through, potentially allowing enough time for the development of prebiotic chemistry. Furthermore, should lava lakes, such as Erta Ale in Ethiopia, exist on Titan, liquid water cryolavas could exist on even greater timescales, much like an impact melt pool. Schurmeier *et al.* (2023) suggest that certain labyrinth features seen on the surface of Titan could be the result of uplift caused by large, cryovolcanic laccoliths. The size of laccolith predicted by their modeling indicates that the emplaced cryomagmas may cool on large timescales (Schurmeier *et al.* 2023). Such an environment could be amenable to prebiotic or biotic chemistry if contact with surface organics or if biotic molecules from the subsurface sea below were incorporated into the cryomagmas comprising the laccoliths.

In general, however, surficial cryovolcanic features may not be as long-lived as impact crater pools (Davies *et al.* 2010). Yet, there could be potential for organisms to live in these environments if they used certain strategies for survival. Such strategies might include anti-freeze proteins, the use of extracellular polymeric substances (EPS) to stick to other organisms or material for stability, cryoprotection, and increased nutrient uptake (Decho and Gutierrez 2017; Zawierucha *et al.* 2017), and/or could use dormancy or cryobiosis if cryovolcanic eruptions were repeated and the surrounding environment remelted. As with any icy environment on Titan, any life in cryovolcanic features would need to be psychrophilic – organisms that can withstand or even thrive in extreme stresses associated with extremely cold environments (Feller and Gerday 2003). Terrestrial psychrophiles have developed adaptations for survival in extremely low temperatures, such as anti-freeze proteins and EPS that can locally decrease the freezing point of liquids (Feller and Gerday 2003). It would thus not be unexpected that Titanian life could develop similar survival mechanisms.

It is difficult to find sufficient analogs to study what kinds of life could develop in cryovolcanic environs. Such extreme temperatures combined with water-ammonia cryovolcanism do not exist on Earth. Thus, until there is further exploration of cryovolcanic environments on Titan and other icy moons, we must postulate about extreme life using thought experiments (Martin *et al.* 2020; McKay and Smith 2005; Sandström and Rahm 2020; Stevenson *et al.* 2015), and tangentially related environments such as glacial and Antarctic lakes, fumaroles, and other environments where psychrophiles can be found employing creative survival strategies. Such thought experiments and potentially useful analogs will be further discussed in the following sections, as they can be applied to Titanian impact crater melt pools as well.

Table 2.1 outlines putative cryovolcanic features discussed in the literature. It includes descriptions of the features and the likelihood that these features could be cryovolcanic in nature. Sources are included in the table description.

Table 2.1: Putative cryovolcanic features on Titan, descriptions of the features, and the likelihood that they are indeed of cryovolcanic origin (Barnes *et al.* 2006; Elachi *et al.* 2005; Hayes *et al.* 2008; Le Corre *et al.* 2009; Lopes *et al.* 2007; Lopes *et al.* 2012; Lopes *et al.* 2013; Moore and Howard 2010; Moore and Pappalardo 2011; Schurmeier *et al.* 2023; Soderblom *et al.* 2009; Stiles *et al.* 2009; Wall *et al.* 2009; Wood *et al.* 2010)

Feature Name	Feature Location	Morphology	Evidence For / Against Cryovolcanism	Likelihood of Cryovolcanic Origin
Anbus Labyrinthus & Other nearby labyrinth terrain features	130-177E, 32-43N	Labyrinth terrain with elevated topography. Features appear dome-shaped with radial channels, maze-like valleys, and plateaus.	Topography, faulting patterns, and scaling relations suggest that the labyrinth features are intrusive cryovolcanic emplacements.	Fair-High
Ara Fluctus	118.24W, 39.48N	Flow-like terrain, seemingly extending from a non-circular source	Non-circular depression indicates a non-impact origin, likely cryovolcanic (e.g., a caldera-like feature). SARTopo data does not yet exist for this region.	Fair
Doom Mons	40.4W, 14.7S	Tall, geographically high feature and rounded feature	Flow-like features appear to originate from a source on Doom Mons, indicating that the mountain could be a shield volcano or volcanic dome, SARTopo data supports a dome or shield volcano hypothesis.	High
Erebor Mons	36.2W, 5.0S	Large mountain feature (40 km in diameter, 1000 m in height), encompassed by lower elevation lobate features	Less thick lobate features appear to be flows emanating from a source on Erebor Mons. A lack of other fluvial features in the area and the apparent methane-dry region	High

Table 2.1: Putative cryovolcanic features on Titan, descriptions of the features, and the likelihood that they are indeed of cryovolcanic origin (Barnes *et al.* 2006; Elachi *et al.* 2005; Hayes *et al.* 2008; Le Corre *et al.* 2009; Lopes *et al.* 2007; Lopes *et al.* 2012; Lopes *et al.* 2013; Moore and Howard 2010; Moore and Pappalardo 2011; Schurmeier *et al.* 2023; Soderblom *et al.* 2009; Stiles *et al.* 2009; Wall *et al.* 2009; Wood *et al.* 2010)

			suggest that these flows are not fluvial in nature.	
Ganesa Macula	16 87.3W, 50.0N	Circular, 180 km diameter radar-dark site with radar-bright edges, flow-like features, and a central depression.	Ta flyby indicated flow-like and lobate features originating from an apparent dome, mimicking cryolava channels. Originally proposed to be a volcanic dome or shield volcano and has been compared to Venusian pancake domes. Central depression was originally interpreted to be a caldera or a volcanic crater. T23 flyby indicated depositional fans, likely fluvial or lacustrine. SARTopo analysis by Stiles et al. 2009 showed topography is not of a dome or shield.	Little to none
"Hot Cross Bun" Feature	203W, 38.5N	Dome-shaped, labyrinth terrain originally interpreted as a cryovolcanic laccolith	More heavily eroded than other features, which makes interpretation of composition and origin difficult. Uplifted terrain with similar spectra to the surrounding environment indicates emplacement of some material or some other deformative process.	Fair
Hotei Regio	78W, 26S	700 km wide region with many potentially geologically young features. Among these are a basin with tall (100-200 m thick) lobate flow-like features	Finer-resolution imagery lends evidence to sediment-filled valleys and potential paleosea structures. Topographic data revealed 100-200 m thick lobate features that are radar bright at 5 μm and are unlikely to be fluvial. A 20-30 km wide	Overall region: Fair Radar-bright flows and caldera-esque features: High

Table 2.1: Putative cryovolcanic features on Titan, descriptions of the features, and the likelihood that they are indeed of cryovolcanic origin (Barnes *et al.* 2006; Elachi *et al.* 2005; Hayes *et al.* 2008; Le Corre *et al.* 2009; Lopes *et al.* 2007; Lopes *et al.* 2012; Lopes *et al.* 2013; Moore and Howard 2010; Moore and Pappalardo 2011; Schurmeier *et al.* 2023; Soderblom *et al.* 2009; Stiles *et al.* 2009; Wall *et al.* 2009; Wood *et al.* 2010)

			feature appears to be surrounded by radial faulting, suggesting cryovolcanic activity. Dendritic channels in the south appear to originate in mountainous terrain surrounding the basin and are enriched in water ice.	
Leilah Fluctus	77.8W, 50.5N	Radar-bright, flow-like features stemming from fan-like structures and potential drainage sites	Flow-like features stem from fluvial channels and thus are likely fluvial in origin themselves	Little to none
Mohini Fluctus	38.5W, 11.8S	Region contains flow deposits and thick lobate features emanating from Doom Mons and another caldera-like feature.	Flow features seemingly originate from single, putative cryovolcanic sources (a potential dome or shield volcano and a potential caldera or volcanic pit), apparent thickness of lobate flows is more indicative of a cryovolcanic origin than a fluvial or depositional one.	High
Rohe Fluctus	37.8W, 47.3N	Flow-like features and channels originating from a circular, depressed source	The flow-like features are seemingly stemming from a single, non-fluvial, depressed source that is reminiscent of a caldera, making a fluvial origin less likely than a cryovolcanic one	Fair
Sotra Patera (Facula)	40.0W, 14.5S	Large, deep, ovoid depressions and flow-like features appearing to emanate from Doom Mons	Ovoid depressions are deep and non-circular and are unlikely to be of impact origin. Interpretations of the pits include collapse of a volcanic feature. A lack of fluvial channels in the	High

Table 2.1: Putative cryovolcanic features on Titan, descriptions of the features, and the likelihood that they are indeed of cryovolcanic origin (Barnes *et al.* 2006; Elachi *et al.* 2005; Hayes *et al.* 2008; Le Corre *et al.* 2009; Lopes *et al.* 2007; Lopes *et al.* 2012; Lopes *et al.* 2013; Moore and Howard 2010; Moore and Pappalardo 2011; Schurmeier *et al.* 2023; Soderblom *et al.* 2009; Stiles *et al.* 2009; Wall *et al.* 2009; Wood *et al.* 2010)

			area suggest flow-like features are not fluvial in nature.	
T3 SAR swath flow feature	70W, 20N	A flow-like feature bright in both SAR and VIMS data. The flow appears to emanate from a caldera-like feature. There are also several lobate features and two crater-like pits	Spectral data for the putative cryovolcanic features in this swath correlate well in both VIMS and SAR data, spectra of the features were analyzed and do not match that of pure water ice but possibly a slurry mixture of methane, CO_2, and water. Whether or not this mixture is indicative of a cryolavas is unknown	Fair
Tortola Facula	143.1W, 8.8N	30 km diameter region with a central, depressed, dark feature, a young, non-cratered surface, and flow-like features seemingly emanating from a single source.	The depressed dark feature was originally proposed to be a caldera and the source of the flow features was proposed to be a cryovolcanic dome. However, the radar-dark central feature appears caldera-like, but T43 flyby data indicated dunes and hummocks and no central caldera feature.	Little to none
Tui Regio	125W, 24S	150 km wide by 1500 km long region containing 5 μm radar-bright lobate features are interpreted to constitute a flow field emanating from a single, point source. Tui has a similar spectrum to Hotei Regio, which has also been interpreted to be potentially	Low-resolution imagery and low-quality SARTopo data make interpretation difficult. The lobate flows may actually be lower topographically than the surrounding area, and the morphology suggests possible paleoseas and paleochannels. However, the spectra of flow features exhibit no spectral signatures	Fair

Table 2.1: Putative cryovolcanic features on Titan, descriptions of the features, and the likelihood that they are indeed of cryovolcanic origin (Barnes *et al.* 2006; Elachi *et al.* 2005; Hayes *et al.* 2008; Le Corre *et al.* 2009; Lopes *et al.* 2007; Lopes *et al.* 2012; Lopes *et al.* 2013; Moore and Howard 2010; Moore and Pappalardo 2011; Schurmeier *et al.* 2023; Soderblom *et al.* 2009; Stiles *et al.* 2009; Wall *et al.* 2009; Wood *et al.* 2010)

		cryovolcanic. Tui Regio is geologically young.	indicative of evaporitic materials, meaning that they could potentially be cryovolcanic in origin.	
Western Xanadu	140W, 10S	Lobate and flow-like features along with circular pits and depressions	Heavy erosion in the area makes true cryovolcanic or erosional origins difficult to determine. The area is also seemingly intersected by young material, possibly indicating recent cryovolcanism. There is no SARTopo data for this region.	Fair
Winia Fluctus	30W, 45N	Radar-bright, flow-like features emanating from various smooth-looking, fanlike structures	Winia Fluctus may not be a flow feature, but instead a large depression. It is likely a fluvial or aeolian valley	Little to none

2.3.2 *Sites of Astrobiological Significance*

A promising site for putative lifeforms residing in cryovolcanic environments is Hotei Regio. Certain features in this region rank high in probability of cryovolcanic origin. Additionally, abnormal brightness in SAR data at 5-μm for flow-like features in the region suggests that there is likely ongoing geologic activity in the region (Soderblom et al. 2009). The exact nature of this ongoing geology remains unclear, but if cryovolcanic processes are occurring in the present or have occurred in the recent past, potential warm spots on the surface or in the near surface with liquid water pools or flows may still exist. This region is thus of high importance to analyze with future studies and surface-going missions.

A spectroscopically similar feature, also bright at 5-μm wavelengths, is Tui Regio. Tui Regio was originally interpreted to be a cryovolcanic flow field, supported at the time by spectral data and feature interpretation (Barnes et al. 2006). However, a lack of fine-resolution data makes definitive

interpretation difficult. Initial, yet lower quality SARTopo data suggests that lobate flow features in the region may actually be depressions (Moore and Howard 2010), but a lack of high-quality data and similar spectroscopy to features with high likelihood of cryovolcanic origins in Hotei Regio does not preclude potential cryovolcanism in Tui Regio as well. If the flow features are indeed elevated flows and not depressions, they could signal that a cryovolcanic source would be present in the area. Thus, Tui Regio represents another intriguing environment to further analyze. A lack of cryovolcanism in the region could limit potential astrobiological significance, but further in-situ analysis is needed to determine Tui Regio's true origins.

Sotra Patera is a deep pit-like depression located in a region assumed to be cryovolcanic in origin (Lopes et al. 2013). From Cassini data, Lopes et al. (2013) have interpreted Sotra Patera to be a cryovolcanic caldera. Doom Mons, located nearby, has been interpreted by Lopes et al. (2013) to be a volcanic shield or dome. Flow features referred to as Mohini Fluctus radiate from the mountain. These flow features appear to be a product of some processes occurring at or in Doom Mons, indicating that these could be cryovolcanic flows emanating from a cryomagmatic source that formed Doom Mons (Lopes et al. 2013). The entire region that encapsulates these features has been deemed to be highly likely to be cryovolcanic in origin and could be an exciting astrobiological target as well.

The labyrinth features described by Schurmeier et al. (2023) appear very amenable to astrobiological conditions if the laccolith origin is indeed correct. Long-lived cooling cryomagma pools that form the laccolith could provide a safe environment for prebiotic chemistry to occur. These locations could be of interest to future surface-going missions. However, there are two major caveats. First, the channels and valleys dissecting the putative cryovolcanic domes could make for difficult terrain to land a rotorcraft in or drive a rover into. Further, highly detailed studies of the area would be needed before considering a surface-going mission to the area. Second, there is no direct evidence for extrusive cryovolcanic features in the area. If life were to develop in the subsurface laccoliths, it is unlikely significant evidence of such life could be detected from the surface. For now, this area, while astrobiologically promising, is unlikely to be explored at the surface any time soon.

Other features such as features in Western Xanadu, the T3 SAR swath flow feature, Rohe Fluctus, and northern labyrinth terrain (Schurmeier et al. 2023), are less studied, but rank 'Fair' to 'High' in likelihood of cryovolcanic activity at some point in time. Thus, these features are also useful to study when considering the astrobiology of cryovolcanic features. However, further studies of these features are needed to determine their true astrobiological potential.

Overall, the above cryovolcanic locations determined to have fair to high likelihoods of cryovolcanic origins should be high on the list of priority sites for further exploration by both Dragonfly – following completion of its primary mission directives – and for future missions to Titan.

2.4 IMPACT CRATERS

The primary method for generating large volumes of liquid water on the surface of an icy satellite such as Titan is through an energetic impact event. The thick, Titanian atmosphere breaks up impactors less than 1-2 kilometers in size (Artemieva and Lunine 2003; Neish and Lorenz 2012), making small impact events infrequent, or even impossible. However, larger objects (>1 km in diameter) are relatively unaffected by the atmosphere and impact the surface in energetic impact events (Artemieva and Lunine 2003), producing craters such as Menrva, Selk, and Sinlap. A 1 km diameter impactor is estimated to create a ~ 10 km diameter crater on the surface of Titan (Artemieva and Lunine 2003). Artemieva and Lunine (2003) created 3D hydrodynamic simulations of a 2 km diameter impactor impacting Titan's crust and found that these large impact events can produce enough thermal energy to generate as much as 10^1 to 10^2 Gt of impact melt from Titan's water ice crust, much of which would fall back into the crater, creating an impact crater pool hundreds of meters thick (Artemieva and Lunine 2003; 2005). An icy lid would then form over top of the pool, and the water column below would freeze from the top down with increasing time since the event. Interestingly, Artemieva and Lunine (2003) found that the amount of liquid water in the simulated impact crater pools is sufficiently large that the water column would take between 10^2-10^3 years to completely freeze through – potentially long enough for prebiotic chemistry and/or abiogenesis to occur.

However, Artemieva and Lunine (2003)'s results reflect a 2 km diameter impactor hitting Titan's surface, which would result in crater with a diameter between 10-20 km (which is comparable in size to Ksa Crater, between 29-45 km in diameter, depending on the study), and an impact crater pool several hundred meters thick (Artemieva and Lunine 2003). Most observed craters on Titan exceed 10-20 km in diameter (Table 2.2), some such as Menrva, Forseti, and Selk greatly so. The impact events that created these larger craters would likely generate deeper pools with larger volumes of water. Consequently, these crater pools would take even longer to freeze completely.

For example, Artemieva and Lunine (2005) investigated the effects of larger impacts on Titan to determine if impact events could feed material into its atmosphere. Their findings revealed that a 10 km diameter impact should generate a crater approximately 150 km in diameter, which would

subsequently be filled with 10,000 km^3 of melt, creating a 5 km deep annular pool or moat. Artemieva and Lunine (2005) did not calculate freezing timescale for this scenario, but in a similar model creating a 150 km diameter impact crater, O'Brien et al. (2005) did and found that it would take 10^3 -10^4 years for a 150 km diameter impact crater pool to completely freeze through. Such a timescale is impressive, but there are even larger craters that exist on Titan that could boast even longer freezing timescales for their impact crater pools.

Consider Menrva, the largest known crater on Titan with a diameter of 425 km (Solomonidou et al. 2020). The magnitude of the impact event that formed Menrva suggests that an immense amount of liquid water melt would be generated from the event, and that such a large volume of water would freeze on a significantly longer timescale than a 20 km diameter crater. A Forseti-sized crater would take 10^3 to 10^4 years to freeze through according to O'Brien et al. (2005), or up to 10^6 years according to Thompson and Sagan (1992). Menrva's crater pool would likely remain partially liquid for much longer. Thus, Menrva and other large impact craters on Titan are compelling astrobiological targets.

Additionally, impact events facilitate the mixing of surface organics with liquid water, a crucial process to the emergence of prebiotic chemistry (Neish et al. 2018; O'Brien et al. 2005). Much of Titan is coated in complex organic sediments (tholins) that have rained out from the atmosphere (Sagan and Khare 1979). When an object impacts the surface of Titan, it kicks up the fine organics, causing them to become airborne (Artemieva and Lunine 2003). Some of these organic molecules will fall back down into the newly formed crater pool (Artemieva and Lunine 2003; 2005).

Additionally, if amino acids or other complex organics conducive to life already exist either within the impactor or on the surface of Titan, Pierazzo and Chyba (1999) predict that approximately 0.1% - 10% of these molecules could survive a large impact event on Titan and could be introduced into the crater pool. Thus, a vital mix of liquid water, complex organic molecules, and amino acids that would be conducive to prebiotic chemistry could form in an impact crater pool, further establishing large craters on Titan as prime targets for the search for life (O'Brien et al. 2005).

2.4.1 *Characteristics of the Crater Pool*

Depending on the depth of the central crater pool – or annular moat should a central peak form – it may possess euphotic, mesophotic, and aphotic zones. On Earth, these zones are used to denote the amount of light penetrating to each zone. The euphotic zone represents the depth from the surface of the liquid

body to where 1% of the surficial solar intensity reaches Lee et al. (2007). The mesophotic zone is the zone below that still contains light but is very dim. The aphotic zone spans the depth of the liquid column to which no light penetrates. These three zones of the water column exist in bodies of water on Earth and have varying implications for the diversity and richness of taxa of macrobial and microbial life present in each zone. The depths of these zones in impact crater pools would have implications for the kinds of life that could develop, the primary production processes they use, and the types of photopigments and biotic waste they could produce. These biological byproducts could serve as important biosignatures. This subject will be the primary focus of Chapter 3.

2.5 IMPACT CRATERS ACROSS TITAN

There are currently about 90 known putative impact crater features on the surface of Titan (Hedgepeth et al. 2020; Solomonidou et al. 2020). 38 of these are very likely true impact craters (Hedgepeth et al. 2020; Solomonidou et al. 2020). Low resolution data or lack of necessary data prevents the other 52 features from being unequivocally identified as impact craters. The relatively small number of craters on Titan as compared to other Saturnian icy moons is partially due to atmospheric shielding that breaks up smaller impactors and also due to active geologic processes such as viscous relaxation, crater slumping, aeolian erosion and/or infill, fluvial erosion, and others that erase or minimize the presence of impact craters over time (Hedgepeth et al. 2020; Neish et al. 2016; Solomonidou et al. 2020; Wood et al. 2010).

Table 2.2: Putative impact craters of Titan, their sizes, putative crater pool depths, and volumes. (Hedgepeth et al. 2020; Neish and Lorenz 2012; Neish et al. 2018; O'Brien et al. 2005; Solomonidou et al. 2020; Wood et al. 2010)

Name	Approximate Diameter (km)	Putative Crater Depth (m)	Putative Melt Volume (km^3)	Estimated Impact Crater Pool Depth (m)
Afekin	115	110-530	3860	372
Beag	26	-	30	56.5
Crater 1H	70	290	761	198
Crater 3H	67	-	660	187
Crater 4H	67	-	660	187
Crater 5H	63	-	540	173
Crater 6H	59	-	435	159

Table 2.2: Putative impact craters of Titan, their sizes, putative crater pool depths, and volumes. (Hedgepeth et al. 2020; Neish and Lorenz 2012; Neish et al. 2018; O'Brien et al. 2005; Solomonidou et al. 2020; Wood et al. 2010)

Crater 7H	55	-	346	146
Crater 8H	43	-	155	107
Crater 9H	40	-	122	97
Crater 11H	38	-	103	91
Crater 12H	34	-	72	79
Crater 13H	34	-	72	79
Crater 14H	29	-	43	65
Crater 15H	27	-	34	59
Crater 16H	27	-	34	59
Crater 18H	23	-	20	48
Crater 19H	23	-	20	48
Crater 20H	20	-	13	41
Crater 21H	17	-	7.4	42
Crater 22H	17	-	7.4	42
Crater 23H	16	-	6.1	30
Crater 24H	16	-	6.1	30
Crater 25H	16	-	6.1	30
Crater 26H	12	-	2.4	21
Crater 27H	11	-	1.8	19
Crater 28H	10	-	1.3	17
Crater 29H	10	-	1.3	17
Crater 30H	9	-	0.93	15
Crater 3NL	20	250	13	41
Crater 4NL	23	-	20	48
Crater 5NL	32	-	59	73
Crater 6NL	34	340	72	79
Crater 7NL	11	-	1.8	19
Crater 8NL	20	-	13	41
Crater 9NL	18	-	9	35
Crater 10NL	25	105-385	26	53
Crater 6W	5	-	0.14	7
Crater 7W	9	-	0.93	15

Table 2.2: Putative impact craters of Titan, their sizes, putative crater pool depths, and volumes. (Hedgepeth et al. 2020; Neish and Lorenz 2012; Neish et al. 2018; O'Brien et al. 2005; Solomonidou et al. 2020; Wood et al. 2010)

Crater 8W	4	-	0.07	6
Crater 9W	7	-	0.41	11
Crater 10W	5	-	0.14	7
Crater 11W	8	-	0.63	13
Crater 12W	3	-	0.03	4
Crater 13W	15	-	4.9	28
Crater 14W	7	-	0.41	11
Crater 15W	10	-	1.3	17
Crater 16W	9	-	0.93	15
Crater 17W	16	-	6.1	30
Crater 18W	14	-	3.9	25
Crater 19W	14	-	3.9	25
Crater 20W	17	-	7.4	33
Crater 21W	20	-	13	41
Crater 22W	25	-	26	53
Crater 23W	31	-	53	70
Crater 24W	41	300-340	132	100
Crater 25W	42	-	143	103
Crater 26W	70	-	761	198
Crater 29W	4	-	0.07	6
Crater 30W	4	-	0.07	6
Crater 31W	3	-	0.03	4
Crater 32W	8	-	0.63	13
Crater 33W	8	-	0.63	13
Crater 34W	9	-	0.93	15
Crater 35W	9	-	0.93	15
Crater 36W	9	-	0.93	15
Crater 37W	11	-	1.8	19
Crater 38W	13	-	3.0	23
Crater 39W	16	-	6.1	30
Crater 40W	21	-	15	43
Crater 41W	18	-	9.0	35

Table 2.2: Putative impact craters of Titan, their sizes, putative crater pool depths, and volumes. (Hedgepeth et al. 2020; Neish and Lorenz 2012; Neish et al. 2018; O'Brien et al. 2005; Solomonidou et al. 2020; Wood et al. 2010)

Crater 42W	23	-	20	48
Crater 43W	32	-	59	73
Crater 44W	29	-	43	65
Crater 45W	34	-	72	79
Crater 46W	29	-	43	65
Crater 47W	42	-	143	103
Crater 48W	10	-	1.3	17
Crater 49W	63	-	539	173
Forseti	140	140-405+	7345	477
Guabonito	70-90	-	1732	272-450
Hano	100	400	2444	311
Ksa	29-45	390-800	43	27-65
Menrva	425	430	277,315	1955
Momoy	40	690-805	122	97
Nath	68	-	693	191
Paxsi	130	-	5764	434
Selk	80	300-470	1178	185-234
Sinlap	80-90	70-700	1178	185-234
Soi	80-90	220-240	1178	185-234

Table 2.2 shows all 90 of the known and suspected impact craters on Titan, their approximate diameters (some numbers vary between sources), the proposed depths of the impact crater, the putative melt volumes, and the estimated depths of impact crater pools given the values in the table.

The proposed depths of the impact craters are from (Hedgepeth et al. 2020). Wakita et al. (2022) in particular note that previous calculations for Titanian impact crater depths did not take into account the different material characteristics of the proposed methane-clathrate and/or methane-saturated ice layer. They modeled impacts into the surface of Titan with these proposed layers and found that crater radii and depths could be different than predicted, either smaller or larger depending on the amount of methane present and the thickness of the layers (Wakita et al. 2022). Therefore, the depths currently recorded may or may not be accurate to the actual depths of these craters.

Putative melt volumes in Table 2.2 were calculated using Eq. 1 in O'Brien et al. (2005):

$$V_{melt} = 6.8x10^{-3}R_c^{3.27}$$

However, O'Brien et al. (2005) note that melt volumes for Titan may differ due to the difference in composition of Titan's crust and the flavor of impactor encountered by Titan. Thus, these values are loosely approximate and should not be taken as gospel. Regardless, the volume of liquid

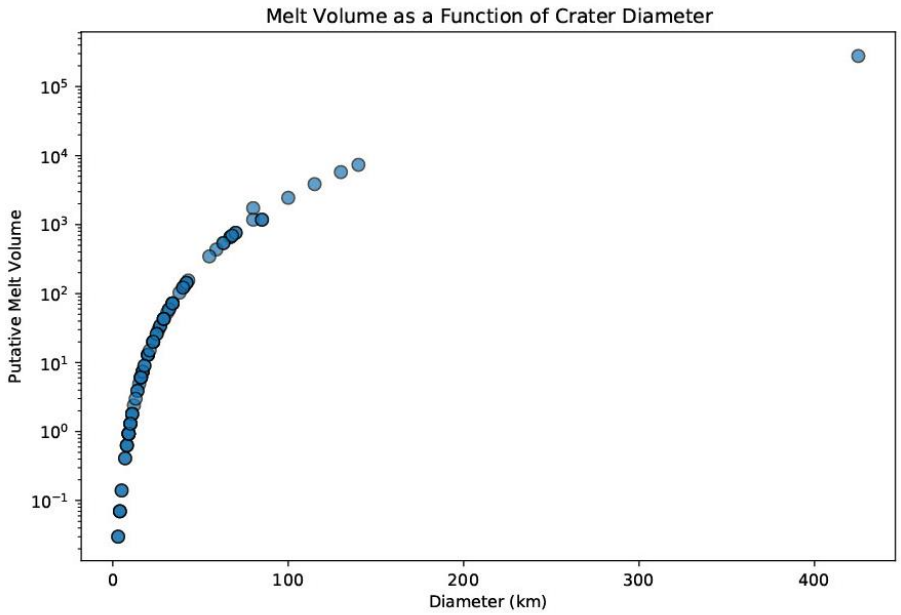

Figure 2.1: Putative impact crater pool melt volumes as a function of crater diameter.

melt increases with increasing impactor and resultant crater size (O'Brien et al. 2005, relationship shown in Figure 2.1) and thus adds evidence to the notion that there should exist larger pools in larger craters that should take longer to freeze.

Impact crater pool depths were calculated from the melt volumes and known diameters using a simple calculation of volume in a cylinder with the diameters and melt volumes of the above craters to roughly estimate putative depths. I use the volume for a cylinder instead of a hemisphere as craters tend not to be perfectly hemispheric in shape. Instead, they tend to take on a flattened bowl shape. A more accurate calculation of depth from diameter and volume for a crater would be a "partial hemisphere", in which the rounded part of the hemisphere is lobbed off, creating two flat surfaces enclosing the volume with different sized radii. However, even these depths will not be particularly accurate, as this method assumes the diameter of the melt pool will be the same as the diameter of the crater. This assumption will only be true if the melt fills the entire crater, which may not be accurate in many cases. As I do not know the slopes of the impact crater walls nor the precise shape of each crater, a rough approximation is made. Actual depths will likely differ, but an order of magnitude calculation

will suffice for this thesis. Ultimately, as we will see in Chapter 3, the exact crater pool depth is not needed. In the modeling done in Chapter 3, the most important data is in the trends. Putative depth values will likely change as more data is gleaned from Titan in the future.

While there are 90 published putative impact craters, only those craters 20 km in diameter or larger are promising locations where prebiotic chemistry may have developed in the past. Pools in craters less than 20 km in diameter would have likely frozen through completely too quickly for prebiotic chemistry or abiogenesis to have occurred or would have done so on a level too low to be detectable by future sampling missions. However, when viewing the distribution of crater sizes, shown in Figure 2.2, 40 craters are less than 20 km in diameter, and 50 are 20 km in diameter or larger. Thus, over 50% of the putative craters could have impact crater pools that could remain liquid to some degree for long enough for prebiotic chemistry or abiogenesis to occur, according to Artemieva and Lunine (2003). The large number of Titanian craters that could host impact crater pools on an astrobiologically amenable timescale is rather promising and renders impact craters worthy sites of exploration both by Dragonfly and future missions.

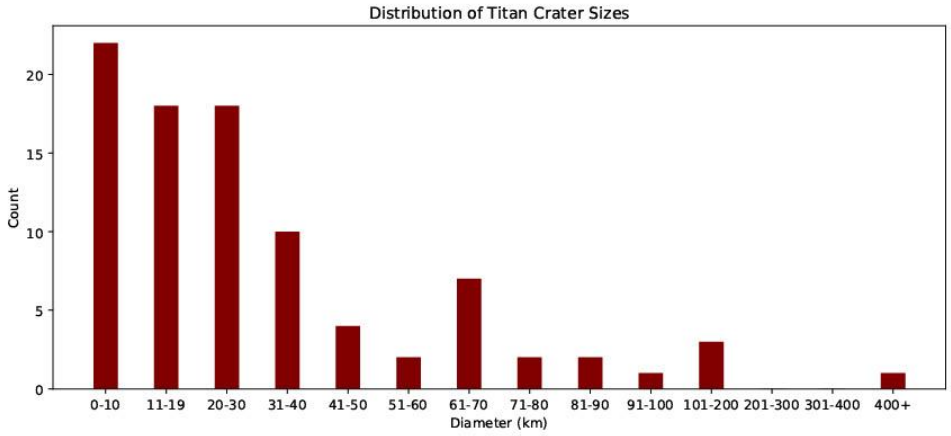

Figure 2.2: Distribution of crater sizes for Titan impact craters (Hedgepeth *et al.* 2020). More than 50% of the putative craters catalogued are above the 20 km diameter mark studied by Artemieva and Lunine (2003).

2.6 LIFE IN CRATER POOLS

Because the surficial solar insolation on Titan is much less than that on Earth, photosynthesis could be a secondary metabolic mechanism for Titanian LAWKI, with photoautotrophs comprising a smaller portion of a putative ecology. If we assume the baseline of photosynthetically active radiation (PAR)

needed for photosynthesis on Earth to be the same Titan, then a larger portion of a putative ecology of an impact crater pool would likely be chemotrophs or could use photosynthesis as an ancillary process in mixotrophic organisms. Alternatively, photosynthesis (or a similar process), should it develop on Titan, could develop to be more efficient in lower light conditions, and thus the various photic zones in the impact crater pool or in the liquid hydrocarbon lakes and seas could yield varying ratios of phototrophs and chemotrophs. This subject will be explored in further detail in Chapter 3.

In the mesophotic and dysphotic zones of the impact crater pool, where very little to no sunlight penetrates, energy for spontaneous assembly of cellular membranes or genetic material would likely need to come from thermal and chemical energy instead of sunlight, indicating chemoautotrophy as a more likely metabolic process for potential life in these zones. Some potential sources of energy for these organisms may be available in impact crater pools. Microorganisms in Lake Whillans in Antarctica, for example, generate energy for life processes via methane or ammonium oxidation (Fox 2018). Both methane and ammonia, along with other hydrocarbons, are available to microorganisms potentially developing in Titanian crater pools, allowing for life even in mesophotic or dysphotic waters. Methane or other carbon-containing molecules could be prime candidates for an electron donor in chemotrophic metabolic pathways (Fisk and Giovannoni 1999). Electron acceptors such as CO_2, H_2, O_2 or NH_3 (Fisk and Giovannoni 1999) could also be present in the crater pool. Should abiogenesis occur, it may not be unreasonable to expect methanotrophic life in the crater pool's water column.

2.6.1 *Biosignatures in Crater Pools*

As previously mentioned, understanding the biosignatures left by putative prebiotic chemistry or biota is just as significant as understanding what kind of life could exist in an environment. If photosynthesis or an analogous process developed in an impact crater pool, primary photopigments, such as chlorophyll-a (Chl-*a*) and chlorophyll-b (Chl-*b*) or accessory photopigments (esp. carotenoids, anthocyanins, and other low-light accessory photopigments) or some analog could be left behind in the frozen waters, provided they wouldn't degrade heavily over time. Products of methanogenesis or other metabolic processes should be studied in organisms on Earth, as similar signatures could be left behind if life used methanogenesis or another metabolic process that breaks down carbon-containing compounds for energy. Thus, it is important to study populations and ecologies of psychrophiles, methanogens, and other lifeforms that survive in environments that could be analogous to Titan impact

crater pools to keep an inventory of possible signatures to look for in future datasets from future missions.

2.7 TERRESTRIAL ANALOGS FOR CRYOVOLCANISM AND IMPACT CRATER POOLS

It is useful for astrobiologists exploring life on icy bodies to study what terrestrial analogs are available, either in the field or in the lab. While no environments on Earth are truly analogous to Titanian environments, there are some phenomenological terrestrial features which may prove insightful in imagining what LAWKI on Titan might look like and what life history strategies such organisms might employ.

For slow, top-down freezing impact pools, useful analogs most notably include over 400 isolated sub-glacial lakes in Antarctica (Fox 2018). With low light conditions, a small percentage of impact melt in the form of the euphotic zone may allow for the development of photosynthetic processes, meaning that the bulk of impact melt ecosystems could likely rely on chemoautotrophic processes. The same phenomenon occurs for microorganisms inhabiting sub-glacial lakes, which are often buried under tens to thousands of meters of ice, and thus are often devoid of solar radiation. These sub-glacial lake organisms are also isolated post-freezing from surrounding ecosystems and surficial nutrients, as organisms that might develop in Titanian crater pools would be.

While cryovolcanism does not occur on Earth, we can look to terrestrial volcanic systems to gather insights into the types of organisms that could develop in cryovolcanic features and regions on Titan. An intriguing analog for icy volcanic formations is the fumarolic caves on Mt. Erebus, Ross Island, Antarctica (Tebo et al. 2015). The fumarolic caves are largely dark and are sometimes completely devoid of sunlight. Subsurface cryomagmatic life would likely be chemoautotrophic, as it would not encounter sunlight until eruption. Thus, autotrophic processes utilizing chemical energy from warm, cryovolcanic processes or from methane, ammonia, or other hydrocarbons would be the necessary drivers for life processes in these environments.

For both icy-lidded crater pools and cryovolcanic formations and melt, cryoconite ecosystems – consortia of organisms living in icy environments such as glaciers – may be promising analogs for putative microbial communities that could have lived in those environments (Zawierucha et al. 2017). Cryoconite holes are a form of melt pool found in glaciers, frozen lakes, or sea ice (Fountain et al.

2004). They are filled with liquid water and covered by an icy lid (Fountain *et al.* 2004). Communities of microorganisms can be found in these holes (Fountain *et al.* 2004; Zawierucha *et al.* 2017). While cryoconite holes are smaller features and their formation mechanisms are different from impact crater pools, such extremophilic and psychrophilic communities and their associated biosignatures may be useful to study in anticipation of missions to icy moons like Titan that boast impact crater pools. As well, understanding the life-history strategies employed by these organisms and associated ecologies may help inform the strategies that could be used by Titanian LAWKI.

In laboratory environments, certain studies have already been conducted to begin to model the limits of survival of organisms in extremely cold and frozen environments, such as those that would be found in cryovolcanic features and impact crater pools. A fantastic example of such a quantitative

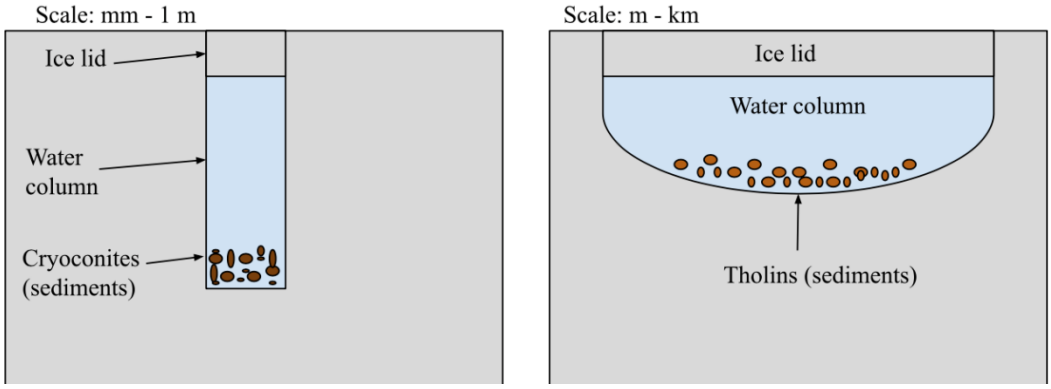

Figure 2.3: Comparison of cryoconite hole and impact crater pool environments (adapted from Fountain *et al.* (2004)).

experiment comes from Mudge *et al.* (2021), who tested the ability for *Colwellia psychrerythraea* to survive in varying levels of salinity and low temperatures in cold brines and observed the metabolic pathways employed by the microbes under different adverse conditions. The microbes produced 500+ protein biosignatures (Mudge *et al.* 2021). Proteins produced by the *C. psychrerythraea* strain tested allowed the team to determine the unique metabolic pathways employed by the organism to combat low nutrient, low temperature, and extreme saline conditions. Understanding proteomic biosignatures that could be produced by life on icy moons and planets can substantially inform any future detections of certain protein segments and what they might indicate about prebiotic or biotic chemistry that could be or have taken place on that body. Further studies like these are needed in anticipation of exploratory missions to icy bodies.

2.8 CONCLUSION

2.8.1 *Current Gaps and Future Directions*

Impact craters are promising and accessible astrobiological targets. As such, Selk Crater has already been selected as one of the prime mission targets for Dragonfly, with an initial landing in the sand sea surrounding the crater upon Dragonfly's arrival at Titan in the 2030s (Lorenz *et al.* 2021). Selk Crater provides an opportunity to access exposed water-ice deposits that likely interacted with the organic sediments of the Belet dune field, and thus is a prospective environment where prebiotic chemistry or abiogenesis could have been initiated and biosignatures could be found.

Selk is not the only sizeable impact crater that could offer a promising environment for prebiotic chemistry. 50 impact craters are 20 km in diameter or larger, with part of the impact crater pool column remaining liquid on timescales that could be promising to the development of prebiotic chemistry or abiogenesis, according to (Artemieva and Lunine 2003). Nine others are the size of Selk or larger. The very largest craters, Hano, Afekin, Paxsi, Forseti, and Menrva, could host some portion of liquid water for 10^4-10^6 years or much longer (Artemieva and Lunine 2005; O'Brien *et al.* 2005; Thompson and Sagan 1992), providing even more time for prebiotic chemistry to potentially occur. Menrva perhaps is one of the most promising sites for prebiotic chemistry, as such a large impact event could have potentially excavated the subsurface ocean, including ammonia and/or prebiotic or biotic molecules from the ocean into the water column. These craters are some of the most promising sites on the surface of Titan when searching for signs of or environments at one point amenable to potential life and should be at the top of the list of sites to explore on the surface. Dragonfly will take on the task of exploring Selk Crater and will determine whether Selk may have once hosted a habitable environment (Barnes *et al.* 2021; Lorenz *et al.* 2021). Future surface-going missions should heavily consider Menrva crater for astrobiological exploration.

Because life has yet to be found on any celestial body other than Earth, large and numerous gaps exist in our understanding of if and how life might develop elsewhere. Until missions such as Dragonfly are flown and gather data on the surface of Titan, much of trying to understand astrobiology on Titan is left to guesswork. However, there are several ways we can continue to further our understanding and refine predictions for where and what life might be on icy moons such as Titan. Modelling, analog work, and metagenomic studies can all help to inform our knowledge about life in extreme environments.

CHAPTER 3

ATTENUATION OF LIGHT AND THE EUPHOTIC ZONE IN TITAN LIQUIDS – IMPLICATIONS FOR LIFE

3.1 ABSTRACT

Titan's average surface temperature of 94 K (well below the freezing point of water) appears to render it inhospitable to terrestrial life as we know it. However, Titan remains an astrobiologically auspicious moon due to its liquid hydrocarbon meteorological cycle, a thick, protective atmosphere, a subsurface liquid water ocean, and global sand seas of complex organic compounds; any or all of which could provide the seeds for prebiotic chemistry. Additionally, three primary environments exist on the surface and in the near-surface of Titan that allow for the short – or long – term existence of liquids: liquid water impact crater pools, intrusive and extrusive cryovolcanic features, and liquid methane and ethane lakes and seas. Here, I investigate the astrobiological potential of transient liquid water impact crater pools and long-lived liquid hydrocarbon lakes and seas by determining the attenuation of incoming solar irradiance with depth in these liquids and determining how much and what wavelengths of solar energy may be available to putative prebiotic chemistries. Additionally, I model the euphotic zone in these liquid columns. I further determine the potential for the development of various types of biochemistries that could arise in these liquid environments and examine the potential biosignatures they could leave behind in these liquid or once-liquid environs.

3.2 INTRODUCTION

Liquid water is requisite for the development and persistence of life as we know it (LAWKI). However, the surface of Titan is 94 K, precluding the existence of liquid water on its surface save for in two environments; cryovolcanic features and impact crater pools created by large impact events. Cryovolcanism has been proposed but not confirmed to exist on Titan (Barnes *et al.* 2006; Lorenz 1996; Lopes *et al.* 2007; Lopes *et al.* 2012; Lopes *et al*. 2013; Schurmeier *et al.* 2023). Should cryovolcanism be an active process on Titan, liquid water slurries could be ejected onto the surface in large enough

quantities to stay semi-liquid for some time, or could pool in dikes, sills, or other intrusive features in the subsurface. These could represent possible environments where LAWKI could develop.

Large impact events have occurred numerous times on Titan. Titan's thick atmosphere provides protection against a large number of impactors. However, for objects with a diameter of 1 km or larger, the atmosphere has limited effect, resulting in violent impacts into the surface (Artemieva and Lunine 2003). In such a powerful impact event, large amounts of liquid water melt are generated from the icy crust of Titan (Artemieva and Lunine 2003; 2005). A large percentage of this melt will settle into the newly formed crater as a melt pool or pond before being slowly frozen through (Artemieva and Lunine 2003; 2005). As on Earth, the lower density of water ice compared to liquid water will cause the pool to freeze from the top down, eventually freezing the entire water column solid. The time over which freezing occurs is dependent on a number of factors, including inherent characteristics of the impactor (diameter, mass, shape, speed of entry, angle of entry), characteristics of the surface at that location, the size and depth of crater created, amount of liquid water melt generated, and the fraction of water that settles back into the crater after the impact event (i.e., the fraction of water that was not vaporized or lost from the crater as impact ejecta). It is difficult to predict and model all these factors.

However, Artemieva and Lunine (2003) modeled impacts of a 2 km diameter impactor into the surface of Titan (creating a 10-20 km diameter impact crater) and found that it would take 10^2 to 10^4 years for the impact crater pool to freeze completely, a timescale potentially amenable to the development of prebiotic chemistry or abiogenesis (Artemieva and Lunine 2003; 2005; Thompson and Sagan 1992). O'Brien *et al.* (2005) and Thompson and Sagan (1992) modeled an impact event on Titan that would generate an approximately 150 km diameter crater and found that a crater pool for such a crater would freeze in a maximum of 10^4 and 10^6 years, respectively. As seen in Chapter 2, many craters exist on Titan with diameters of 10-20 km or greater (Hedgepeth *et al.* 2020), with Menrva crater dwarfing the rest of the crater population with a diameter of around 420 km. The freezing timescale of the crater pool at Menrva should be much greater than that of both the modeled 10-20 km diameter and 150 km diameter craters. Additionally, the impactor that created Menrva could have excavated the subsurface ocean, making Menrva very promising for putative life.

LAWKI requires liquid water and several key elements (carbon, hydrogen, nitrogen, oxygen, phosphorus, and sulfur – or CHNOPS) to form the basis of all essential organic molecules it comprises and uses. CHNOPS elements appear to be present on Titan in varying amounts in the form of complex organic molecules (although oxygen is severely lacking). These molecules form in Titan's upper atmosphere and rainout onto the surface as complex organic "sediments" (Coates *et al.* 2007; Sagan and Khare 1979; Thompson and Sagan 1992). Not only do these complex organic sediments form

magnificent equatorial dunes (Radebaugh *et al.* 2008), they may also become entrained in the liquid water melt ponds produced by large impact events (Artemieva and Lunine 2003), providing the seeds for prebiotic chemistry or abiogenesis in these environments. Thus, in this paper, I explore the attenuation of photosynthetically available solar radiation with depth in Titan impact crater pools to determine what, if any, amount of solar radiation may be available to be used by putative life in these environments.

Additionally, Titan is singular in the solar system in that it possesses stable bodies of liquid hydrocarbons (mainly liquid methane and ethane, in varying amounts) on its surface (Elachi *et al.* 2005; Lunine and Atreya 2008; Stofan *et al.* 2007). The conventional wisdom in astrobiology is to, "Follow the [liquid] water", as LAWKI requires liquid water as a solvent both to assemble and to persist. However, recent work has explored the possibility of methane-based life forms or cells that could assemble and persist in the liquid hydrocarbon lakes and seas of Titan (McKay and Smith 2005; Sandström and Rahm 2020; Stevenson *et al.* 2015). While opinions vary if hydrocarbon-based life could assemble at Titan temperatures, the possibility still exists. We would thus be remiss not to explore the attenuation of light with depth in hydrocarbon lakes and seas that grace Titan's poles as well as in crater pools. In consideration of the idea that alternate-solvent life might be possible, the various energies available to such organisms on Titan should be investigated.

3.2.1 *Photic Zones and Their Significance*

Photic zones are oceanographic and limnological designations of zones of various depth in the vertical water column. Each of these zones is defined by the percentage of surficial solar illumination that remains after attenuation by the water column in each zone (Lee *et al.* 2007). Light hitting the surface of a body of water is both scattered and absorbed by scatterers and absorbers in the water column, in addition to the water molecules themselves (Pegau *et al.* 1997). The amount of attenuation is dependent upon both the amount of each constituent as well as each constituent's inherent optical properties. In liquid water and water ice, red light is absorbed readily and attenuates fastest in the visible spectrum. Blue light, on the other hand, is not as readily absorbed and penetrates to the greatest depths of all the colors of the visible spectrum. The wavelengths of light and the depths to which they penetrate have implications for photosynthesis, the types of photopigments used by life at various depths, and the organisms and ecosystems that can exist at those depths. Thus, it is important to delineate photic zones to best describe the amount of light and thus the kinds of organisms that exist there.

There are three main photic zones that are commonly used in the literature, although the names and subzones belonging to each main zone vary across literature and subfields: the photic/euphotic zone, mesophotic zone, and dysphotic/aphotic zone. Here, I will be primarily concerned with the photic zone, as the mesophotic and dysphotic zone contain little to no solar radiation. The photic/euphotic zone is the uppermost layer of the water column, extending from the surface of the water column to the depth at which only 1% of the surficial photosynthetically available radiation (PAR) penetrates (Lee *et al.* 2007). The majority of photosynthesis in the water column occurs in the euphotic zone, and it is home to many taxa of diatoms, algae (both microscopic and macroscopic), photosynthetic bacteria, and various other forms of photoautotrophic life and the macrobes that depend upon (or consume) them. These photoautotrophs form the basis of the food-energy chain of marine ecologies, and significant effects on microscopic phototrophs can result in a trophic cascade that has far reaching consequences for the marine food chain.

For terrestrial oceans, the boundary between the euphotic and mesophotic zones typically occurs 10s to 100s m deep. It should be noted that the depth of the euphotic zone is not a constant value temporally or spatially; it can vary greatly with weather, waviness, and the presence or absence of organisms such as phytoplankton, zooplankton, higher plants and nekton, and "pollutants" such as sediments, detritus, products of organisms, plants, and other objects in the column that can scatter or absorb light. However, we can look at general trends of light attenuation and euphotic zone depths under varying conditions and draw inferences about how friendly a body of water (or liquid hydrocarbons) may be to photosynthetic organisms in general.

Developing hypotheses regarding the possible types of primary producer that could exist in impact crater pools is an important first step in understanding the resulting materials and potential biosignatures such life may generate. The flavor of primary production used by a group or ecology of microbes also lays the foundation for the specific biogeochemical cycles they may participate in, as well as the amount of biomass they could produce. These factors can determine the various biosignatures putative life may leave behind.

In defining the euphotic zone in Titan liquids, we must make a few tweaks to the terrestrial definition. First, on Earth, the euphotic zone spans the depths of the liquid column in which between 1% and 100% of the surficial solar intensity penetrates (Lee *et al.* 2007). Below the euphotic zone boundary, less than 1% of the surficial solar intensity remains, and photosynthesis is much less likely to occur or will occur in low amounts. However, the average surficial solar intensity at Earth's surface

is much higher than that on Titan's surface (as solar illumination decreases with distance as $\frac{1}{r^2}$ and Titan's thick atmosphere further absorbs and scatters light).

On Earth, the average solar irradiance at the surface is on the order of 100 W/m^2, with the irradiance that reaches the surface being dependent on cloud cover and the presence or lack of atmospheric pollution (Ohmura 2006). However, on Titan, the average top of atmosphere solar intensity is on the order of 10 W/m^2, with the thick atmosphere further attenuating light by another 1-10% (Hendrix and Yung 2017). To find a reasonable average solar irradiance in the visible light range, I integrated radiance values taken near the surface of Titan by the Huygens ULVS instrument (Tomasko *et al.* 2005) over the 480-800 nm range and found an average surface irradiance of 0.336 W/m^2.

Given that the euphotic zone boundary in a water column on Earth occurs at 1% of the surface intensity, under ideal conditions, this boundary would occur at a solar irradiance level of around 1-1.5 W/m^2. Under less ideal conditions the euphotic zone may occur at lower intensities, but in general such irradiances at the euphotic zone boundary are similar to or greater than the surface solar irradiance at Titan, before light has even been attenuated in media.

Thus, just looking for the depth at which 1% of the surface intensity penetrates on Titan is likely insufficient to accurately describe a euphotic zone on Titan. Such low light levels might initially spell bad news for the potential for the development of photosynthesis or an analogous process on Titan. However, I will use three different thresholds to define the euphotic zone on Titan, operating under the assumption that, should photosynthesis or an analogous process develop on Titan, it would be more efficient than photosynthesis on Earth to better harvest the dim light on Titan. Such an assumption is not completely unrealistic, as photosynthesizing bacteria and phytoplankton have been found surviving in low light conditions (Beatty *et al.* 2005; Tanabe *et al.* 2007). An operational taxonomic unit (OTU; the microbial equivalent of a species) of green-sulfur bacteria has even been found on Earth photosynthesizing using geothermal light emitted from a hydrothermal vent as an auxiliary energy source (Beatty *et al.* 2005). The photon flux at and around these smokers was estimated to be between 10^4 and 10^{11} photons cm^{-2} s^{-1} sr^{-1} (3.63e^{-11} to 3.63e^{-4} W/m^2, (Langhans *et al.* 1997; Beatty *et al.* 2005)), a very low level of light.

It is difficult to say with certainty what the bare minimum level of light is needed for photosynthesis to occur, given that the amount needed varies by organism, the photopigments they use, and whether the organism can supplement light energy with other forms of metabolism such as chemotrophy.

Thus, operating under the assumption that photosynthesis or an analogous process is not impossible on Titan, I seek to evaluate the attenuation of light in liquid water impact crater pools and liquid hydrocarbon bodies in order to evaluate how much light is available to putative life at these sites.

3.3 METHODS

I conduct my analysis with a simplified, iterative, 1-D and multilayer Beer-Bouguer-Lambert law for light attenuation with depth in i.) Crater pool columns of liquid water and water ice and ii.) liquid hydrocarbon lakes and seas, (here, taken to be primarily composed of methane). In both environments, I model the attenuation of light in both "pure" materials (aka free of impurities) and these materials with impurities. The impurities tested in the icy lid of the impact crater pools are air bubbles and tholins, both of which would likely be found in this layer. The primary impurity investigated in the water layer of the impact crater pool column and the liquid hydrocarbon lakes and seas will be suspended tholin sediments.

The presence of impurities (and perhaps others) is highly likely in these environments and can greatly decrease transmission of solar irradiance through ice and liquids. Impurities serve as the primary source for attenuation of solar irradiance with depth in ice, water, and liquid methane. This attenuation can often be seen on Earth, where very bubbly ice transmits very little to no light through to the water or ground below due to increased scattering off interfaces between two different indices of refraction (ice and air). Similarly, dirty ice or water transmits less light due to absorption of light by particulates on or in the ice or water (Xu *et al.* 2012). Pure ice, on the other hand, can transmit light to great depths as there is little inherent scattering and absorption in the ice to reduce the transmission of light (Cooper *et al.* 2021; Warren 2019).

From model results, I investigate the depths of the primary euphotic zone in both impact crater pools and liquid hydrocarbon bodies. Additionally, I investigate patterns of light attenuation per wavelength with depth of visible light for several ratios of icy-lid to liquid water in the crater pool starting with a purely water impact crater pool – representing the immediate aftermath of a high-energy impact event into Titan's surface – then investigate the changes in light attenuation when ratios are 1:99, 10:90, 25:75, 50:50, 75:25, 90:10, 99:1, and when the pool freezes through completely.

The icy lid is first represented as "pure", bubble-free ice with optical properties described by a combination of attenuation coefficients from (Cooper *et al.* 2021; Grenfell and Perovich 1981; Warren

and Brandt 2008) (Figure 3.3, Table 1 in *Appendix 1*). Where data was not available, values were linearly interpolated from known values.

Then, various number densities and radii of bubbles and/or complex organics within the ice are then added to test the change in attenuation with the addition of these impurities. As it is not precisely known the amount of each that could be contained within icy lids of impact crater pools, reasonable endmember and average values from literature (Perovich and Gow 1996) are assumed. I do the same for liquid water and hydrocarbon columns. For euphotic zone depths in liquid hydrocarbon bodies, this equation is reduced to a more simplified problem with no icy lid and with the optical properties of water being replaced with those for pure methane.

For the intensity of light at the surface of Titan (and thus the surface of the icy lid), I use spectral data for the solar intensity arriving at Titan by wavelength from Huygens' Upward-Looking Visible Spectrometer (ULVS; from Tomasko *et al.* (2005), shown in Figure 3.1); this is the amount of solar irradiance that reaches the surface of Titan through its thick, extended atmosphere. I use wavelengths of λ = 480-800 nm throughout this paper, as these are the wavelengths captured by Huygens that are most photosynthetically relevant. UV light is not included in this study despite also being used in photosynthetic processes as it is nearly completely attenuated by Titan's atmosphere.

3.3.1 *Model*

To begin, I use the Beer-Bouguer-Lambert Law, expressed as:

$$I_z = I_o e^{-kz} \tag{3.1}$$

where I_o represents light intensity at the surface of the material and z represents depth in the material. k is the attenuation coefficient, which traditionally is represented by the linear sum:

$$k = k_{absorption} + k_{scattering} \tag{3.2}$$

Or, alternatively:

$$k = \kappa + \sigma \tag{3.3}$$

Where κ and σ are the same as $k_{absorption}$ and $k_{scattering}$ respectively.

I alter this definition of the attenuation coefficient to match the works of Grenfell (1983) and Grenfell (1991); both for more precision in my multilayered approach and to allow for the adjustment

of the number densities and volume fraction of each absorbing and scattering constituent in both ice and liquid layers. As the exact composition nor the number of scatterers and/or absorbers in impact crater pool icy lids and liquid hydrocarbon bodies on Titan are not known, nor is it known how these might vary between different locations across Titan, the introduction of a range of possible values into the model is necessary. From Grenfell (1983), I adopt the definition:

$$\frac{d\tau}{dz} = -(\kappa + \sigma) \tag{3.4}$$

The Beer-Bouguer-Lambert Law can therefore be expressed as:

$$I_z = I_o e^{\tau} = I_o e^{-\sum_j (\kappa_j + \sigma_j) dz} \tag{3.5}$$

Where τ is the optical density of the layer/material and is summed as I take the calculation of each layer of ice and water individually. $\sum_j \kappa_j$ is the total absorption coefficient of all the constituents in a layer. $\sum_j \sigma_j$ is the total scattering coefficient of all the constituents in a layer. I adopt Grenfell (1991)'s interpretation of the absorption coefficient:

$$\kappa_{j,layer} = \sum_i k_{abs,i} V_i \tag{3.6}$$

Where the subscript i denotes each absorbing constituent in the layer, and V_i represents the volume fraction of each material in the layer.

σ, on the other hand, is the volume scattering coefficient, which I also adopt from Grenfell (1991):

$$\sigma_{j,layer} = \sum_i \int_{r_{i,min}}^{ri,max} Q_{i,scat} \pi {r_i}^2 N_i(r) dr \tag{3.7}$$

Here, σ is a sum over all scattering constituents, r_i is the scattering radius of each constituent i, Q_i is the scattering efficiency of each constituent, and $N_i(r)$ is the number size distribution of each constituent.

For both bubbles and tholins, I assume a scattering coefficient of $Q = 1$ following geometric optics, and I assume those bubbles and tholin particles that will contribute to scattering will have an effective scattering radius of $r_{eff} \gg \lambda$ (Hedman 2023).

I also integrate σ over a range of possible values of r to arrive at an equation including the average of possible radii and number distributions:

$$\sigma_i = \pi \overline{r_{i,eff}^2} \eta_i \tag{3.8}$$

Where $\overline{r_{i,eff}}$ is the average possible scattering radius for the constituent and η_i is the average number density for the constituent (Hedman 2023).

I arrive at the final equation for each layer:

$$I_z = I_o e^{-(\sum_i k_i V_i + \sum_i \pi Q_i \overline{r_{i,eff}^2} \eta_i} \tag{3.9}$$

In which I assess the following values for conditions on Titan in impact crater pools and the liquid hydrocarbon lakes and seas.

Table 3.1: Case scenarios for model runs.

Run	Water	Ice Lid	Bubbles in Ice Lid	Tholins in Ice Lid	Tholins in Water Column	Methane	Tholins in Methane
Case 1	✓	✕	✕	✕	✕	✕	✕
Case 2	✕	✓	✕	✕	✕	✕	✕
Case 3	✓	✓	✕	✕	✕	✕	✕
Case 4	✓	✓	✓	✕	✕	✕	✕
Case 5	✓	✓	✕	✓	✕	✕	✕
Case 6	✕	✕	✕	✕	✕	✓	✕
Case 7	✕	✕	✕	✕	✕	✓	✓

3.3.2 *Parameters*

I_o – For layer 1, I_o is represented by values of radiance at Titan's surface from Tomasko *et al.* (2005), Figure 3.1, and the integration irradiance for these values. For consecutive layers, (i.e., a layer of water below a layer of ice in an impact crater pool), I_o is the resultant I_z calculated for the layer directly above.

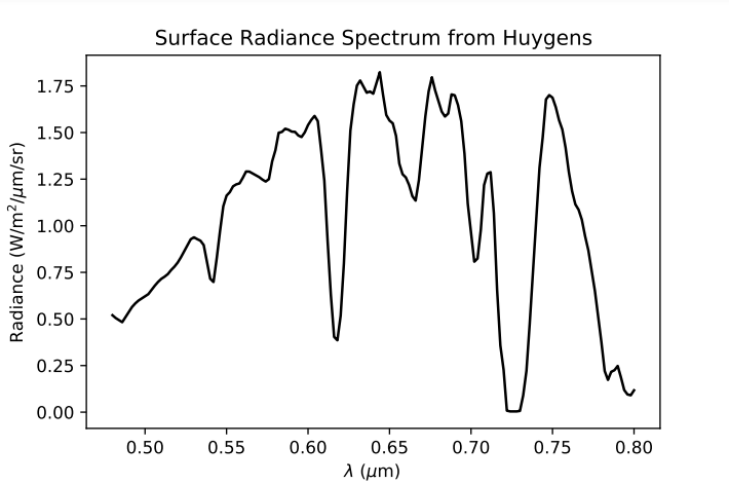

Figure 3.1: The surface spectrum of visible light (in this paper taken to be 400-800 nm) as seen from Huygens' Upward-Looking Visible Spectrometer (ULVS) instrument. This data was taken during the Huygens descent at 5 km above the surface. Wavelengths below 480 nm are not shown here as this light is preferentially scattered by the Titanian atmosphere, and little reaches the spacecraft or the surface. (Adapted from Tomasko *et al.* 2005, Figure 3.17c)

ATTENUATION COEFFICIENTS – Because theoretical absorption and scattering coefficients can be mathematically tricky to derive and reliable measurements for attenuation coefficients of different materials often already exist in the literature, I adapt existing measurements of absorption coefficients for water, ice, tholins, and liquid methane. Where certain values for the coefficients do not exist in the literature, I linearly interpolate from known values. For scattering coefficients, I use those for ice and water that already exist in the literature, but for bubbles and tholins, I use Equation 3.8. The complete list of the coefficients used will be tabulated in the Appendices. Where indices of refraction were presented in the literature, absorption coefficients were calculated from the equation $\kappa = \frac{4\pi b}{\lambda}$ where b is the imaginary part of the complex index of refraction of the material.

- *Water* – Absorption and scattering coefficients for pure water are taken from Buiteveld *et al.* (1994) (shown in Figure 3.2 and Table 1 in *Appendix 1*). Pure water values were chosen as pollutants such as tholins would later be added into the model.

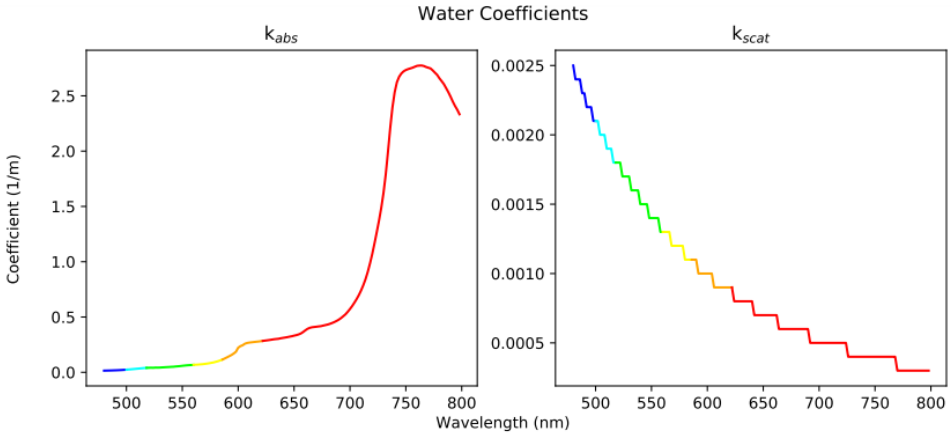

Figure 3.2: Attenuation coefficients of pure, liquid water, adapted from Buiteveld *et al.* (1994).

- *Ice* – Absorption coefficients of ice are a conglomeration of values recorded by Cooper *et al.* (2021), Grenfell and Perovich (1981), and Warren and Brandt (2008). Each study measured different wavelengths, so multiple were needed to cover the entire 480-800 nm waveband. Values for pure ice were used when possible. Cooper *et al.* (2021) measured areas with clean ice, but ultimately those measurements will have larger scattering coefficients associated with them as the ice was not generated in a lab where bubble growth can be largely controlled for. Thus, for ice, I do not include the scattering coefficients in the attenuation coefficients, as doing so and accounting for bubbles in the model would double count the effect of bubbles in the ice. For pure water and ice, scattering is minimal in the visible spectrum (Warren 2019). Small Rayleigh scattering effects in ice are usually caused by birefringence between crystals or small defects in the ice structure (Warren 2019). In reality, the scattering coefficients of ice in the visible spectrum, like those of water, are likely orders of magnitudes smaller than the absorption coefficient, and thus have little effect on attenuation at the tested scales.

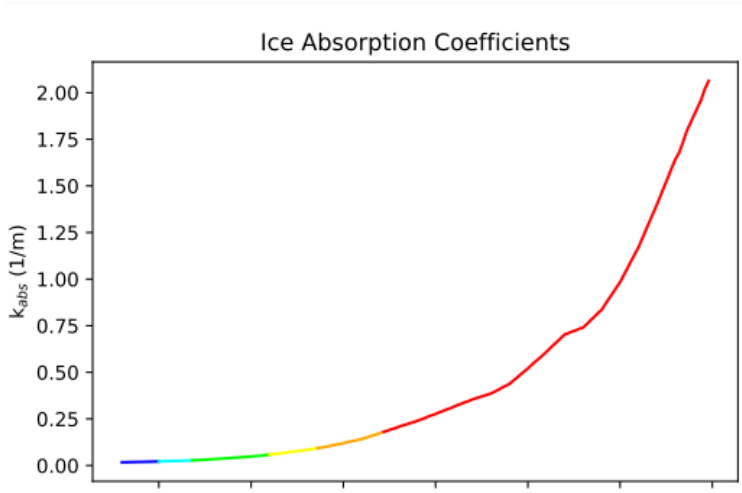

Figure 3.3: Absorption coefficients of water ice, from Cooper *et al.* (2021), Grenfell and Perovich (1981), and Warren and Brandt (2008).

- *Methane* – Methane absorption coefficients are from Martonchik and Orton (1994). Martonchik and Orton (1994) measured the complex index of refraction of liquid methane at 90 K for a range of wavelengths. Scattering coefficients were not measured and difficult to find in the literature. Thus, I assume that, like for pure water and pure ice, scattering by the liquid methane itself is minmal, and I use the absorption coefficients as the attenuation coefficients for the liquid methane.

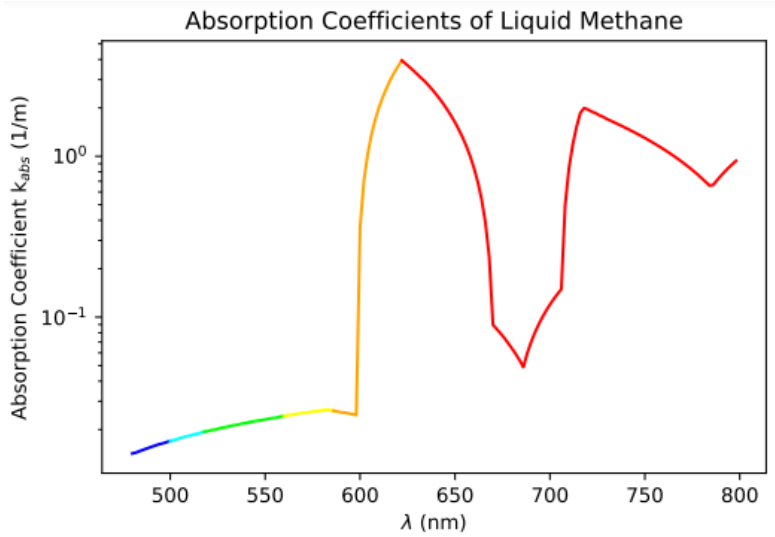

Figure 3.4: Absorption coefficients of pure, liquid methane at 90 K, from Martonchik and Orton (1994).

- *Ethane* – Optical constants for ethane were sought in order to determine if there would be differences in attenuation between methane, ethane, and varying mixtures of the two. However, the literature on optical constants for ethane in the visible wavelengths – including liquid ethane

– is surprisingly lacking. Refractive indices at sub-60 K temperatures have been measured for ethane and ethylene ice mixtures (Hudson *et al.* 2014; Satorre *et al.* 2017). However, both papers make these measurements at a single wavelength. These measurements cannot be extrapolated to the entire visible spectrum for ethane ice or liquid ethane at 90 K. Measurements of the indices of refraction and absorption properties of ethane ice have been made in a broader waveband in the infrared (Pearl *et al.* 1991), but again, this is not sufficient for determining the attenuation coefficients in the visible spectrum. Thus, I concede to representing the hydrocarbon lakes and seas of Titan as solely composed of methane. This representation should theoretically be an appropriate assumption for most Titanian seas, barring Kraken Mare.

- *Tholins* – Absorption coefficients for tholins were taken from Vuitton *et al.* (2009). Scattering coefficients for tholins were calculated using Equation 3.8 and vary as scattering radii and average effective number densities are varied in the model.

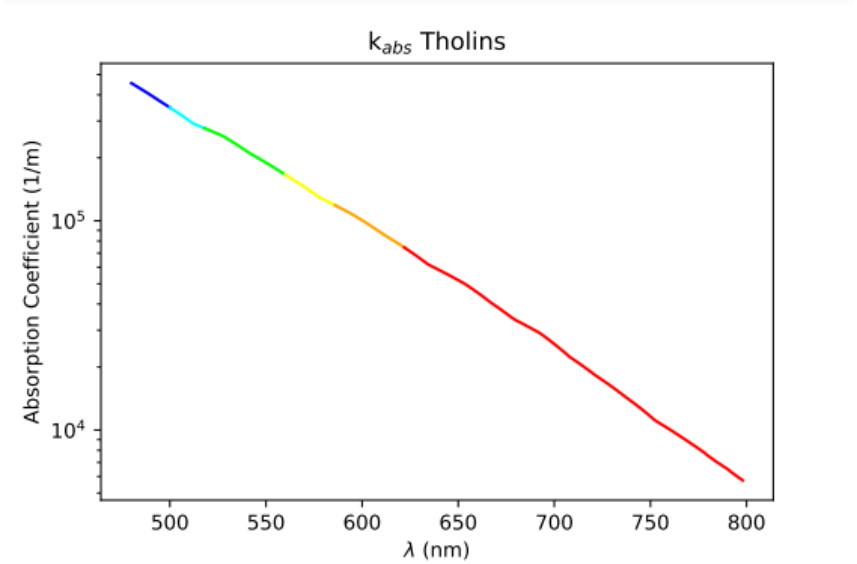

Figure 3.5: Absorption coefficients of tholins, from Vuitton *et al.* (2009).

- *Air bubbles* – Absorption by air trapped inside air bubbles is assumed to be zero, as "pure air" should not in and of itself scatter or absorb light. Scattering as an effect of inclusions of bubbles of various sizes and number densities are calculated from Equation 3.8.

EFFECTIVE SCATTERING RADII AND NUMBER DENSITIES – Values used for effective scattering radii, volume fractions, and number densities for tholins and air bubbles in various media are listed is Tables 3.2, 3.3, and 3.4.

Table 3.2: Values of model parameters for attenuation in the crater pool when bubbles are introduced to the icy lid.

Run	V_{ice}	V_{air}	$r_{eff,bub}$ (mm)	η_{bub} (bubbles/m^3)
Case 4a	0.9	-	1	10^3
Case 4b	0.9	-	1	10^5
Case 4c	0.9	-	0.5	10^3
Case 4d	0.9	-	4	10^3

Table 3.3: Values of model parameters for attenuation in the crater pool when tholins are introduced to the icy lid.

Run	V_{ice}	V_{thol}	$r_{eff,thol}$ (mm)	η_{thol} (tholins/m^3)
Case 5a	0.99+	10^{-6}	1	10^3
Case 5b	0.99+	10^{-7}	1	10^3
Case 5c	0.99+	10^{-8}	1	10^3
Case 5d	0.99+	10^{-8}	4	10^3
Case 5e	0.99+	10^{-8}	1	10^4
Case 5f	0.99+	10^{-8}	1	10^5

Table 3.4: Values of model parameters for attenuation of light in a liquid methane body with suspended tholins in the methane column.

Run	$V_{methane}$	V_{thol}	$r_{eff,thol}$ (mm)	η_{thol} (tholins/m^3)
Case 7a	0.99+	10^{-6}	1	10^3
Case 7b	0.99+	10^{-7}	1	10^3
Case 7c	0.99+	10^{-8}	4	10^3
Case 7d	0.99+	10^{-8}	1	10^3
Case 7e	0.99+	10^{-8}	1	10^4
Case 7f	0.99+	10^{-8}	1	10^5

DEPTHS – For a pool in an 80 km diameter Selk-sized crater with 1178 km^3 of liquid melt, z is calculated to be 234 m, representing the depth of the impact crater pool when modeling the crater as a flattened cylinder. As mentioned in Chapter 2, craters are not perfect hemispheres and are often more accurately shaped like a flattened bowl. Ultimately, for this study, the trends of attenuation of light are more important than the shape of the crater. For the hydrocarbon lakes and seas, I let z approach infinity as the exact depths of the lakes and seas on Titan are not known.

3.4 RESULTS

3.4.1 *Impact Crater Pool – Pure Water Endmember*

I begin with a check for the attenuation of light in an impact crater pool filled with pure water and that has no icy lid, representing the crater pool immediately after formation but with no impurities present in the water. I use three different euphotic zone boundaries to assess different possibilities for a more efficient photosynthesizing life form on Titan. For the first boundary, I take the boundary of the euphotic zone to be 1% of the surface intensity of Titan. To find this value, I integrated the radiances measured by Huygens ((Tomasko *et al.* 2005), Figure 3.17c) using:

$$I = \int_{480\ nm}^{800\ nm} R(\lambda) d\lambda \tag{3.10}$$

Where I is the irradiance in W m^{-2} and R is the radiance in W m^{-2} μm^{-1} sr^{-1}. The result is an average surficial irradiance value over the range of 480-800 nm of 0.336 W m^{-2}. 1% of this value, $3.36e^{-3}$ W m^{-2}, will be used as the first boundary of a euphotic zone on Titan. This limit will serve as the euphotic zone boundary in a scenario where photosynthesis on Titan is very efficient and the euphotic zone spans a similar range on Titan as it does on Earth.

For the second boundary, I use a limit of $3.63e^{-6}$ W m^{-2} as an intermediate value between the photon flux at the lower and higher ends of the visible spectrum given off by the black smoker at which Beatty *et al.* (2005) found and collected green-sulfur bacteria photosynthesizing without sunlight. This boundary would represent the boundary of the euphotic zone in a scenario where photosynthesis is either ultra-efficient or is used as an auxiliary metabolic process as in the case of the green-sulfur bacteria.

For the third boundary, I use the limit of what would be considered the mesophotic zone on Earth for Titanian liquids. Photosynthesis still occurs in the mesophotic zone, but at a lower rate, and generally light levels are too low for light-loving organisms such as phytoplankton and certain algal organisms. The conditions of the mesophotic zone on Earth would more closely resemble the euphotic zone on Titan, and as such, using the lower limit of the mesophotic zone on Earth to describe the lower limit of the euphotic zone on Titan may be sufficient. The mesophotic zone is less studied and more poorly defined than the euphotic or dysphotic zones (Castellan *et al.* 2022). Generally, for marine waters, the mesophotic zone is defined as 30-150 m in depth (Castellan *et al.* 2022), but this does not hold for all conditions, and of course would be different on Titan. Castellan *et al.* (2022) report that the

bottom of the mesophotic zone most accurately corresponds to an irradiance of 0.0001 mol photons m^{-2} day^{-1} – or 0.0012 W m^{-2}.

The results for the pure water impact crater pool are shown in Figure 3.6. This scenario represents the conditions immediately following an impact event, after the impact melt has settled back into the crater and before freezing has begun. This scenario is idealistic in that there are no additional scatterers or absorbers in the water. Figure 3.6 represents the maximum transmission of each wavelength of light through the water. The addition of any additional materials – such as ice, bubbles, and tholins – will cause light to be further absorbed and scattered, and light will attenuate faster at shallower depths. The rate of and extent to which attenuation occurs depends on the flavor and number of particles in the water. Inherently, pure water preferentially absorbs red light and transmits blue light (Warren 2019), and this trend is confirmed by these results. For a 234 m deep crater pool with no additional scatterers and absorbers, red light attenuates within the top 25 m of the water column, whereas blue and some cyan and green light reach the bottom depths of the pool.

A similar scenario is shown in Figure 3.7, except in this scenario, the pool has completely frozen through. For pure ice, attenuation trends are nearly identical to pure water (Warren 2019).

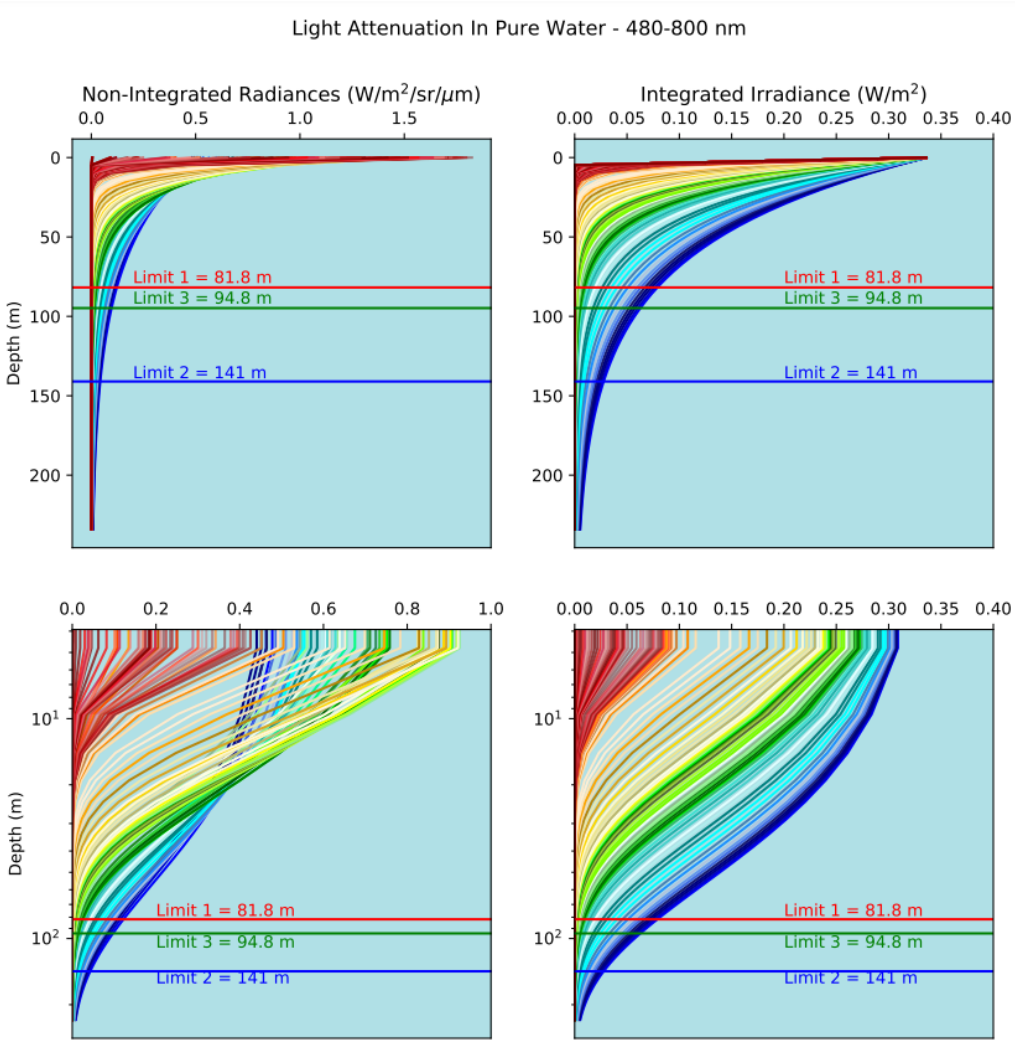

Figure 3.6: Attenuation of light with depth in a pure water impact crater pool with no ice or pollutants.

For general trends, I observed the behavior of all wavelengths from 480-800 nm on a 2 nm interval. For measurements of euphotic zone depths and for more complex scenarios, I used 17 wavelengths across the waveband to simplify calculations and runtime.

To find the depth of the euphotic zone, I integrate the radiance at each depth using Simpson's Rule. I thus find that the depth of the euphotic zone boundary in a pure water pool 234 m deep is located at approximately 83 m in depth for euphotic zone limit 1, 141 m for euphotic zone limit 2 and 95 m for euphotic zone limit 3. Thus, for both limits 1 and 3, nearly 1/3 of the water column receives enough light for "Titanian photosynthesis". For limit 2, over half of the water column receives enough light for "Titanian photosynthesis". Assuming photosynthesis or an analogous process could arise on Titan, and assuming that that process is adapted to lower light conditions, a euphotic zone around 80 m - 90 m

deep for limits 1 and 3 rivals shallower ocean euphotic zones (as a result of cloudy weather and/or impurities in the water) on Earth, which could be promising. However, these euphotic zone depths are for pure water with no icy lid, and thus is our upper endmember for light available in the impact crater pool column.

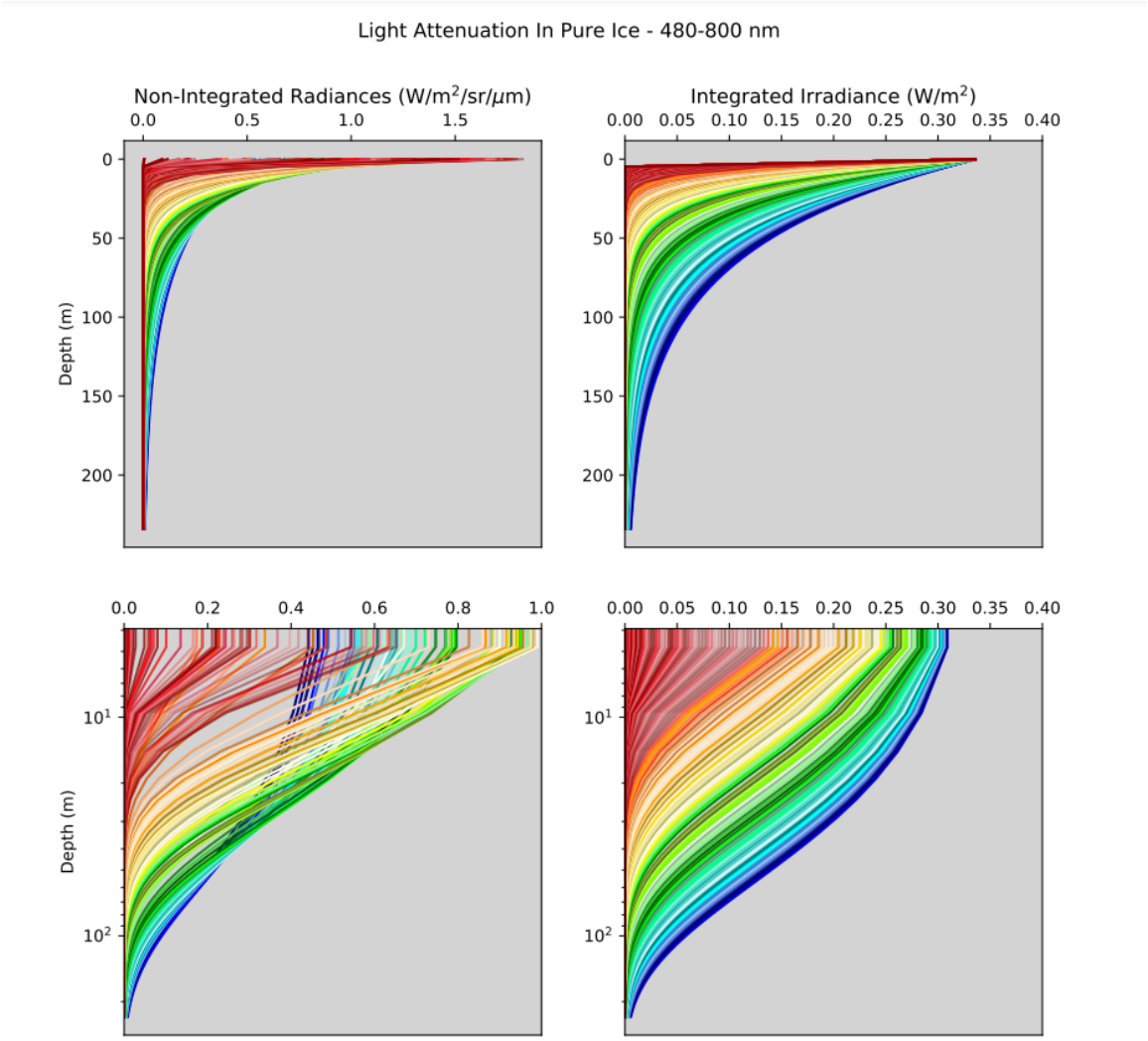

Figure 3.7: Attenuation of light with depth in a pure water ice impact crater pool.

3.4.2 *Impact Crater Pool – Pure Ice Lid, Pure Water Pool*

I first test the scenario in which both the ice lid and the water column of the impact crater pool are free of impurities. This scenario is the idealistic, upper endmember scenario for the timescale on which at least part of the pool is liquid. The results for this run are shown in Table 3.5. Because pure ice and water share similar attenuation properties, it is unsurprising that the euphotic zone does not change much, even with growing melt pool thickness. For limit 1, by the time 50% of the impact crater pool column is frozen, the euphotic zone is subsumed by the ice. This result is also seen for limit 3, the euphotic zone depth is about 20 m deeper than that of limit 1 but is also subsumed by the time 50% of the pool is frozen through. Thus, only the timescale from initial impact to the time 50% of the column is frozen is time amenable to the development of life that could use photosynthesis as a primary metabolic mechanism with our assumptions. This timescale is the absolute maximum for a Selk-sized crater. For limit 2, the euphotic zone is still partially in the liquid water column by the time 50 % of the pool is frozen over but is subsumed as well by the time 75% of the pool is frozen over. Future work could benefit from determining the timescale over which freezing of the impact crater pool occurs. For larger craters, the timescale will be lengthened. Larger crater pools can be modeled using the techniques of this thesis to determine the timescale(s) that would be amenable to photosynthetic organisms for craters larger than Selk.

Table 3.5: Results for the various cases of an impact crater pool with a growing icy lid.

Run	Euphotic Zone Depth, Limit 1 (0.00336 W m^{-2})	Euphotic Zone Depth, Limit 2 (3.36e^{-6} W m^{-2})	Euphotic Zone Depth, Limit 3 (0.0012 W m^{-2})	Ice:Water
Case 3	80.7 m	144 m	100 m	1:99
Case 3	81.5 m	140 m	97.5 m	10:90
Case 3	79.3 m	139 m	97.1 m	25:75
Case 3	N/A, euphotic zone located within ice lid	142 m	N/A, euphotic zone located within ice lid	50:50

Table 3.5: Results for the various cases of an impact crater pool with a growing icy lid.

Case 3	N/A, euphotic zone located within ice lid	N/A, euphotic zone located within ice lid	N/A, light nearly completely attenuated in ice lid	75:25
Case 3	N/A, light nearly completely attenuated in ice lid	N/A, euphotic zone located within ice lid	N/A, light nearly completely attenuated in ice lid	90:10

3.4.3 *Bubbly Ice*

I tested two different number densities of bubbles existing in the icy lid, a lower end value of $\eta = 10^3$ bubbles/m^3 and an upper limit of $\eta = 10^5$ bubbles/m^3. At $\eta = 10^6$ and above, light is attenuated immediately within the icy lid and does not penetrate to the water below, even when the icy lid is only 1% of the entire column. Noticeable differences in attenuation patterns between the pure ice-pure water crater pool and the bubbly ice lid are not seen until a number density of $\eta = 10^3$ bubbles/m^3, though they are small. Attenuation of light increases very quickly with increases in bubble number density.

I additionally tested three different effective scattering radii for the bubbles; $\overline{r_{eff}}$ = 0.5 mm, 1 mm, and 4 mm, keeping a number density of 10^3 constant. A small difference between 0.5 mm and 1 mm can be seen. However, a large difference can be seen between 1 mm and 4 mm. For 1 mm bubbles, light wasn't nearly fully attenuated in the ice lid until the ice lid comprised 50% of the impact crater pool column for limits 1 and 3. For limit 2, the euphotic zone was not subsumed by the ice lid until a time when between 50% and 75% of the pool was frozen over. At 4 mm, light was nearly fully attenuated by the time 25% of the column was frozen for limits 1 and 3. For limit 2, light was nearly fully attenuated in the ice lid by the time 50% of the column was frozen over. Depending on the freezing timescale of the crater pool, the time during which life could potentially develop could be significantly shortened.

There were instances in investigating either changes in effective scattering radius or in effective number density in which the euphotic zone would have been located within the ice lid due to the high attenuation rate. However, some light was still transmitted into the water below, mainly in the blue and/or cyan wavelength ranges. This light could be potentially used by putative life if it were to develop

photosynthesis or an analogous process if it were efficient enough and photopigments that were developed could use only wavelengths on the shorter wavelength end of the visible spectrum, or if photosynthesis was used as an auxiliary metabolic process.

Unfortunately, in literature regarding terrestrial ice, bubble number density for various ices studied in situ is often estimated to be on the order of 10^8 bubbles/m^3. Although, this value can vary across environments, freezing timescales, salinity, etc. Clean glacial and sea ice can both have less bubbles and transmit light through substantial depths, more closely matching our testing range of $<10^3$ to 10^5 bubbles/m^3, so it is not impossible that cleaner ice that allows for transmission of light could exist on Titan. Ultimately, the amount and size of bubbles that could be included in the icy lid will depend heavily on the speed of freezing and the energetics of the impact event.

Table 3.6: Results for the various cases of an impact crater pool with an icy lid with varying effective scattering radii and effective number densities of bubbles.

Run	Euphotic Zone Depth, Limit 1 (0.00336 W m^{-2})	Euphotic Zone Depth, Limit 2 (3.63e^{-6} W m^{-2})	Euphotic Zone Depth, Limit 3 (0.0012 W m^{-2})	Ice:Water
Case 4a	82.4 m	141 m	94.6 m	1:99
Case 4a	82.4 m	140 m	93.2 m	10:90
Case 4a	80.4 m	141 m	94.0 m	25:75
Case 4a	N/A, euphotic zone located within ice lid	145 m	N/A, euphotic zone located within ice lid	50:50
Case 4a	N/A, euphotic zone located within ice lid	N/A, euphotic zone located within ice lid	N/A, euphotic zone located within ice lid	75:25
Case 4b	68.7 m	137 m	84.1 m	1:99
Case 4b	N/A, light completely attenuated in ice lid	N/A, light completely attenuated in ice lid	N/A, light completely attenuated in ice lid	10:90

Table 3.6: Results for the various cases of an impact crater pool with an icy lid with varying effective scattering radii and effective number densities of bubbles.

Case 4c	82.4 m	141 m	94.7 m	1:99
Case 4c	84.5 m	140 m	94.0 m	10:90
Case 4c	82.3 m	142 m	95.6 m	25:75
Case 4c	N/A, euphotic zone located within ice lid	146 m	N/A, euphotic zone located within ice lid	50:50
Case 4d	78.3 m	140 m	93.0 m	1:99
Case 4d	63.0 m	134 m	79.0 m	10:90
Case 4d	N/A, euphotic zone located within ice lid	122 m	N/A, euphotic zone located within ice lid	25:75
Case 4d	N/A, light completely attenuated in ice lid	N/A, light completely attenuated in ice lid	N/A, light completely attenuated in ice lid	50:50

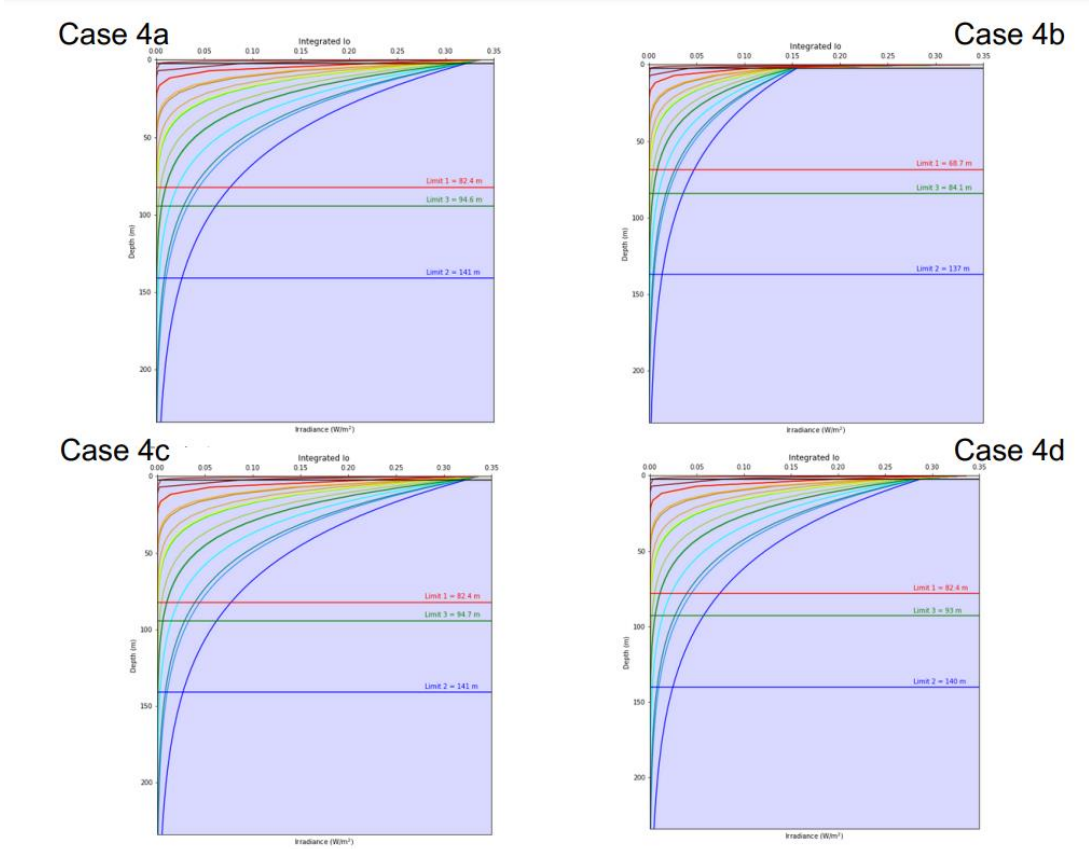

Figure 3.8: Results of Cases 4a-4d when the ratio of ice:water in the impact crater pool column is 1:99.

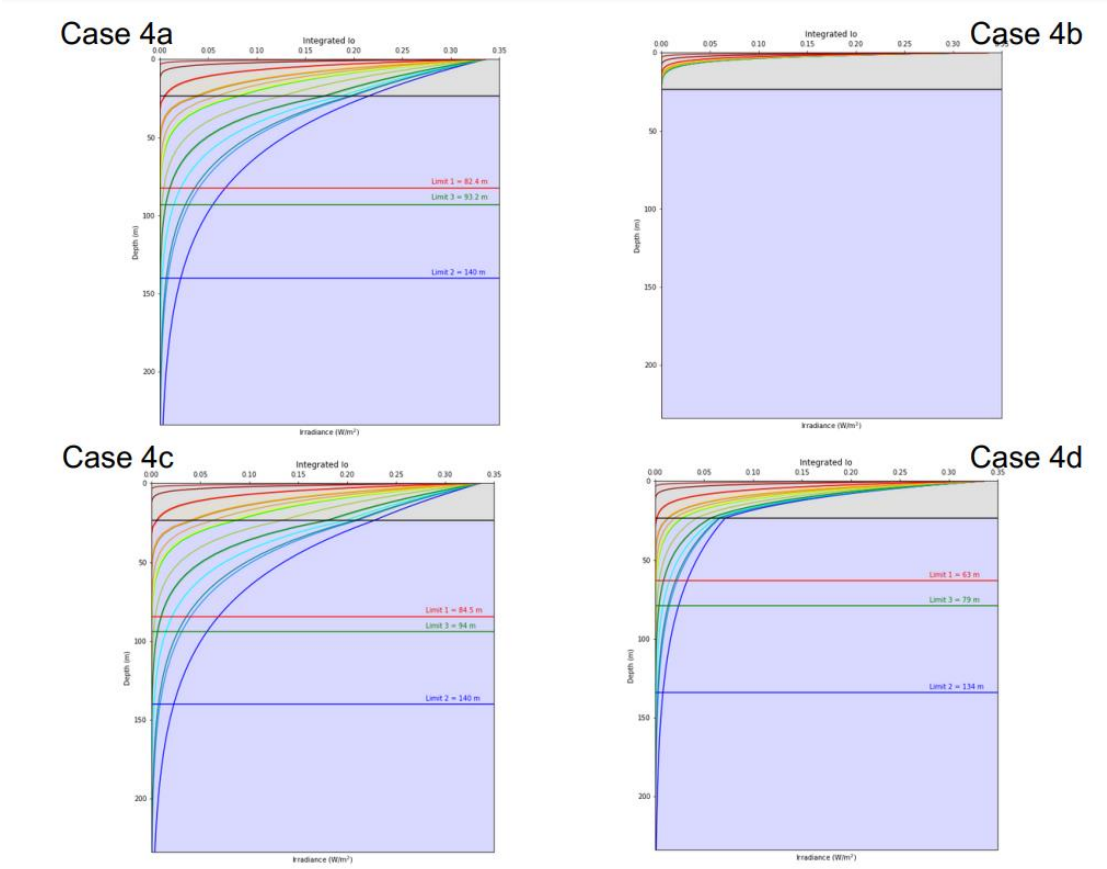

Figure 3.9: Results of Cases 4a-4d when the ratio of ice:water in the impact crater pool column is 10:90.

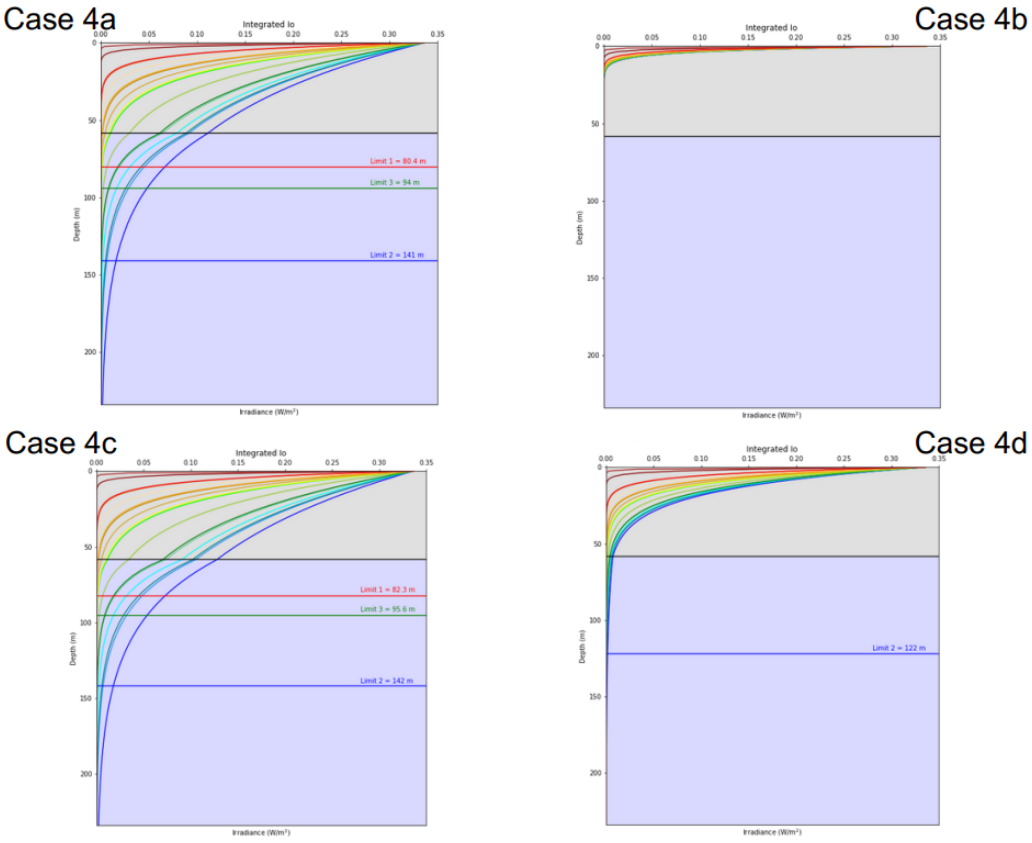

Figure 3.10: Results of Cases 4a-4d when the ratio of ice:water in the impact crater pool column is 25:75.

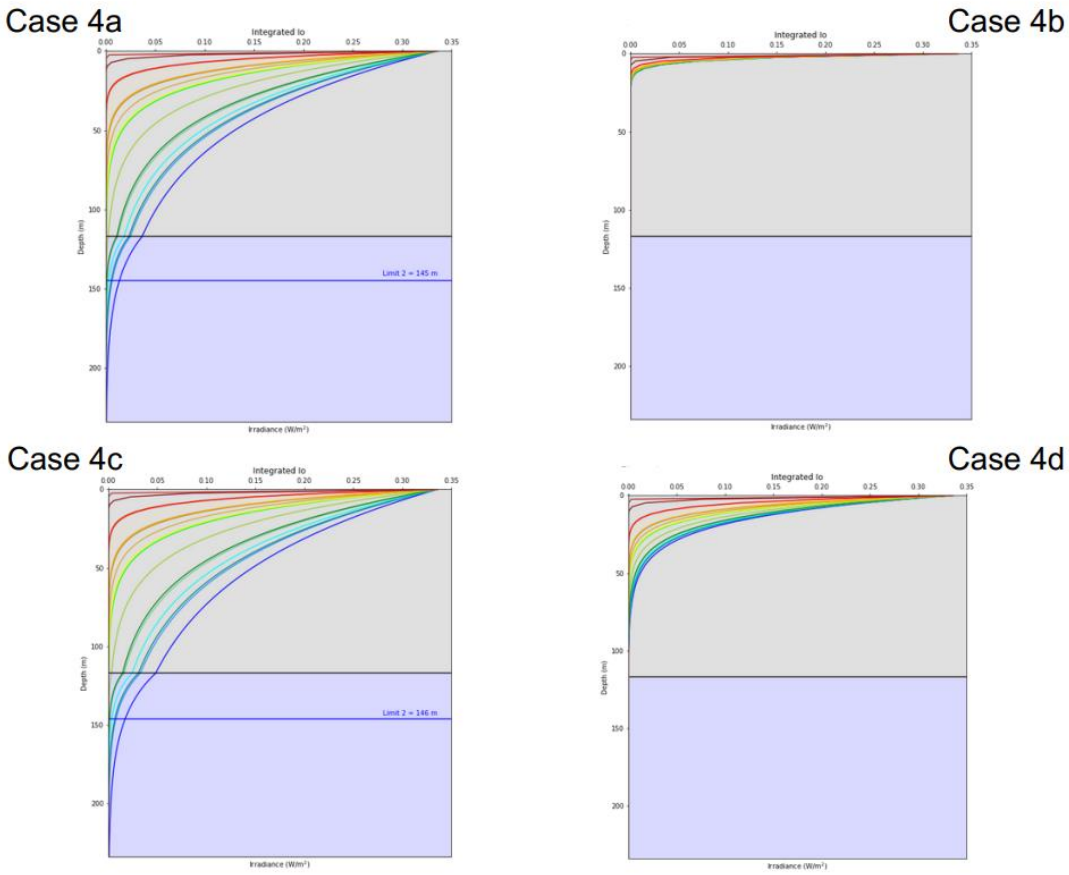

Figure 3.11: Results of Cases 4a-4d when the ratio of ice:water in the impact crater pool column is 50:50.

3.4.4 *Tholins in the Ice Lid, Pure Water Column*

The above scenario was repeated, but this time for tholins instead of bubbles in the icy lid layer. For the scenario where only 1% of the impact crater pool column is frozen, at a tholin fraction of 0.0001% in the ice lid, the effect of attenuation by the tholins begins to become noticeable. At a 0.001% tholin fraction, there is a significant effect on the attenuation of visible light, with the euphotic zone boundary shrinking quickly from over 80 m deep to 28.5 m deep for limit 1. At a 0.01% tholin fraction, light is attenuated immediately within a very thin icy lid.

The volume fraction, number density, and radius of tholins in the icy lid all affect the attenuation of light with depth in the impact crater pool column. For tholins with larger radii, light is attenuated much faster, leading to a shallower euphotic zone depth and quicker total attenuation of light in the ice lid. The most striking effect is seen in the larger volume fractions of tholins located in the ice lid. For Case 5a, light is almost completely attenuated in the icy lid by the time only 10% of the impact crater pool column is frozen for limit 1. This result could be significant if a large fraction of tholins are entrained in the ice lid as a result of being kicked up by the impact event, or, if large amounts of tholins were blown onto the surface layer of the ice lid. Equatorial craters especially could be at risk for large amounts of tholins in or on the lid as they are located in or near dunes. While the mixing of tholins and water is essential for prebiotic chemistry, too many tholins in or on the impact crater pool column could block large amounts of light and would likely rule out photosynthesis as a reasonable metabolic process for life in these pools.

Table 3.7: Results for the various cases of an impact crater pool with an icy lid with varying effective scattering radii and effective number densities of tholins.

Run	Euphotic Zone Depth, Limit 1 (0.00336 W m^{-2})	Euphotic Zone Depth, Limit 2 (3.63e^{-6} W m^{-2})	Euphotic Zone Depth, Limit 3 (0.0012 W m^{-2})	Ice:Water
Case 5a	68.9 m	139 m	85.8 m	1:99
Case 5a	N/A, light almost completely attenuated in ice lid	N/A, light almost completely attenuated in ice lid	N/A, light almost completely attenuated in ice lid	10:90

Table 3.7: Results for the various cases of an impact crater pool with an icy lid with varying effective scattering radii and effective number densities of tholins.

Case 5b	79.1 m	140 m	94.6 m	1:99
Case 5b	67.4 m	137 m	83.9	10:90
Case 5b	N/A, euphotic zone located within ice lid	134 m	67.6 m	25:75
Case 5b	N/A, light completely attenuated in ice lid	N/A, light completely attenuated in ice lid	N/A, light completely attenuated in ice lid	50:50
Case 5c	80.9 m	141 m	94.3 m	1:99
Case 5c	77.4 m	139 m	91.0 m	10:90
Case 5c	74.5 m	138 m	89.3 m	25:75
Case 5c	N/A, euphotic zone located within ice lid	140 m	N/A, euphotic zone located within ice lid	50:50
Case 5d	75.3 m	140 m	92.7 m	1:99
Case 5d	59.8 m	133 m	76.0 m	10:90
Case 5d	N/A, euphotic zone located within ice lid	120 m	N/A, euphotic zone located within ice lid	25:75
Case 5e	77.8 m	140 m	93.3 m	1:99
Case 5e	66.8 m	136 m	82.6 m	10:90
Case 5e	N/A, euphotic zone located within ice lid	128 m	67.2 m	25:75

Table 3.7: Results for the various cases of an impact crater pool with an icy lid with varying effective scattering radii and effective number densities of tholins.

Case 5e	N/A, light completely attenuated in ice lid	N/A, light completely attenuated in ice lid	N/A, light completely attenuated in ice lid	50:50
Case 5f	68.2 m	137 m	83.8 m	1:99
Case 5f	N/A, light completely attenuated in ice lid	N/A, light completely attenuated in ice lid	N/A, light completely attenuated in ice lid	10:90

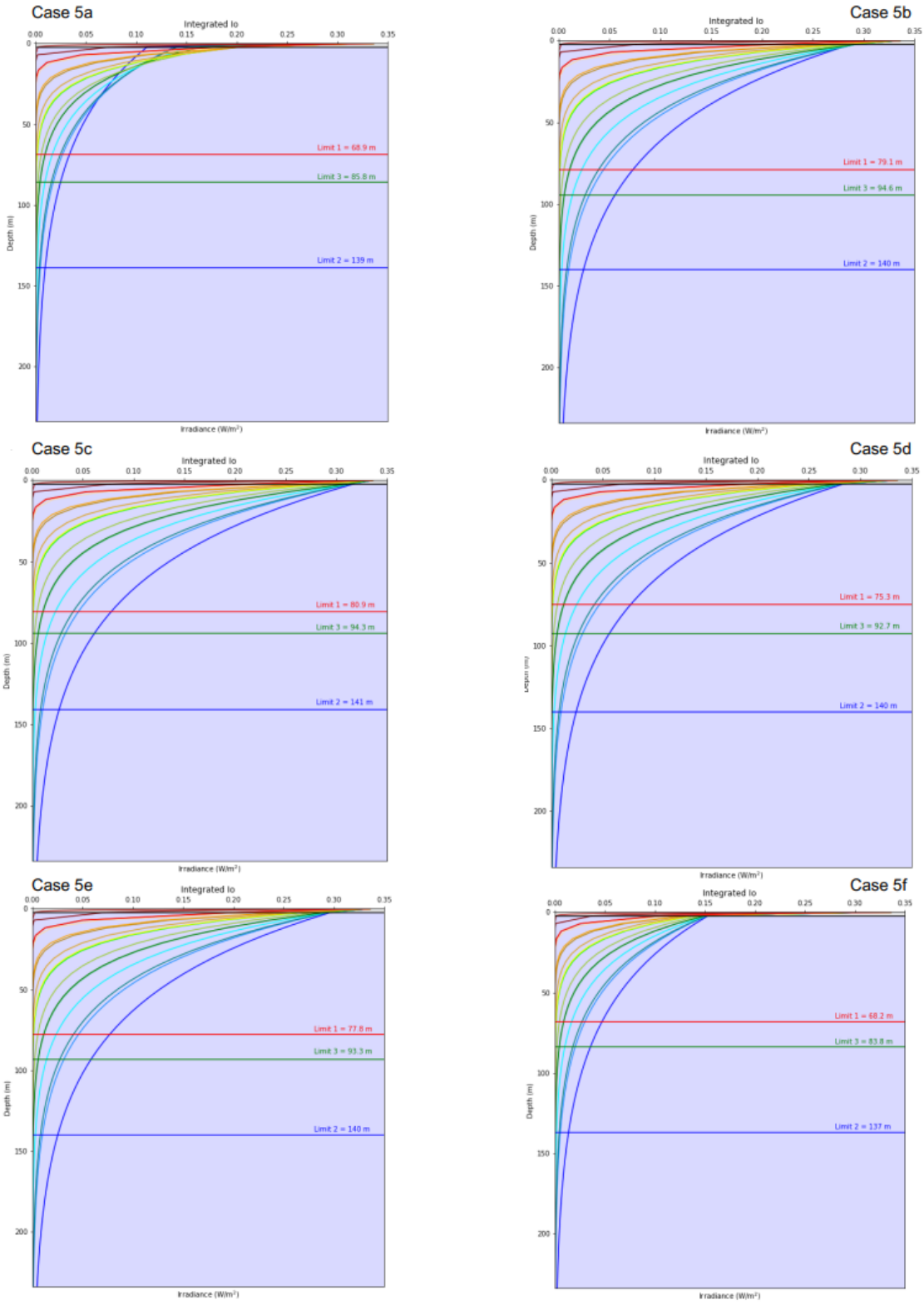

Figure 3.12: Results of Cases 5a-5f when the ratio of ice:water in the impact crater pool column is 1:99.

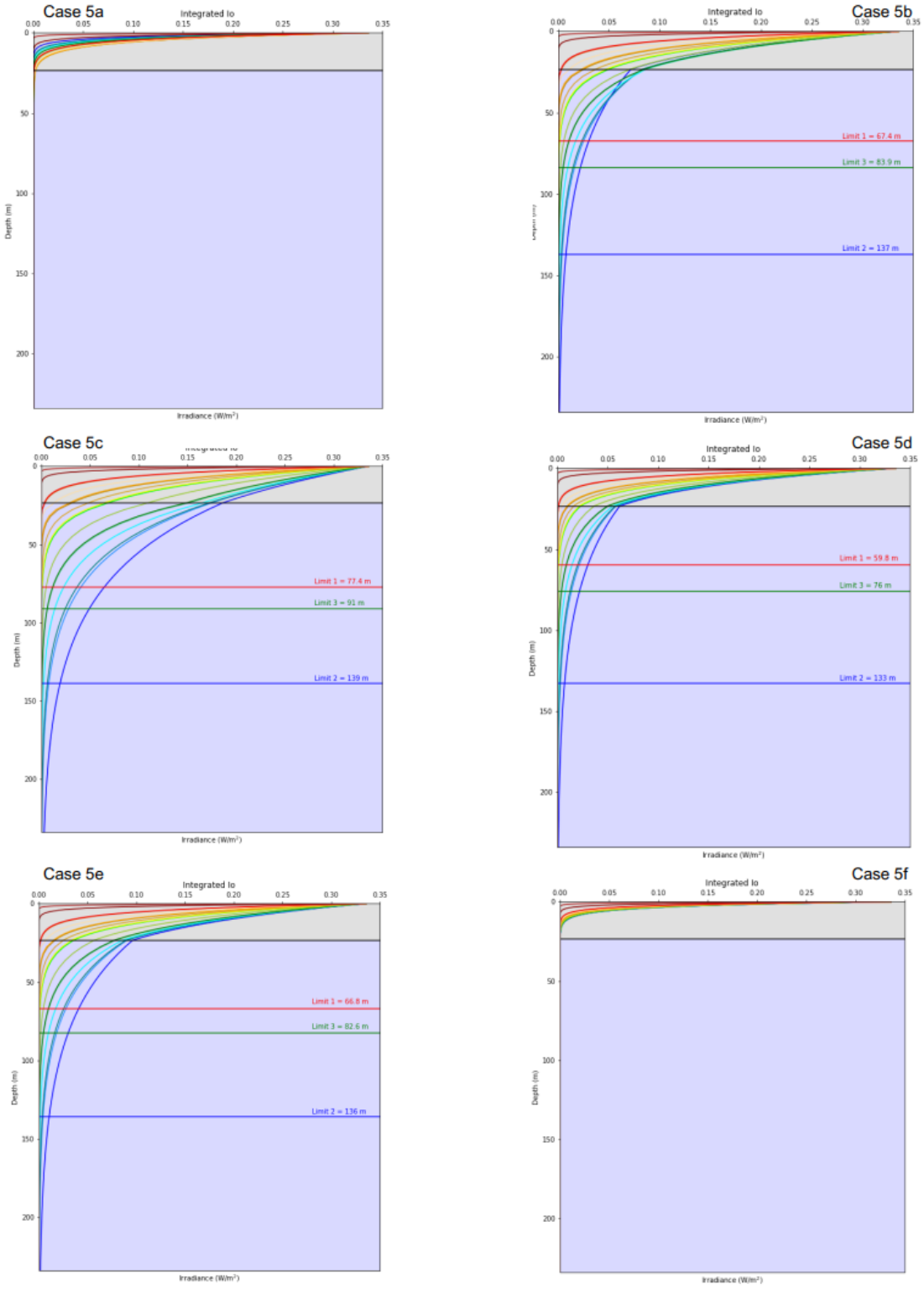

Figure 3.13: Results of Cases 5a-5f when the ratio of ice:water in the impact crater pool column is 10:90.

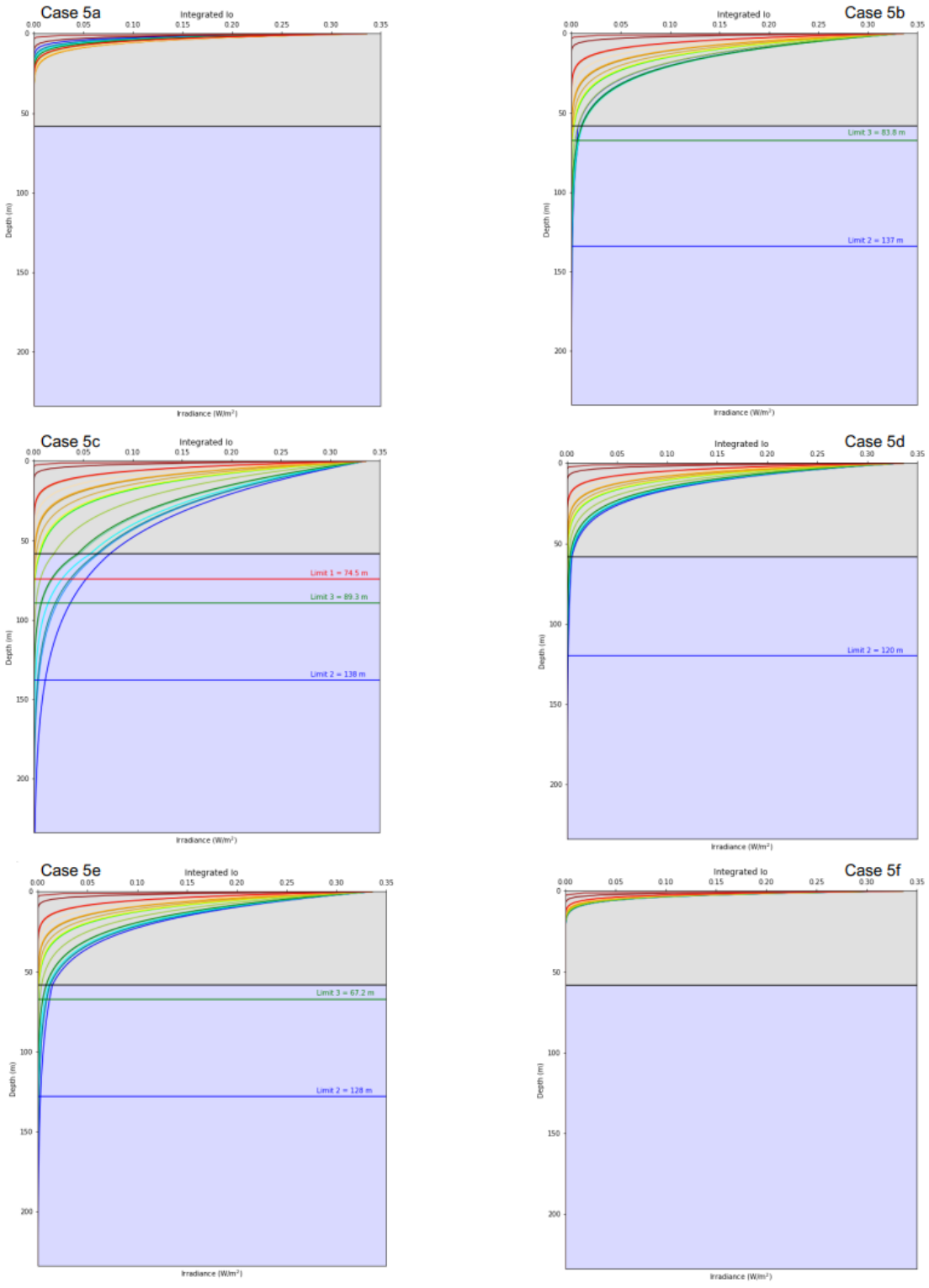

Figure 3.14: Results of Cases 5a-5f when the ratio of ice:water in the impact crater pool column is 25:75.

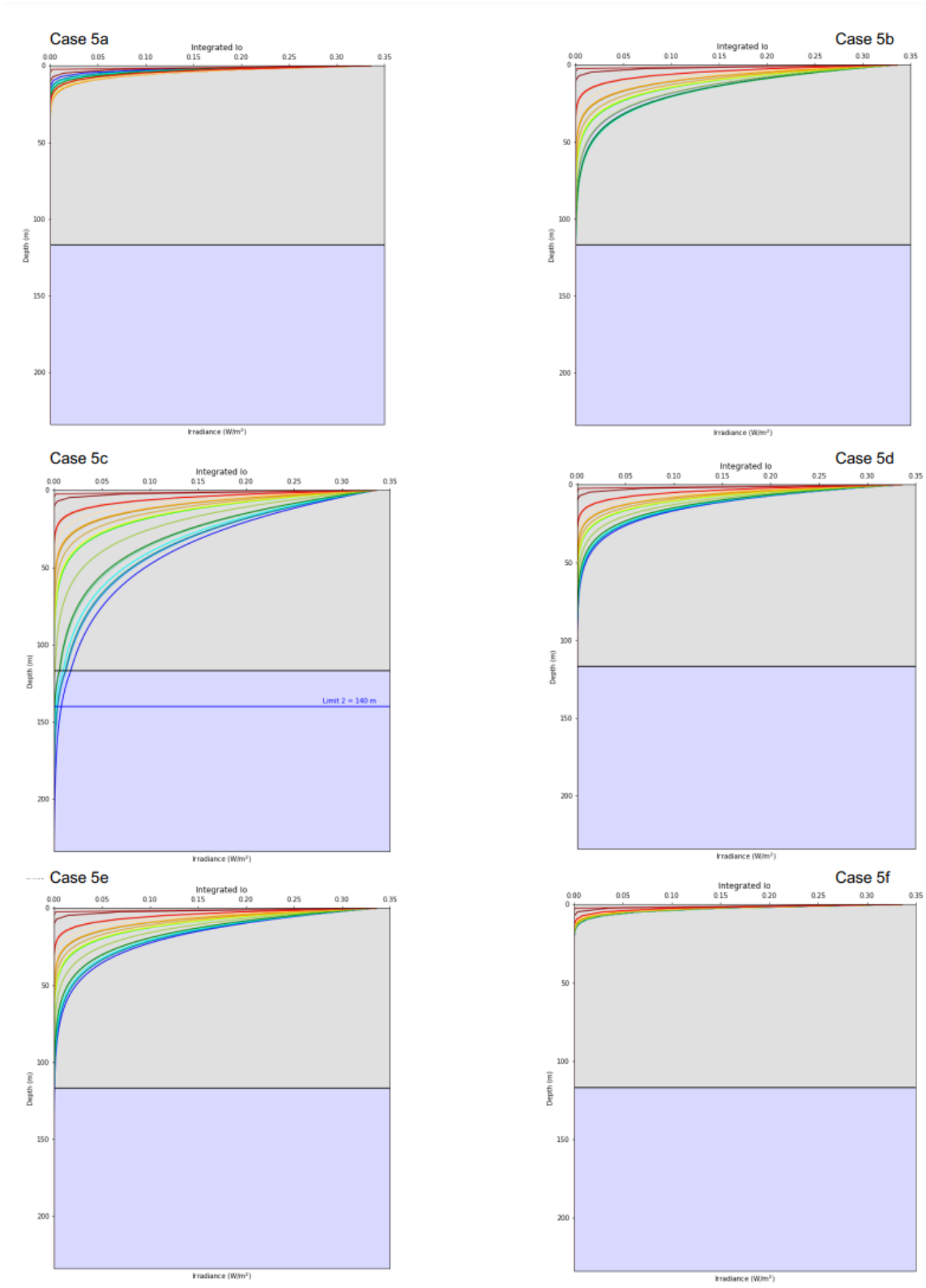

Figure 3.15: Results of Cases 5a-5f when the ratio of ice:water in the impact crater pool column is 50:50.

3.4.5 *Lakes and Seas*

PURE ETHANE ENDMEMBER – The attenuation of light in pure methane is a useful endmember. While choppiness from waves, scattering from bubbles, and absorption from suspended tholins are likely mechanisms for attenuation of light in the hydrocarbon lakes and seas, there could be areas where the "waters" are relatively clear. Determining the attenuation of light in pure methane and an associated euphotic zone represents the maximum amount of light available in the hydrocarbon column in the lakes and seas. As previously mentioned, the lakes and seas of Titan are likely mixes of methane, ethane, and trace other liquid hydrocarbons in varying ratios depending on location (Lunine and Atreya 2008; Stofan *et al.* 2007). However, appropriate optical properties for liquid hydrocarbons are sparse in the literature. Thus, for now, I represent the liquid hydrocarbon lakes and seas as purely methane.

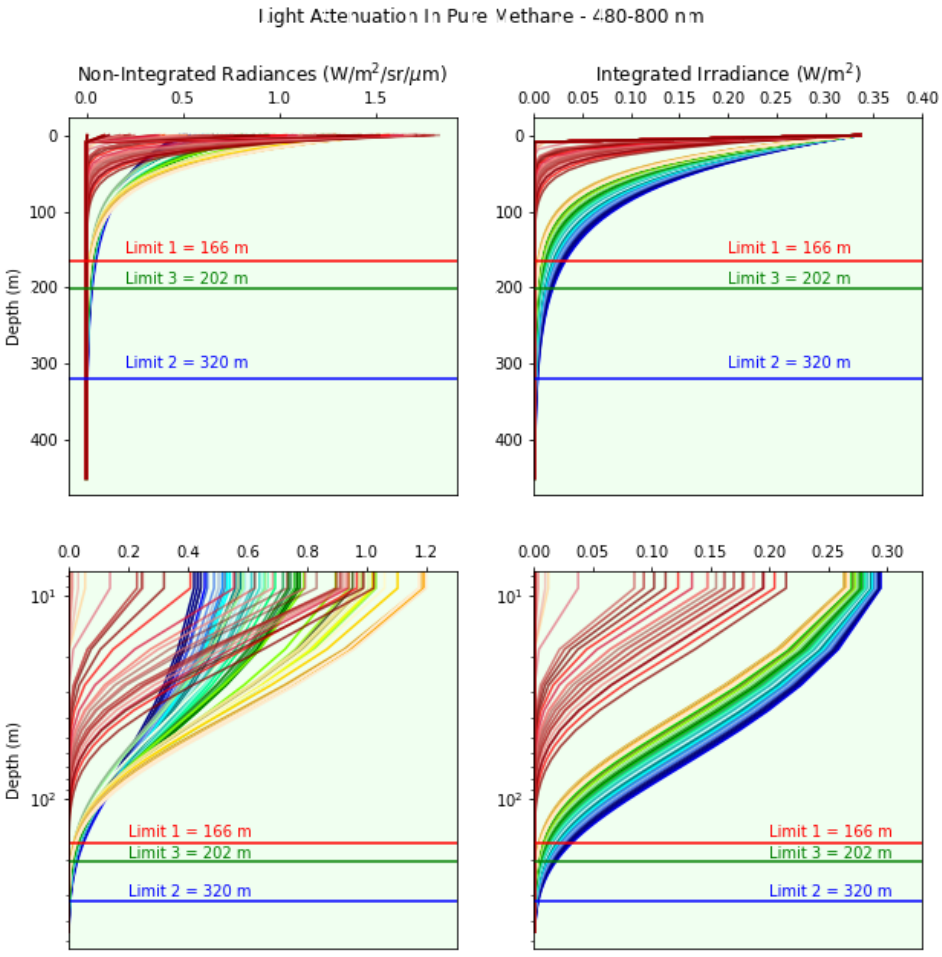

Figure 3.16: Attenuation of light as a function of depth in a pure methane lake or sea.

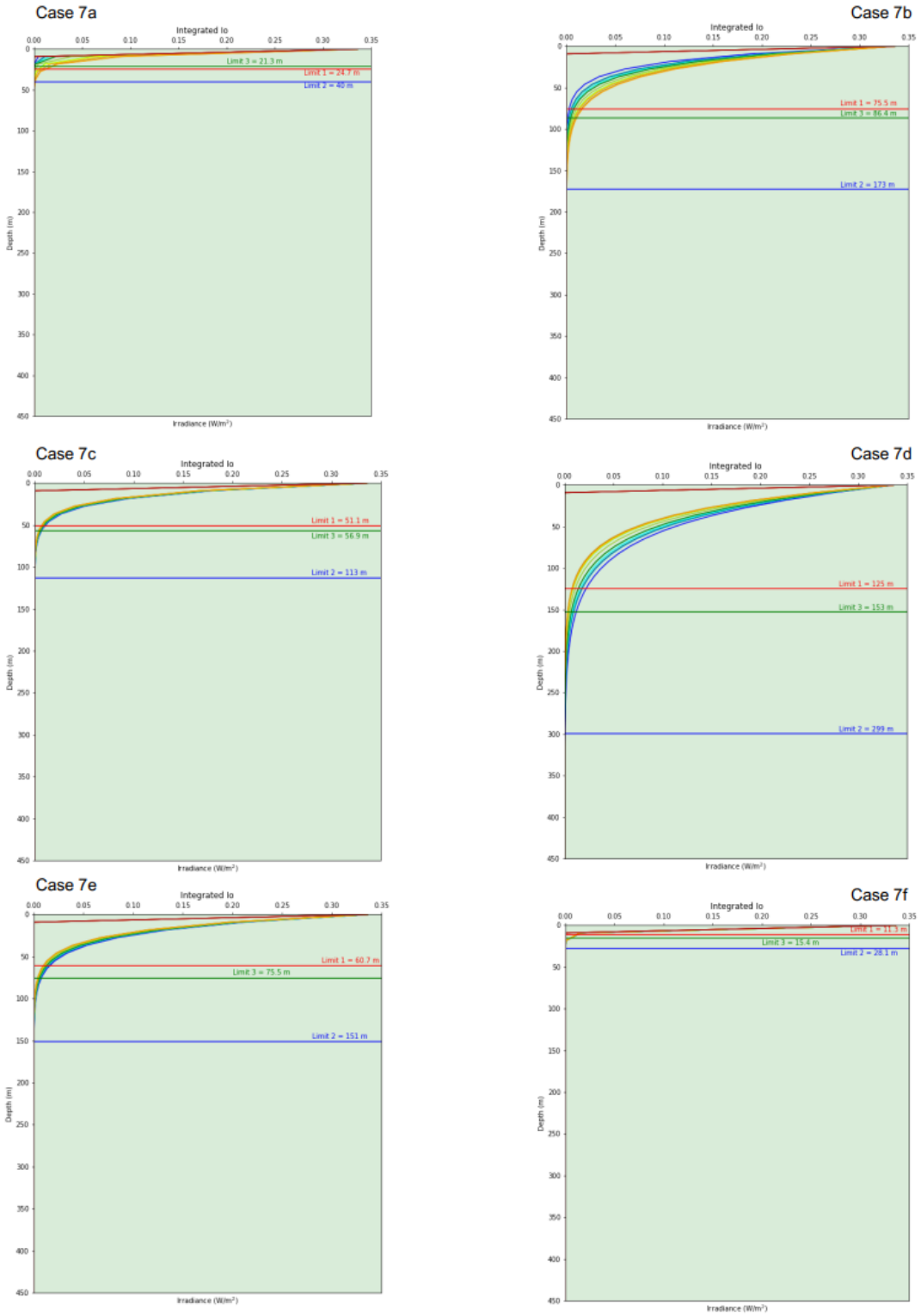

Figure 3.17: Results of Cases 7a-7f.

The results for the pure methane endmember are shown in Figure 3.16. The euphotic zone for pure methane for limit 1 is calculated to be 166 m, around twice that of a pure water impact crater pool. For

limit 2, the euphotic zone depth is 320 m, which is quite deep. For limit 3, the euphotic zone depth is 202 m, much deeper than even limit 2 values for the impact crater pools.

Table 3.8: Results for the various cases of a methane lake or sea with suspended tholins in the liquid hydrocarbon column.

Run	Euphotic Zone Depth, Limit 1 (0.00336 W m^{-2})	Euphotic Zone Depth, Limit 2 (3.63e^{-6} W m^{-2})	Euphotic Zone Depth, Limit 3 (0.0012 W m^{-2})
Case 7a	24.7 m	40 m	21.3 m
Case 7b	75.5 m	173 m	86.4 m
Case 7c	51.1 m	113 m	56.9 m
Case 7d	125 m	299 m	153 m
Case 7e	60.7 m	151 m	75.5 m
Case 7f	11.3 m	28.1 m	15.4 m
Pure Methane	166 m	320 m	202 m

METHANE WITH SUSPENDED SOLIDS – Complex organic sediments are likely constantly coming into contact with the polar hydrocarbon lakes and seas. Tholins could be incorporated into the hydrocarbon bodies from atmospheric rainout, sediments blown into the liquids from the surrounding environment, or lapped up by waves on the shores. Size distributions of tholin sediments on the surface are not known, but it is likely that there are small tholins that could be suspended in the liquid hydrocarbons. Thus, I model the attenuation of light with varying levels of suspended tholin sediments.

The addition of tholins in the liquid methane lake or sea significantly changes the depth of the euphotic zone in most of the tested cases. Case 7d attenuates light the least out of all the tested cases, but still shallows the euphotic zone by nearly 30-50 m depending on which euphotic zone limit is being used. Cases 7a and 7f, with the largest tested tholin volume fraction and tholin number density, respectively, result in the most dramatic shallowing of the euphotic zone depth.

3.5 DISCUSSION

3.5.1 *Photopigments in Titan Liquids as Biosignatures*

For terrestrial photosynthesis, various pigments and photopigments exist that allow photosynthesizing organisms to absorb light energy from the sun and to convert it into energy. The most well-known photopigments are chlorophylls-*a* and -*b* (chlorophyll-*a* is required for terrestrial photosynthesis), but various other photopigments exist as accessory photopigments. Among these are carotenoids, anthocyanins and xanthophylls, among others. If life that could utilize photosynthesis were to develop on Titan, it is unknown if it would use photopigments analogous to terrestrial ones, or something different in structure in function. Because we cannot predict what an alien photopigment would be like, we analyze if photosynthesis may be possible and what biosignatures in the form of photopigments could be left behind by Titan life by looking at terrestrial photopigments.

What, if any, of the terrestrial photopigments such as chlorophylls, carotenoids anthocyanins, and xanthophylls could be utilized by life in Titan impact crater pools and life in Titanian lakes and seas?

IMPACT CRATER POOLS – For the impact crater pools, red light is attenuated nearly immediately in the water column, even with a very small icy lid. Thus, red light will be of little to no use to photosynthesizing life in Titan impact crater pools. Chlorophyll-*a* has two main absorption peaks in the visible spectrum, one in the blue-violet and one in the red. The blue-violet absorption peak occurs at around 450-480 nm (Okamoto *et al.* 1996, Tang *et al.* 2009, among others), wavelengths of light that are heavily attenuated by Titan's atmosphere and don't reach the surface. The red absorption peak occurs around 650-700 nm depending on the form of chlorophyll-*a* (French *et al.* 1972, Lehmer *et al.* 2021, among many others). Chlorophyll-*a* or an analogous photopigment would thus be of no use to putative life in impact crater pools unless it featured a singular absorption peak at wavelengths of 480 nm or greater.

Chlorophyll-*b* features absorption peaks that are redshifted compared to chlorophyll-*a* (Kume *et al*. 2018). For chlorophyll-*b*, the red absorption peak is much shallower than that of the blue absorption peak (Kume *et al.* 2018). The red wavelengths are unusable to life in the impact crater pools, so it is notable that the larger absorption for this chlorophyll occurs in the blue end of the spectrum. As well, the blue absorption peak is shifted toward wavelengths that are not only available to life in the impact crater pool but are those wavelengths that penetrate to the deepest depths and exist the longest

in the liquid column. Thus, a chlorophyll-b-like photopigment could be optimal for photosynthesizing life in Titan impact crater pools.

Anthocyanin pigments feature peak absorbances around the 500-600 nm range (Gould 2004), depending on the organism and specific anthocyanin structure. Anthocyanins are accessory photopigments – the bulk of photosynthetic processes are instead carried out by chlorophylls and carotenoids (Kume *et al.* 2018). Anthocyanin pigments tend to provide benefits to photosynthezing organisms such as plants by attracting pollinators, deterring certain predators, and providing protection against UV radiation and protecting a plant's photosystem against excess sunlight and radiation (Gould 2004, Liu *et al.* 2018).

While anthocyanins act essentially as a sunscreen for certain, harmful wavelengths of light, they do absorb visible wavelengths, and a type of anthocyanin or anthocyanin analog could be used in some sort of photosynthetically analogous process on Titan due to the availability of light in the impact crater pool at its peak absorption wavelengths. While anthocyanin production in terrestrial plants is usually triggered by the presence of UV radiation, which would be absent in the crater pool, anthocyanin production can also be triggered by the presence of blue light (Liu *et al.* 2018), which is available in the impact crater pool. Thus, anthocyanin-like pigments, altered to be the main pigment involved in photosynthetic processes, could be utilized by Titanian life in impact crater pools.

Carotenoids are the other main family of photopigments that drive photosynthesis (Kume *et al.* 2018). Carotenoids such as carotenes have two absorption peaks in the 400-500 nm range (Udensi *et al.* 2022). One of these absorption peaks is located at wavelengths shorter than 480 nm and thus may not be useful to life in impact crater pools, but if the second absorption peak occurs at or at wavelengths longer than 480 nm, some flavor of carotenoid-like photopigment could be used.

Xanthophylls are one family of carotenoids and are similar to chlorophyll-*b* in that they have a peak absorption in the blue, around 480-510 nm (Peterman *et al.* 1997). As mentioned above, peak absorption at these wavelengths of light would be optimal as these are the most available wavelengths of light to the water column. A xanthophyll or xanthophyll-like pigment could be useful to life in the impact crater pool.

The above list of photopigments is by no means exhaustive but should show that each photopigment will absorb different wavelengths of light that may or may not be useful for Titanian LAWKI. For putative life in impact crater pools on Titan, the development of a photopigment that has absorption peaks in the blue or green part of the visible spectrum (such as an anthocyanin, xanthophyll, or chlorophyll-*b*, or perhaps a carotenoid) will be necessary, as these are the wavelengths of light that last the longest in the impact crater pool. Secondary or tertiary peaks in longer wavelengths could be useful as well but may not be necessary.

LIQUID HYDROCARBON LAKES AND SEAS – The inherent optical properties of liquid methane are different from those of water, and thus patterns of light attenuation differ in liquid hydrocarbon bodies. As well, the presence, size, and amount of tholins in the liquid methane column can change which wavelengths of light penetrate deepest into the column and which are quickly attenuated. In all cases, red light is still attenuated in the upper few meters and will not be very useful to putative life. Blue, green, yellow, and orange wavelengths are all available in varying, but usable, amounts in each case. Despite the differences in optical properties, the same photopigments that would be of use to putative life in the impact crater pools would be of use to putative life in the liquid methane column as well, with preference towards a photopigment with peak absorption in the blue or the orange shifting depending on the size and amount of tholins present. Chlorophyll-*b*, xanthophylls, anthocyanins, and carotene carotenoids or analogous pigments could all be useful pigments to life in liquid hydrocarbons.

3.5.2 *Possibility of Photosynthesis in Titan Liquids*

As seen in this chapter, for impact crater pools, in any of the three euphotic zone limits modeled, an amount of light exists for some time in the liquid water column that could be utilized in photosynthesis or an analogous process. However, the timescale over which photosynthesis could potentially be viable changes greatly depending on the freezing timescale of the impact crater pool, the amount and size of tholins and/or bubbles in the icy lid, and the amount and size of tholins suspended in the water column. The range of amenable conditions over which photosynthesis could be possible as a primary metabolic process is small in impact crater pools. Inclusion of more tholins or other absorbing sediments on top of or within the icy lid or suspended in the water column would greatly decrease the timescales over which there could be enough light to support photosynthesis. As well, bubbly ice would also decrease the amount of light transmitted through the icy lid and thus would decrease the amount of time over which photosynthesis could be viable.

In the case of photosynthesis on Titan being super-efficient or being used as an accessory metabolic process, the levels of light needed are lowered and the timescale over which photosynthesis may be possible is lengthened. Even so, in the cases studied, the euphotic zone boundary was subsumed by the time 10-75 % of the water column was frozen through, depending on the case studied. If even more tholins or bubbles are present, the euphotic zone is subsumed even quicker. Thus, while organisms using super-efficient photosynthesis or photosynthesis as an accessory metabolism could have a higher likelihood of developing and surviving on longer timescales, they would not be able to photosynthesize

over the entire lifespan of the modeled impact crater pool being liquid to some degree, even if the ice and water were both completely free of impurities.

As well, photosynthetic life would need to develop right away in most impact crater pools, or relatively quickly in large to very large impact crater pools in order to utilize the full timescale over which there is enough light to photosynthesize. This would require a very quick rate of abiogenesis and would likely require phototrophy to develop before (or in tandem with) chemotrophy, which is opposite to what is assumed to have occurred on Earth. Again, we only have a sample size of one to refer to when we study abiogenesis and evolution of life, but it seems highly unlikely that the conditions for a quick abiogenesis and successive development of efficient phototrophy would exist in most impact crater pools on Titan. However, it may not be impossible for very large impact crater pools such as those that may have existed in craters like Menrva, depending on the timescale over which such a pool would freeze.

O'Brien *et al.* (2005) estimate that, for freezing impact crater pools, the time that it would take to freeze approximately half of the column would correspond to only 10% of the total freezing timescale. This percentage would correspond to between 10 and 100,000 years for the predicted lower and upper endmember freezing timescales of 10^2 and 10^6 years, respectively for a Selk-sized crater (Artemieva and Lunine 2003; 2005; O'Brien *et al*. 2005; Thompson and Sagan 1992). The freezing timescales for pools in larger craters such as Menrva, Forseti, Paxsi and Afekin would likely be longer. However, the majority of Titan craters are Selk-sized or smaller. Smaller crater pools pose challenges for the development of photosynthesis in putative impact crater pool organisms. Once 50% of the crater pool column has frozen, very little, if any, light penetrates through the ice lid, depending on the scenario. The presence of ammonia as a constituent of crater melt is not unrealistic, particularly for large impacts such as the one that created Menrva, which could have excavated the "salty" subsurface ocean. However, it is unlikely that the presence of ammonia will significantly extend the freezing timescale. Future, more detailed, studies on the freezing timescales of various impact crater pools would be very useful in further narrowing down whether or not there could be a possibility for the development of photosynthesis in larger crater pools.

Photosynthesis may be difficult, or nearly impossible, on Titan for reasons other than just lower light levels. While carbon dioxide likely exists in some form on Titan, carbon dioxide is solid at Titanian temperatures, and thus would require melting and/or vaporization to free up gaseous carbon dioxide molecules for use in photosynthesis. Carbon dioxide is required, along with water, for terrestrial photosynthesis.

If photosynthesis were to exist in Titanian impact crater pools (and especially in liquid hydrocarbon bodies), photosynthesizing organisms would need to use a different molecule other than carbon dioxide to fuel photosynthesis, and thus would need alternate regulatory proteins and enzymes to carry out the photosynthetic process. This would turn Titanian photosynthesis into a very alien process with different biosignatures. Searching for signatures of photosynthetic materials such as rubisco, glyceraldehyde-3-phosphate, and 3-phosphoglyceric acid that aid in the processing of carbon dioxide in the Calvin Cycle would be of little use. Future studies could focus on determining what materials could be used in "Titanian photosynthesis" and what proteins or other signatures may be left behind by a photosynthesizing organism on Titan.

If we were to look for photosynthesizing organisms on Titan, the most amenable environments are likely in the hydrocarbon lakes and seas. If the existence of hydrocarbon-based lifeforms such as those proposed by McKay and Smith (2005) and Stevenson *et al.* (2015) is possible, there is a higher chance that these organisms could eventually develop photosynthesis or an analogous metabolic process. The liquid hydrocarbon lakes and seas do not have the risk of freezing over like the liquid impact crater pools or cryovolcanic features. Thus, the timescales over which photosynthesis could develop are orders of magnitude greater for liquid hydrocarbon bodies than for impact crater pools. As well, a larger percentage of the liquid column is located within the euphotic zone in all three limits, and thus there is a large volume of environment in liquid hydrocarbon bodies that could be amenable to photosynthesis. Complex organic material would rainout into the lakes and seas and could provide alternate energy sources to carbon dioxide to use in an alien photosynthetic process. Thus, the likelihood of such a process arising in liquid hydrocarbon environments is higher than that of impact crater pools.

3.6 CONCLUSION

For a variety of different scenarios, the depth of the euphotic zone boundary was calculated and is tabulated in Table 3.5-Table 3.8. As a reminder, on Earth, the euphotic zone is the section of the water column that spans the surface of the column to the depth at which the solar insolation has dwindled to 1% of that at the surface (Lee *et al.* 2007). The euphotic zone is the zone in the water column where the majority of photosynthesis in the water column occurs. I keep the same definition for Titan.

The three photic zones in the liquid columns on Earth have varying implications for the diversity and richness of taxa of macrobial and microbial life present in each zone. The depths of these

zones in impact crater pools and the liquid hydrocarbon lakes and seas would similarly have implications for the kinds of life that could develop, the primary production processes they employ, and the types of photopigments they could use in these environments. These photopigments could serve as theoretical biosignatures.

The euphotic zone depth varies with the composition of the attenuated media, the presence and amount of impurities, and the sizes of the impurities. In many of the cases tested for the Titan impact crater pool – even the pure water, pure ice lid endmember – light from the surface was either completely attenuated or the euphotic zone was subsumed by the ice lid by the time 50% of the column was frozen. In the most generous case, the euphotic zone was subsumed in the ice lid by the time 75% of the pool had frozen over. O'Brien *et al.* (2005) estimate that the time for approximately 50% of the impact crater pool liquid column to freeze would only be around 10% of its total lifespan. Thus, abiogenesis and the development of phototrophy would have to develop very quickly in order to utilize the already small amount of light present in the impact crater pool.

Therefore, two conditions (at least) would need to be met if photosynthesis or an analogous process were to develop within organisms inhabiting an impact crater pool. First, photosynthetic processes in impact crater pool organisms would need to be much more efficient, or able to use lower levels of light, than those on Earth. Titanian life would likely need to rely on photopigments that process shorter wavelengths of light such as green and blue, as red and orange light are attenuated rapidly in the pool. The low levels of light compared to on Earth will require adaptation and high efficiency. Organisms such as Antarctic phytoplankton can survive months of nearly aphotic conditions during polar night (Tanabe *et al.* 2007), so this is not impossible. It is unknown if the specific phytoplankton studied by Tanabe *et al.* (2007) used a different means of acquiring energy or if they were actively photosynthesizing during polar night, but the increase in chlorophyll-*a* measured by the researchers during polar night suggests some form of photosynthetic process could have been taking place and could thus be used by putative organisms in dim impact crater pools.

Second, photosynthetic processes would need to develop quickly, likely before chemotrophy. This scenario contradicts the proposed path of the evolution of life on Earth, where photosynthesis appeared later in the biological record, and chemotrophy likely served as the initial metabolism used by LAWKI. Given that our only sample size for life is Earth, it may not be impossible for phototrophy to before chemotrophy, but it is less familiar.

Tanabe *et al*. (2007) studied phytoplankton in the freshwater lakes of Antarctica and found that, with thicker icy lids and lower to no light levels associated with polar night, there were increased concentrations of chlorophyll-*a* in the lakes. Similarly, as ice melted and light levels increased, the

concentrations of chlorophyll-*a* in the water column decreased (Tanabe *et al.* 2007). Should life have developed in impact crater pools on Titan, and if that life developed photosynthesis or an analogous process, we might expect to see signatures of photopigments (or analogous structures) such as chlorophylls or other photopigments that increase photosynthetic efficiency in dim or dark settings. However, it is unlikely we could see chlorophyll-*a* or an analog of chlorophyll-*a* as it absorbs light mainly in the red and blue wavelengths that are unavailable to life in the impact crater pool.

In impact crater pools, generally, the wavelengths that survive the longest with the growing ice lid and addition of impurities are blue and green. Thus, any photopigments used by putative impact crater pool life would need to absorb light in these wavelengths. Carotene carotenoids, anthocyanins, xanthophylls, chlorophyll-*b* or analogous photopigments that absorb at lower wavelengths would be the most likely to result in successful photosynthesis.

The inherent optical properties of liquid methane in the liquid hydrocarbon lakes and seas result in different attenuation patterns than those of the impact crater pools. However, due to the lack of short-wavelength blue and violet light and long-wavelength red light, as well as the availability of blue, green, yellow, and orange light, the same photopigments that could be used in the impact crater pools could be used in photosynthesis in the liquid hydrocarbon bodies as well.

The lack of bio-available carbon dioxide would make terrestrial photosynthesis impossible on Titan. However, alternate energy sources such as complex organic molecules or methane could be used to create an alien photosynthetic process. As well, should photosynthesis develop in a hydrocarbon-based lifeform, it would take on an alien flavor from the familiar terrestrial photosynthesis. Thus, we should expect that if photosynthesis were to develop in Titan environments, it and its byproducts would look different to those of terrestrial photosynthesis.

Compared to putative life in impact crater pools, putative life in the hydrocarbon lakes and seas has the advantage of time. These lakes and seas are not at risk of freezing on astrobiological timescales, and thus even if the euphotic zone spans only a shallow range of depths, it will be stable for millions to perhaps billions of years.

It is difficult to postulate if organisms could arise in the liquid hydrocarbon lakes and seas (McKay and Smith 2005; Sandström and Rahm 2020; Stevenson *et al.* 2015), let alone if they could develop photosynthesis or an analogous process. If hydrocarbon- based life were to arise, it would be nearly impossible to predict what its metabolism would look like, and what photopigment-like structures could develop. Such predictions are well beyond the scope of this thesis but could be an interesting area of future theoretical study.

Ultimately, whether life on Titan could arise and photosynthesize is unknown and will likely remain so for a while yet. However, the results of this thesis suggest that it would be highly unlikely to develop in organisms in impact crater pools. The challenges of lack of time, carbon dioxide, and sufficient light levels would likely prove too great for the development of photosynthesis as we know it. If life utilizing photosynthetic processes were to develop on Titan, it would likely develop in the hydrocarbon lakes and seas. This would require hydrocarbon-based life to exist and exhibit the capacity to develop photosynthesis or an analogous process, but it is not out of the realm of possibility. If photosynthesis did develop on Titan, it would need to take on a rather alien flavor to address lack of carbon dioxide and low light levels. As more is gleaned about the extremes of photosynthesis on Earth, we may learn that certain organisms may require less light than expected or utilize energy sources present on Titan in order to photosynthesize. However, even if photosynthesis cannot develop in impact crater pools, the development of chemotrophic organisms may still be possible. Overall, Titan impact crater pools and the liquid hydrocarbon lakes and seas remain astrobiologically promising sites.

CHAPTER 4

CAVEATS

4.1 ON PUTATIVE IMPACT CRATER POOL DEPTHS

As mentioned in Chapter 2, impact crater pool depths calculated for Titanian craters are only a rough order of magnitude estimation. The calculation used for the volume of melt generated is based on a more simplistic, idealistic equation used by O'Brien *et al.* (2005). In reality, melt generation is more complex, and depends on impact velocity, impactor composition, the angle of impact, among many other considerations. These factors are more thoroughly considered in more complex models such as those used by Artemieva and Lunine (2003) and Artemieva and Lunine (2005). The use of such models is beyond the scope of this thesis.

Additionally, a portion of the melt generated by an impact will be ejected from the crater as ejecta. Yet a smaller portion could potentially drain into the subsurface via fracturing. Thus, the entire volume of the melt generated by the impact will not be retained in the crater structure. Nevertheless, Artemieva and Lunine (2003) determined that, for a 10-20 km diameter crater, a significant portion of the melt will be retained in the crater, enough for the freezing timescale to be astrobiologically significant. I make the assumption that the same can be said for larger craters.

Additionally, I used a flattened cylinder model to calculate the depth of the impact crater pool. In reality, simple crater morphologies more accurately resemble a "squished" hemisphere or bowl. For such a shape, the radius of the crater at the level of the crater pool will be less than the full radius of the crater, unless the melt fully fills the crater. Thus, the depths calculated from the melt volume in this case are not entirely accurate. However, the slope angles of the Titanian craters are unknown, so it is difficult to use the flattened hemisphere approach when calculating pool depths. Between using a flattened cylinder or a normal hemisphere to model pool depths, the flattened cylinder approach is more accurate. Crater depths tend to be much shallower than crater radii for large craters, and thus a hemisphere with equal radii in all directions would be an inaccurate representation. In my modeling, the actual depth of the crater pool is less important than the general trends of light attenuation with depth in the impact crater pool column.

4.2 ON OPTICAL PROPERTIES USED IN CHAPTER 3

The scope of the research in Chapter 3 is limited to wavelengths between 480 and 800 nm as this is the range of light used in photosynthesis and likely to be used in any process analogous to photosynthesis that could independently evolve on other celestial bodies. As well, visible and UV wavelengths below 480 nm are preferentially scattered in the Titan atmosphere, and thus negligible amounts of irradiance at these wavelengths reach Titan's surface. This study could be repeated with near-infrared or infrared light to assess whether the amount of solar flux reaching Titan's surface at these wavelengths could be utilized by putative prebiotic and biotic chemistries as thermal energy inputs, provided they are not attenuated immediately by either the Titan liquids or icy lids overlying impact crater pools as they freeze.

Absorption data for ethane at astrophysical temperatures is lacking. Refractive indices at sub-60 K temperatures have been measured for ethane and ethylene ice mixtures (Hudson *et al.* 2014; Satorre *et al*. 2017). However, both papers make these measurements at a single wavelength. Future work could follow the lead of (Martonchik and Orton 1994) to study the optical constants of liquid ethane, and these values could be applied to our model to analyze if there are differences that arise between the two hydrocarbons. As well, signals from Cassini instrumentation have been measured when attenuated in Titan liquids (Hayes *et al*. 2011). Perhaps knowledge from these data could be used to help determine attenuation coefficients of Titan liquids for more accurate future modeling.

4.3 ON PUTATIVE ASTROBIOLOGY ON TITAN

The "life" hypothesized to benefit from the solar intensity propagating through the impact crater pool or liquid hydrocarbon lakes and seas is assumed to be capable of photosynthesis or a photosynthesis-adjacent process for simplicity in this study. We obviously have no idea if photosynthesis or a similar process would develop through independent evolution if life were to exist on another celestial body like Titan. Nor is photosynthesis the most efficient metabolic process and may not have the potential to develop in dim locations such as the surface or near-surface of Titan because it may not be a biologically favorable process. However, proposing a complete alien metabolism that would best fit various Titanian environments and would be statistically most likely to develop is well beyond the scope of this thesis. There are potentially other sources of energy that could be used by putative life in these environments, and this should be a focus of future astrobiological studies.

BIBLIOGRAPHY

Artemieva N. and Lunine J. 2003. Cratering on Titan: impact melt, ejecta, and the fate of surface organics. Icarus 164:471–480.

Artemieva N. and Lunine J.I. 2005. Impact cratering on titan ii. global melt, escaping ejecta, and aqueous alteration of surface organics. Icarus 175:522–533.

Barnes J.W., Brown R.H., Radebaugh J., Buratti B.J., Sotin C., Le Mouelic S., Rodriguez S., Turtle E.P., Perry J., Clark R., *et al.* 2006. Cassini observations of flow-like features in western Tui Regio, Titan. Geophysical Research Letters 33.

Barnes J.W., Turtle E.P., Trainer M.G., Lorenz R.D., MacKenzie S.M., Brinckerhoff W.B., Cable M.L., Ernst C.M., Freissinet C., Hand K.P., *et al.* 2021. Science goals and objectives for the Dragonfly Titan rotorcraft relocatable lander. The Planetary Science Journal 2:130.

Beatty J.T., Overmann J., Lince M.T., Manske A.K., Lang A.S., Blankenship R.E., Van Dover C.L., Martinson T.A., and Plumley F.G. 2005. An obligately photosynthetic bacterial anaerobe from a deep-sea hydrothermal vent. Proceedings of the National Academy of Sciences 102:9306–9310.

Buiteveld H., Hakvoort J.H., and Donze M. 1994. Optical properties of pure water. SPIE Proceedings.

Castellan G., Angeletti L., Montagna P., and Taviani M. 2022. Drawing the borders of the mesophotic zone of the mediterranean sea using satellite data. Scientific Reports 12.

Coates A.J., Crary F.J., Lewis G.R., Young D.T., Waite J.H., and Sittler E.C. 2007. Discovery of heavy negative ions in Titan's ionosphere. Geophysical Research Letters 34.

Cooper M.G., Smith L.C., Rennermalm A.K., Tedesco M., Muthyala R., Leidman S.Z., Moustafa S.E., and Fayne J.V. 2021. Spectral attenuation coefficients from measurements of light transmission in bare ice on the Greenland ice sheet. The Cryosphere 15:1931–1953.

Davies A.G., Sotin C., Matson D.L., Castillo-Rogez J., Johnson T.V., Choukroun M., and Baines K.H. 2010. Atmospheric control of the cooling rate of impact melts and cryolavas on Titan's surface. Icarus 208:887–895.

Decho A.W. and Gutierrez T. 2017. Microbial extracellular polymeric substances (EPSS) in ocean systems. Frontiers in Microbiology 8.

Elachi C., Wall S., Allison M., Anderson Y., Boehmer R., Callahan P., Encrenaz P., Flamini E., Franceschetti G., Gim Y., *et al.* 2005. Cassini radar views the surface of Titan. Science 308:970–974.

Feller G. and Gerday C. 2003. Psychrophilic enzymes: Hot topics in cold adaptation. Nature Reviews Microbiology 1:200–208.

Fisk M.R. and Giovannoni S.J. 1999. Sources of nutrients and energy for a deep biosphere on Mars. Journal of Geophysical Research: Planets 104:11805–11815.

Fountain A.G., Tranter M., Nylen T.H., Lewis K.J., and Mueller D.R. 2004. Evolution of cryoconite holes and their contribution to meltwater runoff from glaciers in the McMurdo dry valleys, Antarctica. Journal of Glaciology 50:35–45.

Fox D. 2018. The hunt for life below Antarctic ice. Nature 564:180–182.

French C.S., Brown J.S., and Lawrence M.C. 1972. Four universal forms of chlorophyll-*a*. Plant Physiology 49:421–429.

Gould K.S. 2004. Nature's swiss army knife: The diverse protective roles of anthocyanins in leaves. Journal of Biomedicine and Biotechnology 2004:314–320.

Grenfell T.C. 1983. A theoretical model of the optical properties of sea ice in the visible and near infrared. Journal of Geophysical Research: Oceans 88:9723–9735.

Grenfell T.C. 1991. A radiative transfer model for sea ice with vertical structure variations. Journal of Geophysical Research 96:16991.

Grenfell T.C. and Perovich D.K. 1981. Radiation absorption coefficients of polycrystalline ice from 400-1400 nm. Journal of Geophysical Research 86:7447.

Guzmán Marmolejo A. and Segura A. 2015. Methane in the solar system. Boletín de la Sociedad Geológica Mexicana 67:377–385.

Hayes A., Aharonson O., Lunine J., Kirk R., Zebker H., Wye L., Lorenz R., Turtle E., Paillou P., Mitri G., *et al.* 2011. Transient surface liquid in Titan's polar regions from Cassini. Icarus 211:655–671.

Hayes A., Aharonson O., Wall S., Sotin C., Le Gall A., Lopes R., Janssen M., and Cassini RADAR Team. 2008. Joint Analysis of Titan's Surface Using The Cassini VIMS And Radar Instruments. In AAS/Division for Planetary Sciences Meeting Abstracts #40, vol. 40 of AAS/Division for Planetary Sciences Meeting Abstracts, page 34.06.

Hedgepeth J.E., Neish C.D., Turtle E.P., Stiles B.W., Kirk R., and Lorenz R.D. 2020. Titan's impact crater population after Cassini. Icarus 344:113664.

Hedman M.M. 2023. Personal communication.

Hendrix A.R. and Yung Y.L. 2017. Energy options for future humans on Titan. Journal of Astrobiology Outreach 05.

Hudson R., Gerakines P., and Moore M. 2014. Infrared spectra and optical constants of astronomical ices: II. Ethane and ethylene. Icarus 243:148–157.

Huygens C. 1659. Systema Saturnum 1.

Kargel J.S. 1995. Cryovolcanism on the icy satellites. Comparative Planetology with an Earth Perspective page 101–113.

Kume A., Akitsu T., and Nasahara K.N. 2018. Why is chlorophyll-*b* only used in light-harvesting systems? Journal of Plant Research 131:961–972.

Lange R.D. 2008. Cassini-Huygens mission overview and recent science results. 2008 IEEE Aerospace Conference.

Langhans R.W., Sager J.C., and McFarlane J.C. 1997. page 1–30. Iowa Agriculture and Home Economics Experiment Station.

Le Corre L., Le Mouélic S., Sotin C., Combe J.P., Rodriguez S., Barnes J., Brown R., Buratti B., Jaumann R., Soderblom J., *et al.* 2009. Analysis of a cryolava flow-like feature on Titan. Planetary and Space Science 57:870–879.

Lee Z., Weidemann A., Kindle J., Arnone R., Carder K.L., and Davis C. 2007. Euphotic zone depth: Its derivation and implication to ocean-color remote sensing. Journal of Geophysical Research: Oceans 112.

Lehmer O.R., Catling D.C., Parenteau M.N., Kiang N.Y., and Hoehler T.M. 2021. The peak absorbance wavelength of photosynthetic pigments around other stars from spectral optimization. Frontiers in Astronomy and Space Sciences 8.

Liu Y., Tikunov Y., Schouten R.E., Marcelis L.F., Visser R.G., and Bovy A. 2018. Anthocyanin biosynthesis and degradation mechanisms in solanaceous vegetables: A review. Frontiers in Chemistry 6.

Lopes R., Mitchell K., Stofan E., Lunine J., Lorenz R., Paganelli F., Kirk R., Wood C., Wall S., Robshaw L., *et al.* 2007. Cryovolcanic features on Titan's surface as revealed by the Cassini Titan Radar mapper. Icarus 186:395–412.

Lopes R.M., Kirk R.L., Mitchell K.L., LeGall A., Barnes J.W., Hayes A., Kargel J., Wye L., Radebaugh J., Stofan E.R., *et al*. 2013. Cryovolcanism on Titan: New results from Cassini Radar and VIMS. Journal of Geophysical Research: Planets 118:416–435.

Lopes R.M.C., Stofan E.R., Wall S.D., Wood C., Kirk R.L., Lucas A., Mitchell K.L., Lunine J.I., Turtle E.P., Radebaugh J., Malaska M., and Cassini RADAR Team. 2012. Titan's "Hot Cross Bun": A Titan Laccolith? In AAS/Division for Planetary Sciences Meeting Abstracts #44, vol. 44 of AAS/Division for Planetary Sciences Meeting Abstracts, page 201.06.

Lorenz R.D. 1996. Pillow lava on Titan: Expectations and constraints on cryovolcanic processes. Planetary and Space Science 44:1021–1028.

Lorenz R.D. 2017. Drifting buoy and autonomous submersible designs for the scientific exploration of Titan's seas. In OCEANS 2017 - Aberdeen, pages 1–8.

Lorenz R.D., MacKenzie S.M., Neish C.D., Gall A.L., Turtle E.P., Barnes J.W., Trainer M.G., Werynski A., Hedgepeth J., and Karkoschka E. 2021. Selection and characteristics of the Dragonfly landing site near Selk crater, Titan. The Planetary Science Journal 2:24.

Lunine J.I. 2017. Ocean worlds exploration. Acta Astronautica 131:123–130.

Lunine J.I. and Atreya S.K. 2008. The methane cycle on Titan. Nature Geoscience 1:159–164.

Martin K.P., MacKenzie S.M., Barnes J.W., and Ytreberg F.M. 2020. Protein stability in Titan's subsurface water ocean. Astrobiology 20:190–198.

Martonchik J.V. and Orton G.S. 1994. Optical constants of liquid and solid methane. Applied Optics 33:8306.

McKay C. and Smith H. 2005. Possibilities for methanogenic life in liquid methane on the surface of Titan. Icarus 178:274–276.

Mitchell J.L. and Lora J.M. 2016. The climate of Titan. Annual Review of Earth and Planetary Sciences 44:353–380.

Moore J.M. and Howard A.D. 2010. Are the basins of Titan's Hotei Regio and Tui Regio sites of former low latitude seas? Geophysical Research Letters 37.

Moore J.M. and Pappalardo R.T. 2011. Titan: An exogenic world? Icarus 212:790–806.

Mudge M.C., Nunn B.L., Firth E., Ewert M., Hales K., Fondrie W.E., Noble W.S., Toner J., Light B., and Junge K.A. 2021. Subzero, saline incubations of *Colwellia psychrerythraea* reveal strategies and biomarkers for sustained life in extreme icy environments. Environmental Microbiology 23:3840–3866.

Neish C. and Lorenz R. 2012. Titan's global crater population: A new assessment. Planetary and Space Science 60:26–33.

Neish C., Molaro J., Lora J., Howard A., Kirk R., Schenk P., Bray V., and Lorenz R. 2016. Fluvial erosion as a mechanism for crater modification on Titan. Icarus 270:114–129.

Neish C.D., Lorenz R.D., Turtle E.P., Barnes J.W., Trainer M.G., Stiles B., Kirk R., Hibbitts C.A., and Malaska M.J. 2018. Strategies for detecting biological molecules on Titan. Astrobiology 18:571-585.

Ohmura A. 2006. Observed long-term variations of solar irradiance at the earth's surface. Space Science Reviews 125:111–128.

Okamoto K., Yanagi T., Takita S., Tanaka M., Higuchi T., Ushida Y., and Watanabe H. 1996. Development of plant growth apparatus using blue and red led as artificial light source. Acta Horticulturae page 111–116.

O'Brien D.P., Lorenz R.D., and Lunine J.I. 2005. Numerical calculations of the longevity of impact oases on Titan. Icarus 173:243–253.

Pearl J., Ngoh M., Ospina M., and Khanna R. 1991. Optical constants of solid methane and ethane from 10,000 to 450 cm^{-1}. Journal of Geophysical Research 96:17477.

Pegau W.S., Gray D., and Zaneveld J.R. 1997. Absorption and attenuation of visible and near-infrared light in water: Dependence on temperature and salinity. Applied Optics 36:6035.

Perovich D.K. and Gow A.J. 1996. A quantitative description of sea ice inclusions. Journal of Geophysical Research: Oceans 101:18327–18343.

Peterman E.J., Gradinaru C.C., Calkoen F., Borst J.C., van Grondelle R., and van Amerongen H. 1997. Xanthophylls in light-harvesting complex ii of higher plants: light harvesting and triplet quenching. Biochemistry 36:12208–12215.

Pierazzo E. and Chyba C.F. 1999. Amino acid survival in large cometary impacts. Meteoritics; Planetary Science 34:909–918.

Radebaugh J., Lorenz R., Lunine J., Wall S., Boubin G., Reffet E., Kirk R., Lopes R., Stofan E., Soderblom L., *et al.* 2008. Dunes on Titan observed by Cassini radar. Icarus 194:690–703.

Roth L., Saur J., Retherford K.D., Strobel D.F., Feldman P.D., McGrath M.A., and Nimmo F. 2014. Transient water vapor at Europa's south pole. Science 343:171–174.

Sagan C. and Khare B.N. 1979. Tholins: Organic chemistry of interstellar grains and gas. Nature 277:102–107.

Sandström H. and Rahm M. 2020. Can polarity-inverted membranes self-assemble on Titan? Science Advances 6.

Satorre M., Millán C., Molpeceres G., Luna R., Maté B., Domingo M., Escribano R., and Santonja C. 2017. Densities and refractive indices of ethane and ethylene at astrophysically relevant temperatures. Icarus 296:179–182.

Schenk P.M. and Moore J.M. 2020. Topography and geology of Uranian mid-sized icy satellites in comparison with saturnian and plutonian satellites. Philosophical Transactions of the Royal Society A: Mathematical, Physical and Engineering Sciences 378:20200102.

Schurmeier L.R., Dombard A.J., Malaska M.J., Fagents S.A., Radebaugh J., and Lalich D.E. 2023. An intrusive cryomagmatic origin for northern radial labyrinth terrains on Titan and implications for the presence of crustal clathrates. Icarus 404:115664.

Soderblom L.A., Brown R.H., Soderblom J.M., Barnes J.W., Kirk R.L., Sotin C., Jaumann R., Mackinnon D.J., Mackowski D.W., Baines K.H., *et al.* 2009. The geology of Hotei Regio, Titan: Correlation of Cassini VIMS and Radar. Icarus 204:610–618.

Solomonidou A., Neish C., Coustenis A., Malaska M., Le Gall A., Lopes R.M., Werynski A., Markonis Y., Lawrence K., Altobelli N., *et al.* 2020. The chemical composition of impact craters on Titan. Astronomy; Astrophysics 641.

Sparks W.B., Hand K.P., McGrath M.A., Bergeron E., Cracraft M., and Deustua S.E. 2016. Probing for evidence of plumes on Europa with HST/STIS. The Astrophysical Journal 829:121.

Sparks W.B., Schmidt B.E., McGrath M.A., Hand K.P., Spencer J.R., Cracraft M., and Deustua S.E. 2017. Active cryovolcanism on Europa? The Astrophysical Journal 839.

Spencer J.R., Barr A.C., Esposito L.W., Helfenstein P., Ingersoll A.P., Jaumann R., McKay C.P., Nimmo F., and Waite J.H. 2009. Enceladus: An active cryovolcanic satellite. Saturn from Cassini-Huygens page 683–724.

Stevenson J., Lunine J., and Clancy P. 2015. Membrane alternatives in worlds without oxygen: Creation of an azotosome. Science Advances 1.

Stiles, B.W. *et al.* 2009. Determining Titan surface topography from Cassini SAR data. Icarus, 202, 584-598.

Stofan E., Lorenz R., Lunine J., Bierhaus E.B., Clark B., Mahaffy P.R., and Ravine M. 2013. TiME – the Titan mare explorer. In 2013 IEEE Aerospace Conference, pages 1–10.

Stofan E.R., Elachi C., Lunine J.I., Lorenz R.D., Stiles B., Mitchell K.L., Ostro S., Soderblom L., Wood C., Zebker H., *et al.* 2007. The lakes of Titan. Nature 445:61–64.

Stone E.C. and Miner E.D. 1981. Voyager 1 encounter with the Saturnian system. Science 212:159–163.

Stone E.C. and Miner E.D. 1982. Voyager 2 encounter with the Saturnian system. Science 215:499–504.

Tagliabue A., Schneider S., Pavone M., and Agha-Mohammadi A.A. 2020. Shapeshifter: A multi-agent, multi-modal robotic platform for exploration of Titan. In 2020 IEEE Aerospace Conference, pages 1–13.

Tanabe Y., Kudoh S., Imura S., and Fukuchi M. 2007. Phytoplankton blooms under dim and cold conditions in freshwater lakes of east Antarctica. Polar Biology 31:199–208.

Tang Y.K., Guo S.S., Ai W.D., and Qin L.F. 2009. Effects of red and blue light emitting diodes (LEDs) on the growth and development of lettuce (*var. youmaicai*). SAE Technical Paper Series.

Tebo B.M., Davis R.E., Anitori R.P., Connell L.B., Schiffman P., and Staudigel H. 2015. Microbial communities in dark oligotrophic volcanic ice cave ecosystems of Mt. Erebus, Antarctica. Frontiers in Microbiology 6.

Thompson W.R. and Sagan C. 1992. Organic chemistry on Titan - surface interactions. In ESA, Symposium on Titan 338:167–176.

Tomasko M.G., Archinal B., Becker T., Bézard B., Bushroe M., Combes M., Cook D., Coustenis A., de Bergh C., Dafoe L.E., *et al.* 2005. Rain, winds and haze during the Huygens probe's descent to Titan's surface. Nature 438:765–778.

Toublanc D. 1995. Photochemical modeling of Titan's atmosphere. Icarus 113:2–26.

Udensi J., Loskutova E., Loughman J., and Byrne H.J. 2022. Quantitative Raman analysis of carotenoid protein complexes in aqueous solution. Molecules 27:4724.

Vuitton V., Tran B.N., Persans P.D., and Ferris J.P. 2009. Determination of the complex refractive indices of Titan haze analogs using photothermal deflection spectroscopy. Icarus 203:663–671.

Wakita S., Johnson B.C., Soderblom J.M., Shah J., and Neish C.D. 2022. Methane- saturated layers limit the observability of impact craters on Titan. The Planetary Science Journal 3:50.

Wall S.D., Lopes R.M., Stofan E.R., Wood C.A., Radebaugh J.L., Hörst S.M., Stiles B.W., Nelson R.M., Kamp L.W., Janssen M.A., *et al.* 2009. Cassini radar images at Hotei Arcus and Western Xanadu, Titan: Evidence for geologically recent cryovolcanic activity. Geophysical Research Letters 36.

Warren S.G. 2019. Optical properties of ice and snow. Philosophical Transactions of the Royal Society A: Mathematical, Physical and Engineering Sciences 377:20180161.

Warren S.G. and Brandt R.E. 2008. Optical constants of ice from the ultraviolet to the microwave: A revised compilation. Journal of Geophysical Research 113.

Wood C.A., Lorenz R., Kirk R., Lopes R., Mitchell K., and Stofan E. 2010. Impact craters on Titan. Icarus 206:334–344.

Xu Z., Yang Y., Wang G., Cao W., Li Z., and Sun Z. 2012. Optical properties of sea ice in Liaodong Bay, China. Journal of Geophysical Research: Oceans 117.

Yung Y.L., Allen M., and Pinto J.P. 1984. Photochemistry of the atmosphere of Titan – comparison between model and observations. The Astrophysical Journal Supplement Series 55:465.

Zawierucha K., Ostrowska M., and Kolicka M. 2017. Applicability of cryoconite consortia of microorganisms and glacier-dwelling animals in astrobiological studies. Contemporary Trends in Geoscience 6:1–10.

APPENDICES

APPENDIX 1

Table 1- Water attenuation coefficients from Buiteveld *et al.* (1994).

λ (nm)	k_{abs} (m^{-1})	k_{scat} (m^{-1})	k_{att} (m^{-1})
480	0.0152	0.0025	0.0177
482	0.0157	0.0024	0.0181
484	0.0162	0.0024	0.0186
486	0.0167	0.0024	0.0191
488	0.0174	0.0023	0.0197
490	0.0181	0.0023	0.0204
492	0.0189	0.0022	0.0211
494	0.0198	0.0022	0.0220
496	0.0209	0.0022	0.0231
498	0.0223	0.0021	0.0244
500	0.0238	0.0021	0.0259
502	0.0255	0.0021	0.0276
504	0.0273	0.0020	0.0293
506	0.0291	0.0020	0.0311
508	0.0310	0.0020	0.0330
510	0.0329	0.0019	0.0348
512	0.0349	0.0019	0.0368
514	0.0368	0.0019	0.0387
516	0.0386	0.0018	0.0404
518	0.0404	0.0018	0.0422
520	0.0409	0.0018	0.0427
522	0.0416	0.0018	0.0434
524	0.0409	0.0017	0.0426
526	0.0427	0.0017	0.0444
528	0.0423	0.0017	0.0440
530	0.0429	0.0017	0.0446

Table 1- Water attenuation coefficients from Buiteveld *et al.* (1994).

532	0.0445	0.0016	0.0461
534	0.04567	0.0016	0.0472
536	0.0470	0.0016	0.0486
538	0.0480	0.0016	0.0496
540	0.0495	0.0015	0.0510
542	0.0503	0.0015	0.0518
544	0.0527	0.0015	0.0542
546	0.0544	0.0015	0.0559
548	0.0564	0.0014	0.0578
550	0.0588	0.0014	0.0602
552	0.0611	0.0014	0.0625
554	0.0631	0.0014	0.0645
556	0.0646	0.0014	0.0660
558	0.0658	0.0013	0.0671
560	0.0672	0.0013	0.0685
562	0.0686	0.0013	0.0699
564	0.0699	0.0013	0.0712
566	0.0718	0.0013	0.0731
568	0.0734	0.0012	0.0746
570	0.0759	0.0012	0.0771
572	0.0787	0.0012	0.0799
574	0.0819	0.0012	0.0831
576	0.0858	0.0012	0.0870
578	0.0896	0.0012	0.0908
580	0.0952	0.0011	0.0963
582	0.1008	0.0011	0.1019
584	0.1079	0.0011	0.01090
586	0.1159	0.0011	0.1170
588	0.1253	0.0011	0.1264
590	0.1356	0.0011	0.1367
592	0.1459	0.0010	0.1469
594	0.1567	0.0010	0.1577

Table 1- Water attenuation coefficients from Buiteveld *et al.* (1994).

596	0.1700	0.0010	0.1710
598	0.1860	0.0010	0.1870
600	0.2224	0.0010	0.2234
602	0.2366	0.0010	0.2376
604	0.2448	0.0010	0.2458
606	0.2587	0.0009	0.2596
608	0.2653	0.0009	0.2662
610	0.2691	0.0009	0.2700
612	0.2715	0.0009	0.2724
614	0.2740	0.0009	0.2749
616	0.2764	0.0009	0.2773
618	0.2785	0.0009	0.2794
620	0.2810	0.0009	0.2819
622	0.2839	0.0009	0.2848
624	0.2868	0.0008	0.2876
626	0.2893	0.0008	0.2901
628	0.2922	0.0008	0.2930
630	0.2955	0.0008	0.2963
632	0.2988	0.0008	0.2996
634	0.3011	0.0008	0.3019
636	0.3038	0.0008	0.3046
638	0.3076	0.0008	0.3084
640	0.3111	0.0008	0.3119
642	0.3144	0.0007	0.3151
644	0.3181	0.0007	0.3188
646	0.3223	0.0007	0.3230
648	0.3263	0.0007	0.3270
650	0.3315	0.0007	0.3322
652	0.3362	0.0007	0.3369
654	0.3423	0.0007	0.3430
656	0.3508	0.0007	0.3515
658	0.3636	0.0007	0.3643

Table 1- Water attenuation coefficients from Buiteveld *et al.* (1994).

660	0.3791	0.0007	0.3798
662	0.3931	0.0007	0.3938
664	0.4019	0.0006	0.4025
666	0.4072	0.0006	0.4078
668	0.4098	0.0006	0.4104
670	0.4122	0.0006	0.4128
672	0.4150	0.0006	0.4156
674	0.4173	0.0006	0.4179
676	0.4223	0.0006	0.4229
678	0.4270	0.0006	0.4276
680	0.4318	0.0006	0.4324
682	0.4381	0.0006	0.4387
684	0.4458	0.0006	0.4464
686	0.4545	0.0006	0.4551
688	0.4646	0.0006	0.4652
690	0.4760	0.0006	0.4766
692	0.4903	0.0005	0.4908
694	0.5071	0.0005	0.5076
696	0.5244	0.0005	0.5249
698	0.5470	0.0005	0.5475
700	0.5722	0.0005	0.5727
702	0.5995	0.0005	0.6000
704	0.6303	0.0005	0.6308
706	0.6628	0.0005	0.6633
708	0.6993	0.0005	0.6998
710	0.7415	0.0005	0.7420
712	0.7893	0.0005	0.7898
714	0.8445	0.0005	0.8450
716	0.9109	0.0005	0.9114
718	0.9871	0.0005	0.9876
720	1.0724	0.0005	1.0729
722	1.1679	0.0005	1.1648

Table 1- Water attenuation coefficients from Buiteveld *et al.* (1994).

724	1.2684	0.0005	1.2689
726	1.3719	0.0004	1.3723
728	1.4870	0.0004	1.4874
730	1.6211	0.0004	1.6215
732	1.7872	0.0004	1.7876
734	1.9917	0.0004	1.9921
736	2.2074	0.0004	2.2078
738	2.3942	0.0004	2.3946
740	2.5319	0.0004	2.5323
742	2.6231	0.0004	2.6235
744	2.6723	0.0004	2.6727
746	2.7021	0.0004	2.7025
748	2.7216	0.0004	2.7220
750	2.7334	0.0004	2.7338
752	2.7413	0.0004	2.7417
754	2.7478	0.0004	2.7482
756	2.7542	0.0004	2.7546
758	2.7628	0.0004	2.7632
760	2.7710	0.0004	2.7714
762	2.7733	0.0004	2.7737
764	2.7742	0.0004	2.7746
766	2.7701	0.0004	2.7705
768	2.7610	0.0004	2.7614
770	2.7542	0.0003	2.7545
772	2.7482	0.0003	2.7485
774	2.7305	0.0003	2.7308
776	2.7097	0.0003	2.7100
778	2.6896	0.0003	2.6899
780	2.6590	0.0003	2.6593
782	2.6332	0.0003	2.6335
784	2.6062	0.0003	2.6065
786	2.5702	0.0003	2.5705

Table 1- Water attenuation coefficients from Buiteveld *et al.* (1994).

788	2.5335	0.0003	2.5338
790	2.4924	0.0003	2.4927
792	2.4481	0.0003	2.4484
794	2.4083	0.0003	2.4086
796	2.3742	0.0003	2.3745
798	2.3332	0.0003	2.3335
800	2.2932	0.0003	2.2935

APPENDIX 2

Table 2 – Ice absorption and attenuation coefficients, from Cooper *et al.* (2021), Grenfell and Perovich (1981), and Warren and Brandt (2008).

λ (nm)	k_{abs} (m^{-1})	k_{scat} (m^{-1})	k_{att} (m^{-1})
480	0.0175	-	0.0175
482	0.0178	-	0.0178
484	0.0181	-	0.0181
486	0.0185	-	0.0185
488	0.0189	-	0.0189
490	0.0193	-	0.0193
492	0.0197	-	0.0197
494	0.0202	-	0.0202
496	0.0207	-	0.0207
498	0.0212	-	0.0212
500	0.0218	-	0.0218
502	0.0223	-	0.0223
504	0.0229	-	0.0229
506	0.0235	-	0.0235
508	0.0240	-	0.0240
510	0.0246	-	0.0246
512	0.0252	-	0.0252
514	0.0261	-	0.0261
516	0.0270	-	0.0270
518	0.0279	-	0.0279
520	0.0288	-	0.0288
522	0.0297	-	0.0297
524	0.0308	-	0.0308
526	0.0320	-	0.0320
528	0.0331	-	0.0331
530	0.0343	-	0.0343
532	0.0356	-	0.0356
534	0.0369	-	0.0369

Table 2 – Ice absorption and attenuation coefficients, from Cooper *et al.* (2021), Grenfell and Perovich (1981), and Warren and Brandt (2008).

536	0.0382	-	0.0382
538	0.0396	-	0.0396
540	0.0411	-	0.0411
542	0.0426	-	0.0426
544	0.0440	-	0.0440
546	0.0455	-	0.0455
548	0.0471	-	0.0471
550	0.0487	-	0.0487
552	0.0503	-	0.0503
554	0.0520	-	0.0520
556	0.0530	-	0.0530
558	0.0562	-	0.0562
560	0.0585	-	0.0585
562	0.0607	-	0.0607
564	0.0631	-	0.0631
566	0.0657	-	0.0657
568	0.0683	-	0.0683
570	0.0707	-	0.0707
572	0.0732	-	0.0732
574	0.0757	-	0.0757
576	0.0782	-	0.0782
578	0.0808	-	0.0808
580	0.0837	-	0.0837
582	0.0868	-	0.0868
584	0.0898	-	0.0898
586	0.0930	-	0.0930
588	0.0965	-	0.0965
590	0.1001	-	0.1001
592	0.1038	-	0.1038
594	0.1076	-	0.1076
596	0.1116	-	0.1116
598	0.1158	-	0.1158

Table 2 – Ice absorption and attenuation coefficients, from Cooper *et al.* (2021), Grenfell and Perovich (1981), and Warren and Brandt (2008).

600	0.1200	-	0.1200
602	0.1244	-	0.1244
604	0.1288	-	0.1288
606	0.1333	-	0.1333
608	0.1377	-	0.1377
610	0.1419	-	0.1419
612	0.1485	-	0.1485
614	0.1549	-	0.1549
616	0.1612	-	0.1612
618	0.1676	-	0.1676
620	0.1739	-	0.1739
622	0.1806	-	0.1806
624	0.1875	-	0.1875
626	0.1941	-	0.1941
628	0.2001	-	0.2001
630	0.2074	-	0.2074
632	0.2147	-	0.2147
634	0.2200	-	0.2200
636	0.2272	-	0.2272
638	0.2324	-	0.2324
640	0.2395	-	0.2395
642	0.2466	-	0.2466
644	0.2537	-	0.2537
646	0.2626	-	0.2626
648	0.2696	-	0.2696
650	0.2765	-	0.2765
652	0.2852	-	0.2852
654	0.2921	-	0.2852
656	0.3008	-	0.3008
658	0.3075	-	0.3075
660	0.3161	-	0.3161
662	0.3246	-	0.3246

Table 2 – Ice absorption and attenuation coefficients, from Cooper *et al.* (2021), Grenfell and Perovich (1981), and Warren and Brandt (2008).

664	0.3312	-	0.3312
666	0.3396	-	0.3396
668	0.3461	-	0.3461
670	0.3545	-	0.3545
672	0.3609	-	0.3609
674	0.3673	-	0.3673
676	0.3736	-	0.3736
678	0.3800	-	0.3800
680	0.3862	-	0.3862
682	0.3962	-	0.3962
684	0.4060	-	0.4060
686	0.4177	-	0.4177
688	0.4274	-	0.4274
690	0.4371	-	0.4371
692	0.4540	-	0.4540
694	0.4708	-	0.4708
696	0.4875	-	0.4875
698	0.5041	-	0.5041
700	0.5206	-	0.5206
702	0.5388	-	0.5388
704	0.5569	-	0.5569
706	0.5731	-	0.5731
708	0.5910	-	0.5910
710	0.6088	-	0.6088
712	0.6283	-	0.6283
714	0.6477	-	0.6477
716	0.6652	-	0.6652
718	0.6843	-	0.6843
720	0.7034	-	0.7034
722	0.7101	-	0.7101
724	0.7186	-	0.7186
726	0.7252	-	0.7252

Table 2 – Ice absorption and attenuation coefficients, from Cooper *et al.* (2021), Grenfell and Perovich (1981), and Warren and Brandt (2008).

728	0.7336	-	0.7336
730	0.7402	-	0.7402
732	0.7588	-	0.7588
734	0.7790	-	0.7790
736	0.7973	-	0.7973
738	0.8173	-	0.8173
740	0.8355	-	0.8355
742	0.8654	-	0.8654
744	0.8952	-	0.8952
746	0.9248	-	0.9248
748	0.9542	-	0.9542
750	0.9835	-	0.9835
752	1.0210	-	1.0210
754	1.0583	-	1.0583
756	1.0971	-	1.0971
758	1.1340	-	1.1340
760	1.1707	-	1.1707
762	1.2171	-	1.2171
764	1.2632	-	1.2632
766	1.3091	-	1.3091
768	1.3548	-	1.3548
770	1.4003	-	1.4003
772	1.4487	-	1.4487
774	1.4985	-	1.4985
776	1.5465	-	1.5465
778	1.5958	-	1.5958
780	1.6433	-	1.6433
782	1.6783	-	1.6783
784	1.7311	-	1.7311
786	1.7906	-	1.7906
788	1.8339	-	1.8339
790	1.8770	-	1.8770

Table 2 – Ice absorption and attenuation coefficients, from Cooper *et al.* (2021), Grenfell and Perovich (1981), and Warren and Brandt (2008).

792	1.9199	-	1.9199
794	1.9625	-	1.9625
796	2.0207	-	2.0207
798	2.0629	-	2.0629
800	2.1049	-	2.1049

APPENDIX 3

Table 3 – Methane absorption and attenuation coefficients, from Martonchik and Orton (1994).

λ (nm)	k_{abs} (m^{-1})	k_{scat} (m^{-1})	k_{att} (m^{-1})
480	0.0142	-	0.0142
482	0.0144	-	0.0144
484	0.0147	-	0.0147
486	0.0150	-	0.0150
488	0.0153	-	0.0153
490	0.0156	-	0.0156
492	0.0159	-	0.0159
494	0.0162	-	0.0162
496	0.0164	-	0.0164
498	0.0167	-	0.0167
500	0.0170	-	0.0170
502	0.0172	-	0.0172
504	0.0175	-	0.0175
506	0.0178	-	0.0178
508	0.0181	-	0.0181
510	0.0183	-	0.0183
512	0.0186	-	0.0186
514	0.0188	-	0.0188
516	0.0191	-	0.0191
518	0.0194	-	0.0194
520	0.0196	-	0.0196
522	0.0199	-	0.0199
524	0.0200	-	0.0200
526	0.0204	-	0.0204
528	0.0206	-	0.0206
530	0.0208	-	0.0208
532	0.0211	-	0.0211
534	0.0213	-	0.0213

Table 3 – Methane absorption and attenuation coefficients, from Martonchik and Orton (1994).

536	0.0215	-	0.0215
538	0.0218	-	0.0218
540	0.0220	-	0.0220
542	0.0223	-	0.0223
544	0.0225	-	0.0225
546	0.0227	-	0.0227
548	0.0229	-	0.0229
550	0.0231	-	0.0231
552	0.0234	-	0.0234
554	0.0236	-	0.0236
556	0.0237	-	0.0237
558	0.0241	-	0.0241
560	0.0242	-	0.0242
562	0.0246	-	0.0246
564	0.0247	-	0.0247
566	0.0249	-	0.0249
568	0.0252	-	0.0252
570	0.0254	-	0.0254
572	0.0255	-	0.0255
574	0.0258	-	0.0258
576	0.0260	-	0.0260
578	0.0261	-	0.0261
580	0.0264	-	0.0264
582	0.0266	-	0.0266
584	0.0265	-	0.0265
586	0.0262	-	0.0262
588	0.0259	-	0.0259
590	0.0256	-	0.0256
592	0.0255	-	0.0255
594	0.0252	-	0.0252
596	0.0249	-	0.0249
598	0.0246	-	0.0246

Table 3 – Methane absorption and attenuation coefficients, from Martonchik and Orton (1994).

600	0.3623	-	0.3623
602	0.6993	-	0.6993
604	1.0340	-	1.0340
606	1.3645	-	1.3645
608	1.6948	-	1.6948
610	2.0210	-	2.0210
612	2.3408	-	2.3408
614	2.6606	-	2.6606
616	2.9988	-	2.9988
618	3.3144	-	3.3144
620	3.6280	-	3.6280
622	3.9396	-	3.9396
624	3.7659	-	3.7659
626	3.5933	-	3.5933
628	3.4217	-	3.4217
630	3.2513	-	3.2513
632	3.0819	-	3.0819
634	2.9335	-	2.9335
636	2.7662	-	2.7662
638	2.5999	-	2.5999
640	2.4347	-	2.4347
642	2.2706	-	2.2706
644	2.1074	-	2.1074
646	1.9433	-	1.9433
648	1.7841	-	1.7841
650	1.6259	-	1.6259
652	1.4667	-	1.4667
654	1.3104	-	1.3104
656	1.1551	-	1.1551
658	1.0007	-	1.0007
660	0.8454	-	0.8454
662	0.6929	-	0.6929

Table 3 – Methane absorption and attenuation coefficients, from Martonchik and Orton (1994).

664	0.5413	-	0.5413
666	0.3887	-	0.3887
668	0.2389	-	0.2389
670	0.0895	-	0.0895
672	0.0843	-	0.0843
674	0.0792	-	0.0792
676	0.0742	-	0.0742
678	0.0689	-	0.0689
680	0.0639	-	0.0639
682	0.0590	-	0.0590
684	0.0540	-	0.0540
686	0.0489	-	0.0489
688	0.0594	-	0.0594
690	0.0696	-	0.0696
692	0.0797	-	0.0797
694	0.0898	-	0.0898
696	0.0998	-	0.0998
698	0.1098	-	0.1098
700	0.1197	-	0.1197
702	0.1296	-	0.1296
704	0.1394	-	0.1394
706	0.1492	-	0.1492
708	0.4952	-	0.4952
710	0.8389	-	0.8389
712	1.1807	-	1.1807
714	1.5206	-	1.5206
716	1.8604	-	1.8604
718	1.9952	-	1.9952
720	1.9548	-	1.9548
722	1.8971	-	1.8971
724	1.8572	-	1.8572
726	1.8001	-	1.8001

Table 3 – Methane absorption and attenuation coefficients, from Martonchik and Orton (1994).

728	1.7607	-	1.7607
730	1.7059	-	1.7059
732	1.6635	-	1.6635
734	1.6230	-	1.6230
736	1.5810	-	1.5810
738	1.5410	-	1.5410
740	1.4995	-	1.4995
742	1.4599	-	1.4599
744	1.4187	-	1.4187
746	1.3796	-	1.3796
748	1.3390	-	1.3390
750	1.3000	-	1.3000
752	1.2600	-	1.2600
754	1.2216	-	1.2216
756	1.1818	-	1.1818
758	1.1439	-	1.1439
760	1.1045	-	1.1045
762	1.0670	-	1.0670
764	1.0280	-	1.0280
766	0.9909	-	0.9909
768	0.9523	-	0.9523
770	0.9155	-	0.9155
772	0.8774	-	0.8774
774	0.8410	-	0.8410
776	0.8032	-	0.8032
778	0.7672	-	0.7672
780	0.7298	-	0.7298
782	0.6942	-	0.6942
784	0.6572	-	0.6572
786	0.6635	-	0.6635
788	0.7096	-	0.7096
790	0.7556	-	0.7556

Table 3 – Methane absorption and attenuation coefficients, from Martonchik and Orton (1994).

792	0.8013	-	0.8013
794	0.8467	-	0.8467
796	0.8920	-	0.8920
798	0.9370	-	0.9370
800	0.9550	-	0.9550

APPENDIX 4

Table 4 – Tholin absorption and attenuation coefficients, from Vuitton *et al.* (2009).

λ (nm)	k_{abs} (m^{-1})	k_{scat} (m^{-1})	k_{att} (m^{-1})
480	454248.1	-	454248.1
482	442951.5	-	442951.5
484	431748.3	-	431748.3
486	420637.3	-	420637.3
488	409617.3	-	409617.3
490	398687.3	-	398687.3
492	387846.2	-	387846.2
494	377092.9	-	377092.9
496	367009.0	-	367009.0
498	357384.6	-	357384.6
500	347812.0	-	347812.0
502	338315.7	-	338315.7
504	328894.8	-	328894.8
506	319548.4	-	319548.4
508	310375.6	-	310375.6
510	301075.5	-	301075.5
512	291947.2	-	291947.2
514	286630.6	-	286630.6
516	281744.8	-	281744.8
518	276896.8	-	276896.8
520	272086.0	-	272086.0
522	267312.2	-	267312.2
524	262574.8	-	262574.8
526	257873.4	-	257873.4
528	252922.0	-	252922.0
530	246466.8	-	246466.8
532	240036.6	-	240036.6
534	233654.5	-	233654.5
536	227343.5	-	227343.5

Table 4 – Tholin absorption and attenuation coefficients, from Vuitton *et al.* (2009).

538	221056.0	-	221056.0
540	214815.1	-	214815.1
542	209084.0	-	209084.0
544	204134.2	-	204134.2
546	199243.7	-	199243.7
548	194388.9	-	194388.9
550	189569.4	-	189569.4
552	184762.0	-	184762.0
554	180012.1	-	180012.1
556	175296.3	-	175296.3
558	170614.4	-	170614.4
560	165943.4	-	165943.4
562	161618.7	-	161618.7
564	157436.1	-	157436.1
566	153283.1	-	153283.1
568	149159.3	-	149159.3
570	145086.5	-	145086.5
572	141015.8	-	141015.8
574	136982.2	-	136982.2
576	132972.3	-	132972.3
578	128990.1	-	128990.1
580	126292.0	-	126292.0
582	123698.9	-	123698.9
584	121101.9	-	121101.9
586	118544.2	-	118544.2
588	115982.5	-	115982.5
590	113459.4	-	113459.4
592	110932.2	-	110932.2
594	108443.1	-	108443.1
596	105907.5	-	105907.5
598	103220.8	-	103220.8
600	100551.9	-	100551.9

Table 4 – Tholin absorption and attenuation coefficients, from Vuitton *et al.* (2009).

602	97900.8	-	97900.8
604	95267.2	-	95267.2
606	92651.0	-	92651.0
608	90052.1	-	90052.1
610	87470.2	-	87470.2
612	85089.9	-	85089.9
614	82929.9	-	82929.9
616	80804.2	-	80804.2
618	78672.0	-	78672.0
620	76573.8	-	76573.8
622	74468.9	-	74468.9
624	72377.5	-	72377.5
626	70319.5	-	70319.5
628	68254.6	-	68254.6
630	68254.6	-	68254.6
632	68254.6	-	68254.6
634	62157.9	-	62157.9
636	60757.2	-	60757.2
638	59483.4	-	59483.4
640	58217.6	-	58217.6
642	56959.7	-	56959.7
644	55709.6	-	55709.6
646	54486.7	-	54486.7
648	53251.9	-	53251.9
650	52024.8	-	52024.8
652	50805.1	-	50805.1
654	49573.8	-	49573.8
656	48177.5	-	48177.5
658	46789.7	-	46789.7
660	45410.3	-	45410.3
662	44039.2	-	44039.2
664	42676.5	-	42676.5

Table 4 – Tholin absorption and attenuation coefficients, from Vuitton *et al.* (2009).

666	41303.0	-	41303.0
668	40031.8	-	40031.8
670	38880.7	-	38880.7
672	37755.2	-	37755.2
674	36617.7	-	36617.7
676	35487.0	-	35487.0
678	34381.4	-	34381.4
680	33467.2	-	33467.2
682	32742.6	-	32742.6
684	32040.6	-	32040.6
686	31324.3	-	31324.3
688	30612.3	-	30612.3
690	29922.5	-	29922.5
692	29218.6	-	29218.6
694	28392.0	-	28392.0
696	27516.0	-	27516.0
698	26627.0	-	26627.0
700	25761.1	-	25761.1
702	24900.0	-	24900.0
704	24043.9	-	24043.9
706	23210.4	-	23210.4
708	22346.1	-	22346.1
710	21716.8	-	21716.8
712	21108.7	-	21108.7
714	20486.4	-	20486.4
716	19867.5	-	19867.5
718	19269.6	-	19269.6
720	18657.6	-	18657.6
722	18083.7	-	18083.7
724	17582.5	-	17582.5
726	17084.0	-	17084.0
728	16588.3	-	16588.3

Table 4 – Tholin absorption and attenuation coefficients, from Vuitton *et al.* (2009).

730	16095.3	-	16095.3
732	15605.0	-	15605.0
734	15117.3	-	15117.3
736	14632.3	-	14632.3
738	14184.0	-	14184.0
740	13738.0	-	13738.0
742	13311.5	-	13311.5
744	12887.3	-	12887.3
746	12465.3	-	12465.3
748	12045.6	-	12045.6
750	11611.3	-	11611.3
752	11196.1	-	11196.1
754	10883.0	-	10883.0
756	10605.0	-	10605.0
758	10345.0	-	10345.0
760	10069.6	-	10069.6
762	9795.8	-	9795.8
764	9539.9	-	9539.9
766	9268.9	-	9268.9
768	9015.7	-	9015.7
770	8763.8	-	8763.8
772	8513.2	-	8513.2
774	8280.2	-	8280.2
776	8032.1	-	8032.1
778	7801.5	-	7801.5
780	7523.7	-	7523.7
782	7311.6	-	7311.6
784	7084.6	-	7084.6
786	6890.7	-	6890.7
788	6697.8	-	6697.8
790	6521.8	-	6521.8
792	6299.1	-	6299.1

Table 4 – Tholin absorption and attenuation coefficients, from Vuitton *et al.* (2009).

794	6109.1	-	6109.1
796	5920.1	-	5920.1
798	5747.8	-	5747.8
800	5592.0	-	5592.0